MALEIMIDE BASED THIOL REACTIVE HYDROGELS AND POLYMERS FROM ORTHOGONALLY FUNCTIONALIZABLE BIODEGRADABLE DENDRONS

by

Sebla Onbulak

B.S., Chemistry, Boğaziçi University, 2009

Submitted to the Institute for Graduate Studies in
Science and Engineering in partial fulfillment of
the requirements for the degree of
Master of Science

Graduate Program in Chemistry
Boğaziçi University

2011

MALEIMIDE BASED THIOL REACTIVE HYDROGELS AND POLYMERS FROM ORTHOGONALLY FUNCTIONALIZABLE BIODEGRADABLE DENDRONS

APPROVED BY:

Assoc. Prof. Amitav Sanyal (Thesis Supervisor)	……...
Assist. Prof. Rana Sanyal	……
Assoc. Prof. Seyda Bucak	……

DATE OF APPROVAL: …….

To My Beloved Father

ACKNOWLEDGEMENTS

I would like to express my most sincere gratitude to my thesis supervisor Assoc. Prof. Amitav SANYAL for his endless patience and assistance throughout this study. It was a great opportunity to work in his laboratory and improve myself thanks to his useful comments and excellent scientific guidance.

I wish to express my thanks to Assoc. Prof. Seyda BUCAK for her careful and constructive review of the final manuscript and to Assist. Prof. Rana SANYAL for her endless help and support during my masters program.

I would like to express my great appreciation to Assist. Prof. Javid RZAYEV from University at Buffalo and Assist. Prof. Andrew P. DOVE from University of Warwick to give me the opportunity to work in their laboratories and provide useful data and informative studies for my projects.

I would like to extend my thanks to Ayla TÜRKEKUL, Burcu SELEN ÇAĞLAYAN, Bilge GEDİK ULUOCAK, Tuğçe NİHAL GEVREK and Serap YAPAR for their patience and help running a large number of NMR, SEM, Fluorescence Microscopy and CHNS experiments supporting my laboratory work.

I would like to express my gratitude to my former and present labmates for their enjoyable company and friendship and contributions to my laboratory work. I would like to thank all my friends and all the members of the Chemistry Department who were exactly like a family for me during these years.

Finally, my deepest thanks go to my family for their endless love, support and encouragement throughout these years.

ABSTRACT

MALEIMIDE BASED THIOL REACTIVE HYDROGELS AND POLYMERS FROM ORTHOGONALLY FUNCTIONALIZABLE BIODEGRADABLE DENDRONS

Hydrogels and polymers with reactive side chains have gained an increased attention in recent years due to their amenability to efficient post-functionalization. Wide applications of such hydrogels and polymers in biomedical and pharmaceutical areas and materials science result in new investigations regarding design and synthesis of biofunctionalizable and biodegradable materials. This thesis consists of two different projects. In the first project, poly (ethylene glycol)-based reactive hydrogels were synthesized using a second generation poly (ester) dendron which has an orthogonal character because of the masked malemide unit at its core and alkyne moieties at its periphery. Hydrogel formation was achieved via Huisgen type [3+2] 'click' cycloaddition and unmasking of maleimide functionalities to their reactive forms was achieved via retro Diels-Alder strategy. Positional control of these groups allow to investigate the efficiency of maleimide incorporation and functionalization of the hydrogel. All the functionalizations were performed under mild, reagent-free conditions via derivatization with different thiol containing molecules. Extent of functionalization was investigated through immobilization of the enzyme FITC-streptavidin onto biotinylated hydrogels.

In the second project, a series of carbonate based homo- and lactide based copolymers containing thiol reactive maleimide groups as their side chains have been synthesized via utilizing organocatalytic ring-opening polymerization (ROP). A novel cyclic carbonate monomer was synthesized and polymerizations were achieved at room temperature by using DBU as an organocatalyst. Latent reactive maleimide functionalities of copolymers were activated via retro Diels-Alder reaction. Quantitative functionalization of the pendant maleimide groups by thiol containing molecules was achieved under mild conditions via nucleophilic thiol-ene 'click' chemistry.

ÖZET

ORTOGONAL OLARAK İŞLEVSELLEŞTİRİLEBİLEN BİYOBOZUNUR DENDRONLARDAN ELDE EDİLEN MALEİMİD KÖKENLİ TİOL REAKTİF HİDROJEL VE POLİMERLER

Yan dallarında reaktif grup bulunduran hidrojel ve polimerler, etkin olarak işlevselleştirilebildiklerinden dolayı son zamanlarda artan bir ilgiye maruz kalmıştır. Bu hidrojel ve polimerlerin biyomedikal ve farmasötikal alanlarlardaki ve malzeme bilimindeki geniş kullanımları, biyoişlevsel ve biyobozunur materyallerin tasarım ve sentezlerinde yeni araştırmaların yapılmasına sebep olmuştur. Bu tez çalışması iki farklı projeden oluşmaktadır. İlk projede, çekirdekteki korunmuş maleimid ve yüzeydeki alkin grupları sayesinde ortogonal özellik gösteren ikinci jenerasyon polyester dendron yardımıyla polietilen glikol kökenli reaktif hidrojeller sentezlenmiştir. Hidrojel oluşumu Huisgen tipi [3+2] 'klik' katılımıyla gerçekleşmiş ve korunmuş maleimid grupları retro Diels Alder tepkimesi sayesinde açılarak reaktif hallerine dönüştürülmüştür. Bu grupların konumsal kontrolü, hidrojele maleimid katılımının ve fonksiyonelleştirilebilme veriminin incelenmesine olanak sağlar. Bütün fonksiyonelleştirme çalışmaları, ağır tepkime koşulları ve reaktif madde gerekmeden çeşitli tiol bağlı moleküllerin türevlendirilmesiyle yapılmıştır. Fonksiyonelleştirme miktarı FITC-streptavidin adlı enzimin hidrojellere bağlanmasıyla ölçülmüştür.

İkinci projede, yan dallarında tiol reaktif maleimid grupları bulunduran karbonat kökenli homo- ve laktit kökenli kopolimerler, organokatalitik halka açma polimerizasyonu yardımıyla sentezlenmiştir. Özgün bir halkalı karbonat monomeri sentezlenmiş polimerizasyonları katalizör olarak kullanılan DBU yardımıyla oda sıcaklığında gerçekleştirilmiştir. Kopolimerlerin reaktivitesi gizlenmiş maleimid grupları retro Diels Alder tepkimesiyle aktive edilmiştir. Yan dallarda asılı maleimid gruplarının tiol içeren moleküllerle kantitatif işlevselleştirimi, ağır tepkime koşulları gerektirmeyen nükleofilik tiol-en 'klik' kimyasıyla gerçekleştirilmiştir.

TABLE OF CONTENTS

ACKNOWLEDGEMENTS iv
ABSTRACT v
ÖZET vi
LIST OF FIGURES vii
LIST OF TABLES ix
LIST OF ACRONYMS / ABBREVIATIONS xv
1. INTRODUCTION 1
1.1. Dendrimers 1
1.1.1. Orthogonally reactive dendrons 2
1.2. Click Chemistry 4
1.3. Diels-Alder Reaction in Polymer Chemistry 5
1.4. Hydrogels 7
1.5. Biodegradable Polymers 11
1.6. Ring Opening Polymerization (ROP) 13
1.6.1. Reactive Polymers via organocatalytic ROP 16
2. AIM OF THE STUDY 18
2.1. Thiol Reactive Hydrogels via Orthogonally ‘Clickable’ Dendrons 18
2.2. Biodegradable and Thiol Reactive Polymers 19
3. RESULTS AND DISCUSSION 20
3.1. Thiol Reactive Hydrogels via Orthogonally ‘Clickable’ Dendrons 20
3.1.1. Synthesis and Characterization 20
3.1.2. Effect of temperature on gelation 22
3.1.3. Effect of masked maleimide density within the gel 23
3.1.4. Swelling Studies 24
3.1.5. Scanning electron microscopy 25
3.1.6. Functionalization of Hydrogels 25
3.1.7. Reason for using a masked maleimide group prior to gelation 28
3.2. Biodegradable and Thiol Reactive Polymers 32
3.2.1. Synthesis of Cyclic Carbonate Monomer 32

3.2.2. Synthesis and Characterization of Homopolymers 33
3.2.3. Synthesis and Characterization of Copolymers 39
3.2.4. Functionalization of PLLA Copolymers 42
4. EXPERIMENTAL 46
4.1. Materials and Methods 46
4.2. Thiol Reactive Hydrogels via Orthogonally 'Clickable' Dendrons 47
4.2.1. Synthesis of Second Generation (G2) Alkyne Dendron 47
4.2.2. Hydrogel Synthesis 48
4.2.3. Hydrogel activation 49
4.2.4. Swelling Studies 50
4.2.5. Scanning Electron Microscopy Studies 51
4.2.6. Functionalization with fluorescent dye BodipyC10SH 51
4.2.7. Functionalization with Streptavidin 51
4.2.8. Activation of G2 alkyne dendron 54
4.2.9. Synthesis of PEG Polymer Conjugates 54
4.3. Biodegradable and Thiol Reactive Polymers 56
4.3.1. Synthesis of Cyclic Carbonate Monomer 56
4.3.2. Synthesis maleimide functional homopolymers 57
4.3.3. Synthesis of activated homopolymer by rDA 58
4.3.4. Synthesis of maleimide functional PLLA copolymers 58
4.3.5. Synthesis of activated copolymer by rDA 59
4.3.6. Functionalization of copolymer with 6-(ferrocenyl)hexanethiol ... 60
4.3.7. Functionalization of copolymer with 1-hexanethiol 61
5. CONCLUSIONS 62
APPENDIX 63
REFERENCES 77

LIST OF FIGURES

Figure 1.1. Schematic representation of a dendron and a dendrimer 1

Figure 1.2. Dendrimer synthesis via divergent and convergent method 2

Figure 1.3. Orthogonal functionalization of biodegradable polyester dendrons 3

Figure 1.4. Huisgen cycloaddition reaction between an azide and an alkyne 4

Figure 1.5. Copper catalyzed Huisgen [3+2] cycloaddition reaction 4

Figure 1.6. Possible ‘Click’ reactions of maleimide functionality 5

Figure 1.7. DA and rDA reactions between maleimide and furan derivatives 5

Figure 1.8. Thermosensitive hydrogels via DA/rDA strategy 6

Figure 1.9. Synthesis and functionalization of a reactive copolymer via DA/rDA strategy 7

Figure 1.10. Synthesis of PEG based hydrogels via Huisgen ‘Click’ reaction 8

Figure 1.11. Hydrogel formation via ‘Click’ reaction of Dendron-Polymer Conjugates 9

Figure 1.12. Synthesis of thiol reactive hydrogels 10

Figure 1.13. Hydrolysis and cleavage of ester linkage 11

Figure 1.14. Common synthetic biodegradable polymers 12

Figure 1.15. Schematic representation of drug delivery via biodegradable polymers 12

Figure 1.16. Common monomers used in ROP 14

Figure 1.17. Structure of $Sn(Oct)_2$ 14

Figure 1.18. Organocatalytic ROP catalysts 15

Figure 1.19. ROP of lactide via dual activation by a thiourea-tertiary mine catalyst system 15

Figure 1.20. Illustration of synthesis and functionalization of allyl-functional cyclic carbonate 17

Figure 1.21. Synthesis of and Michael type thiol-ene conjugation maleimide functional PLA..... 17

Figure 2.1. Synthetic approach towards reactive hydrogels using dendritic constructs 18

Figure 2.2. Synthetic approach towards biodegradable and multifunctional polymers via Michael type ‘Click’ conjugation 19

Figure 3.1. Overall Synthesis masked maleimide functional G2 alkyne dendron 20

Figure 3.2. Synthesis of hydrogels 21

Figure 3.3. TGA thermogram of the hydrogel H3 before and after retro Diels-Alder step 23

Figure 3.4. TGA thermograms of the hydrogels (H2 - H5) 24

Figure 3.5. Effect of PEG chain length on swelling..... 25

Figure 3.6. Representative SEM micrographs of hydrogels 25

Figure 3.7. Functionalization of the hydrogel with fluorescent dye BODIPYC10SH..... 26

Figure 3.8. Covalent biotinylation and FITC-labeled Streptavidin immobilization on hydrogels..... 27

Figure 3.9. Fluorescence microscope images and Fluorescence intensity graph after functionalization with Streptavidin 28

Figure 3.10. Azide cycloaddition to N-Ethylmaleimide 29

Figure 3.11. ^{1}H NMR in $CDCl_3$ of Ethylmaleimide-PEG azide 'Click' cycloadduct 29

Figure 3.12. Synthesis of PEG-polymer conjugates 30

Figure 3.13. Obtained Fluorescence intensities of gels formed using activated and masked maleimide functional dendrons at 50 ºC..... 31

Figure 3.14. Synthesis of maleimide functional carbonate monomer 3..... 32

Figure 3.15. ^{1}H-NMR and ^{13}C-NMR in $CDCl_3$ of maleimide functional carbonate monomer 3 33

Figure 3.16. Synthesis of maleimide functional homo-and copolymers via ring opening polymerization and activation of maleimide groups with retro Diels-Alder strategy 34

Figure 3.17. Plots of number-average molecular weight (M_n) vs % monomer conversion and number-average molecular weight (M_n) vs initial 7 monomer-to-initiator ratio 35

Figure 3.18. ^{1}H-NMR in $CDCl_3$ of latent reactive P3 and reactive P3 Retro homopolymers 36

Figure 3.19. GPC traces of the homopolymer P3 homopolymer after the rDA Reaction, P3 Retro 37

Figure 3.20. MALDI-TOF MS analysis of the polymer P3 and P3 Retro 38

Figure 3.21. ^{1}H-NMR in $CDCl_3$ of polymer P14 and P14 Retro 40

Figure 3.22. GPC traces of copolymer P14 and P14 Retro 41

Figure 3.23. TGA thermograms of the polymer P14 and P14 Retro 42

Figure 3.24. TGA thermograms of copolymers with different maleimide percentages 42

Figure 3.25. Synthesis of functionalized polymers via Michael Addition of thiols to the polymer P13 43

Figure 3.26. ^{1}H-NMR in $CDCl_3$ of (a) P14 Retro, 6-(ferrocenyl)hexanethiol functionalized polymer (P14-Fer) and GPC traces 44

Figure 3.27. ^{1}H-NMR spectra of (a) P14 Retro, 1-hexanethiol functionalized polymer (P14-Hex) and GPC traces 45

Figure 4.1. Synthesis of masked maleimide functional G2 alkyne dendron 3 48

Figure 4.2. Representative hydrogel synthesis 49

Figure 4.3. Activation of hydrogels 50

Figure 4.4. Functionalization of the hydrogel with fluorescent dye BODIPYC10SH 52

Figure 4.5. Biotinylation of hydrogel with Biotin-SH 53

Figure 4.6. Activation of G2 alkyne dendron 54

Figure 4.7. Synthesis of G2 Dendron-PEG polymer conjugates 55

Figure 4.8. Synthesis of N-Ethylmaleimide-PEG polymer conjugate 56

Figure 4.9. Synthesis of maleimide functional carbonate monomer 3 57

Figure 4.10. Synthesis of maleimide functional homopolymer 4 57

Figure 4.11. Activation of maleimide functional homopolymer 4 58

Figure 4.12. Synthesis of maleimide functional copolymer 6 59

Figure 4.13. Activation of maleimide functional copolymer 6 59

Figure 4.14. Functionalization of copolymer 7 with 6-(ferrocenyl) hexanethiol 60

Figure 4.15. Functionalization of copolymer 7 with 1-hexanethiol 61

Figure A.1. ^{1}H NMR spectrum of 2nd generation alkyne dendron 3 64

Figure A.2. FTIR traces of G2 alkyne dendron 3, PEG6K bisazide and the

hydrogel 4 65

Figure A.3. ^{1}H NMR spectrum of Dendron-PEG polymer conjugate 9 (1:1 Alkyne:Azide ratio) 66

Figure A.4. ^{1}H NMR spectrum of Dendron-PEG polymer conjugate (1:2 Alkyne:Azide ratio) 67

Figure A.5. ^{1}H NMR spectrum of N-Ethylmaleimide-PEG polymer conjugate 10 68

Figure A.6. ^{1}H NMR spectrum of maleimide functional carbonate monomer 3 69

Figure A.7. ^{13}C NMR spectrum of maleimide functional carbonate monomer 3 70

Figure A.8. ^{1}H NMR spectrum of maleimide functional homopolymer 4 71

Figure A.9. ^{1}H NMR spectrum of activated homopolymer 5 72

Figure A.10. ^{1}H NMR spectrum of maleimide functional copolymer 6 73

Figure A.11. ^{1}H NMR spectrum of activated copolymer 7 74

Figure A.12. ^{1}H NMR spectrum of 6-(ferrocenyl)hexanethiol functionalized copolymer 8 75

Figure A.13. ^{1}H NMR spectrum of 1-hexanethiol functionalized copolymer 9 76

LIST OF TABLES

Table 3.1. Properties of hydrogels with variations in PEG lengths and Temperature 22

Table 3.2. Properties of synthesized PEG-polymer conjugates with activated dendron 30

Table 3.3. Conditions and characterizations of homopolymers..... 34

Table 3.4. Conditions and characterizations of carbonate monomer 3: L-lactide copolymers 39

LIST OF ACRONYMS / ABBREVIATIONS

AIBN	2,2’-azobisisobutyronitrile
$CDCl_3$	Deuterated chloroform
CH_2Cl_2	Dichloromethane
DA	Diels-Alder
DBU	1,8-Diazabicyclo[5.4.0]undec-7-ene
DMAP	4-Dimethylaminopyridine
EtOAc	Ethyl Acetate
FITC	Fluorescein isothiocynate
FT-IR	Fourier Transform Infrared
GPC	Gel Permeation Chromatography
MALDI-ToF	Matrix-assisted laser desorption and ionization time-of-flight
MeOH	Methanol
MS	Mass Spectroscopy
NaAsc	Sodium Ascorbate
NMR	Nuclear Magnetic Resonance
PEG	Poly(ethylene glycol)
PEGMA	Poly(ethylene glycol) methacrylate
PLA	Polylactide
PLLA	Poly-L-lactide
PMDETA	N,N,N-pentamethyldiethylenetriamine
rDA	Retro Diels-Alder
ROP	Ring Opening Polymerization
SEM	Scanning Electron Microscope
TEA	Triethylamine
TEG	Triethyleneglycol
TGA	Thermogravimetric Analysis
THF	Tetrahydrofuran

1. INTRODUCTION

1.1 Dendrimers

Dendrimers are highly ordered, spherical macromolecules which can be synthesized by stepwise organic reactions. This stepwise mechanism gives them the property of being monodisperse. Its structure has a main core, branched repeating units and functional groups on the periphery. A dendron is a part of the dendrimer that starts from a single, chemically addressable focal point and ends at the periphery (Figure 1.1). Large number of functional groups enables multivalency to the dendritic construct. Besides, branching units determine the interior properties of the dendrimer and they are responsible from the growth of it. Number of the branching points from the core to the surface indicates the generation number.

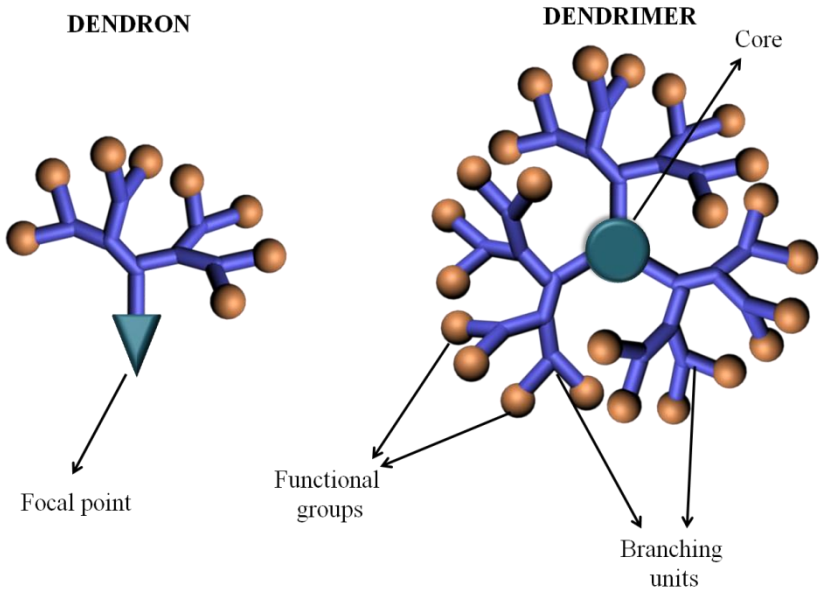

Figure 1.1. Schematic representation of a dendron and a dendrimer.

Due to the steric hindrance along the core and branching units, physical and chemical properties of dendrimers are determined by the functional groups at the surface. Monodisperse character makes the dendrimers attractive to be utilized as drug delivery vehicles [1], light harvesting systems [2] or biomolecular immobilization agents [3]. Also,

they are excellent candidates to form crosslinked systems due to their high branching ability [4].

There are two possible methodologies to synthesize dendrimers. In one of them which is the divergent approach, growth of the dendron starts from the core and later, branching units are added. By this way, very large dendrimers can be prepared but purification becomes harder due to the fast growth [5]. In the second methodology, convergent approach, growth starts from surface groups and continues inwards to the core. Control over dendrimer growth can be established with this approach (Figure 1.2) [6].

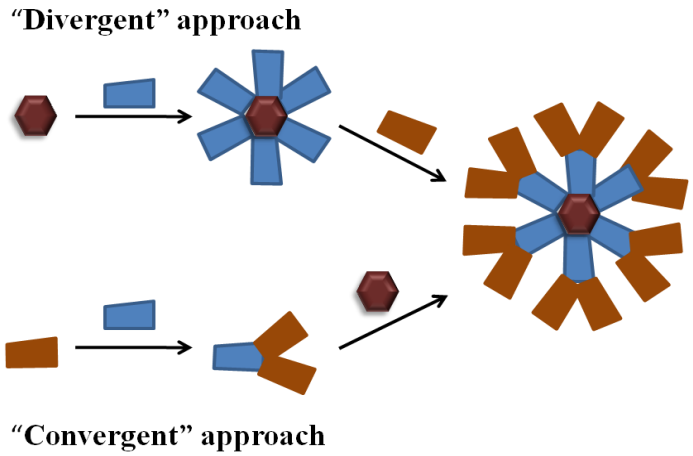

Figure 1.2. Dendrimer synthesis via divergent and convergent method.

1.1.1. Orthogonally Reactive Dendrons

It has been known that dendritic scaffolds use the advantage of being multivalent with large number of functional groups at the periphery. Therefore, utilizing a dendritic macromolecule for formation of multiarm star polymers, hydrogels or dendronized polymers is also favorable. Multivalent character of dendritic structures can be enhanced by incorporating orthogonally functionalizable groups so that they become multifunctional materials [7-9]. These kinds of systems are very attractive since they are widely used in polymer conjugated drug delivery studies. Branched structure of dendritic molecules increases circulation time in the body which is a preferable property for many chemotherapeutic agents [10].

Thiol and amine containing molecules can be utilized to obtain orthogonally functionalizable polymers as reported [11]. Also, some groups demonstrated that chemistry of thiol conjugation and copper catalyzed 1,3-dipolar cycloaddition can supplement to this multifunctionality concept [12-13]. To utilize advantage of orthogonal dendritic scaffolds, in our previous study, we synthesized novel biodegradable polyester dendrons and demonstrated their multifunctionality. Dendron surface was appended with alkyne moeities which undergo lately Huisgen type 'click' cycloaddition reaction with PEG azide. At the same time, maleimide functional core of dendron was functionalized with a thiol containing dye and orthogonal multifunctionality of these kind of systems has been proved [14] (Figure 1.3).

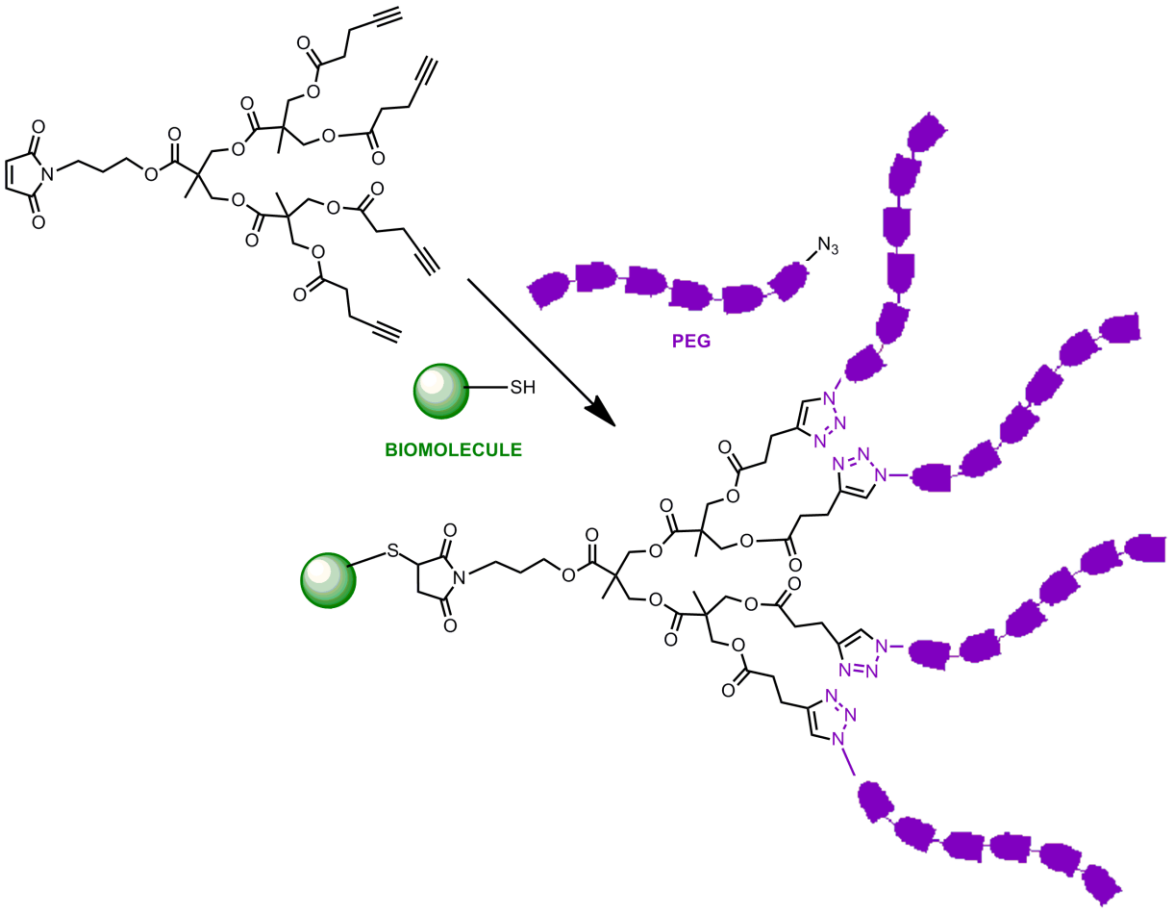

Figure 1.3. Orthogonal functionalization of biodegradable polyester dendrons.

1.2. Click Chemistry

Sharpless and coworkers introduced “Click” Chemistry, a powerful tool in organic synthesis because of its simplicity and efficiency. High selectivity, high yielding capacity and tolerance towards a wide range of functional groups and reaction conditions make “Click” reactions attractive to be used during the synthesis of dendrimers, block copolymers, hydrogel formations, derivatization of cellular surfaces, preparation of enzyme inhibitors and many other studies.

Types of “Click” reactions can be classified as ‘nucleophilic opening of highly strained rings’ such as epoxides, aziridines, ‘protecting group reactions’ such as acetals, ketals, ‘cycloaddition reactions’ such as Diels-Alder [4+2] and Copper catalyzed Huisgen [3+2] cycloadditon reactions [15-17]. Among all of the ‘Click’ reactions, most famous one is Huisgen [3+2] cycloaddition reaction between azide and alkyne functionalities to give a mixture of 1,4 and 1,5-disubstituted triazoles (Figure 1.4).

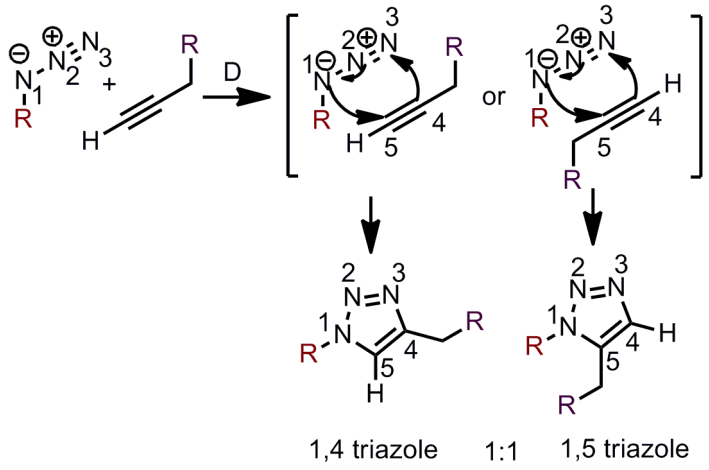

Figure 1.4. Huisgen [3+2] cycloaddition reaction between an azide and an alkyne.

In 2002 Sharpless and Fokin [18] investigated that by introducing a Cu (I) catalyst the reaction forms only the regioisomer, 1,4-disubstituted triazole (Figure 1.5).

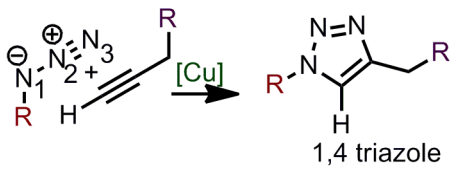

Figure 1.5. Copper catalyzed Huisgen [3+2] cycloaddition reaction.

Metal-free thiol-ene reactions like thiol–ene free-radical addition between electron-rich and electron-poor carbon–carbon double bonds, and the catalyzed thiol Michael addition to electron-deficient carbon–carbon double bonds have emerged during the last century. Especially for biomedical applications, thiol-ene chemistry can be considered as more beneficial since dealing with heavy and toxic metal impurities is prevented by this approach [13]. These alternative 'click' reactions such as Diels-Alder cycloaddition and thiol-maleimide conjugation reaction have emerged and used as valuable tools in synthesis of functionalized macromolecules [19]. With Diels-Alder strategy, active double bond of maleimide moiety has been protected and then, site-specific and highly efficient attachment of thiol containing biomolecules can be achieved via Michael addition reaction (Figure 1.6).

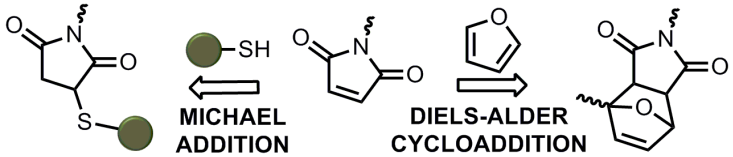

Figure 1.6. Possible 'Click' reactions of maleimide functionality.

1.3 Diels-Alder Reaction in Polymer Chemistry

Diels Alder [4+2] cycloaddition reaction is one of the well known methods in synthesis of polymers and other macromolecules. The Diels-Alder (DA) reaction occurs between an electron poor "dienophile" and an electron-rich "diene" to form a cyclic adduct (Figure 1.7). This reaction is mild-conditioning and high-yielding and no side products are observed. Furan and anthracene derivatives are mostly utilized as diene components. Due to their high reactivity and wide structural variability, maleimides are preferred as dienophiles. Also, maleimides are preferred for 'Click' conjugation strategies since they react not only with dienes via Diels-Alder strategy but also with thiols via Michael type thiol-ene reaction [20-21]. Thermoreversibility of Diels-Alder reaction is also an attractive concept in which formed cycloadduct is converted to the initial reactant via retro Diels-Alder (rDA) reaction.

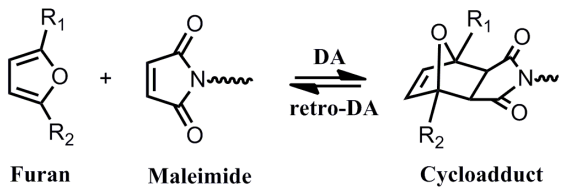

Figure 1.7. DA and retro DA reactions between maleimide and furan derivatives.

In polymer chemistry, DA reaction has been widely used in synthesis of macromolecules such as polymers, dendrimers and crosslinked structures. In literature, Gandini and his co-workers synthesized thermally reversible hydrogels by utilizing a furan functional styrene copolymer and a bismaleimide crosslinker. This study can be considered as the first example which illustrates the efficiency of Diels-Alder/retro Diels-Alder strategy in crosslinked systems [22]. In another example, novel thermosensitive hydrogels were synthesized by aqueous Diels–Alder reaction of between a furan functional acrylate based and a maleimide functional polyethylene glycol based polymer via Diels-Alder cycloaddition. Disassembly of the system occurred upon solvent and temperature variation via retro Diels-Alder reaction [23] (Figure 1.8).

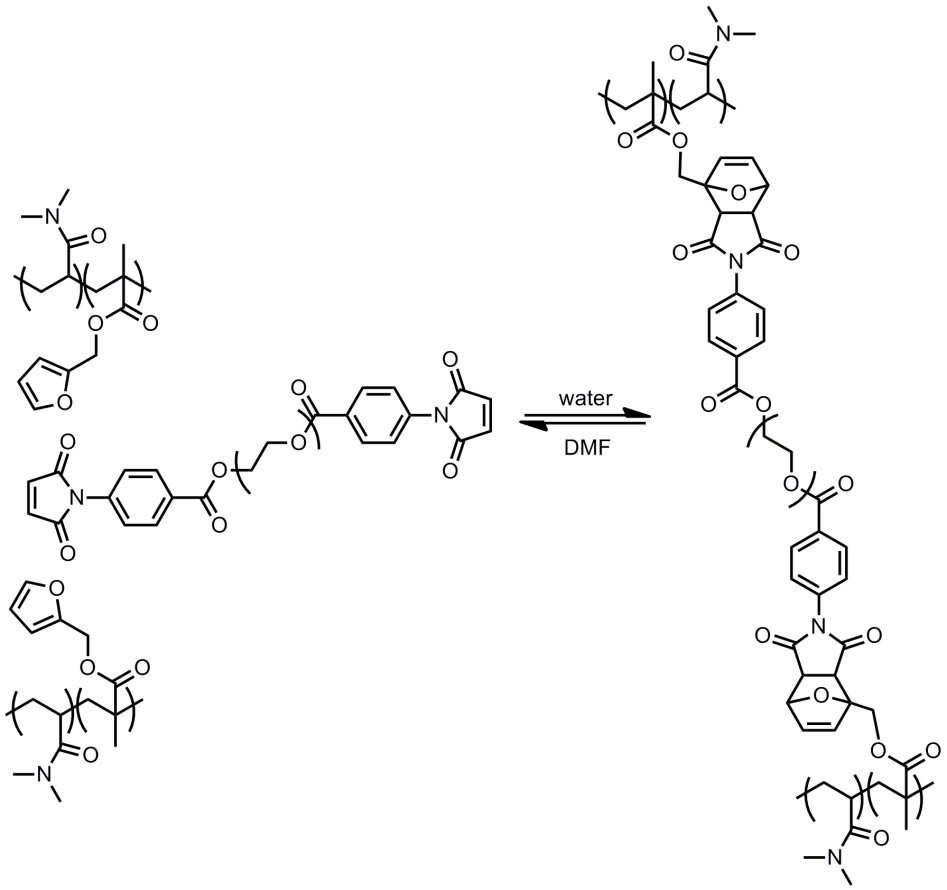

Figure 1.8. Thermosensitive hydrogels via DA/rDA strategy.

Previous work from our research group illustrates a new methodology for the synthesis of reactive polymers having maleimide units as their side chains. A novel acrylate based monomer was prepared and polymerized. Furan protected maleimide unit prevents a possible incorporation of active double bond to the polymer backbone. After

polymerization, maleimide functionalities were activated and furtherly functionalized with thiol containing molecules [24] (Figure 1.9).

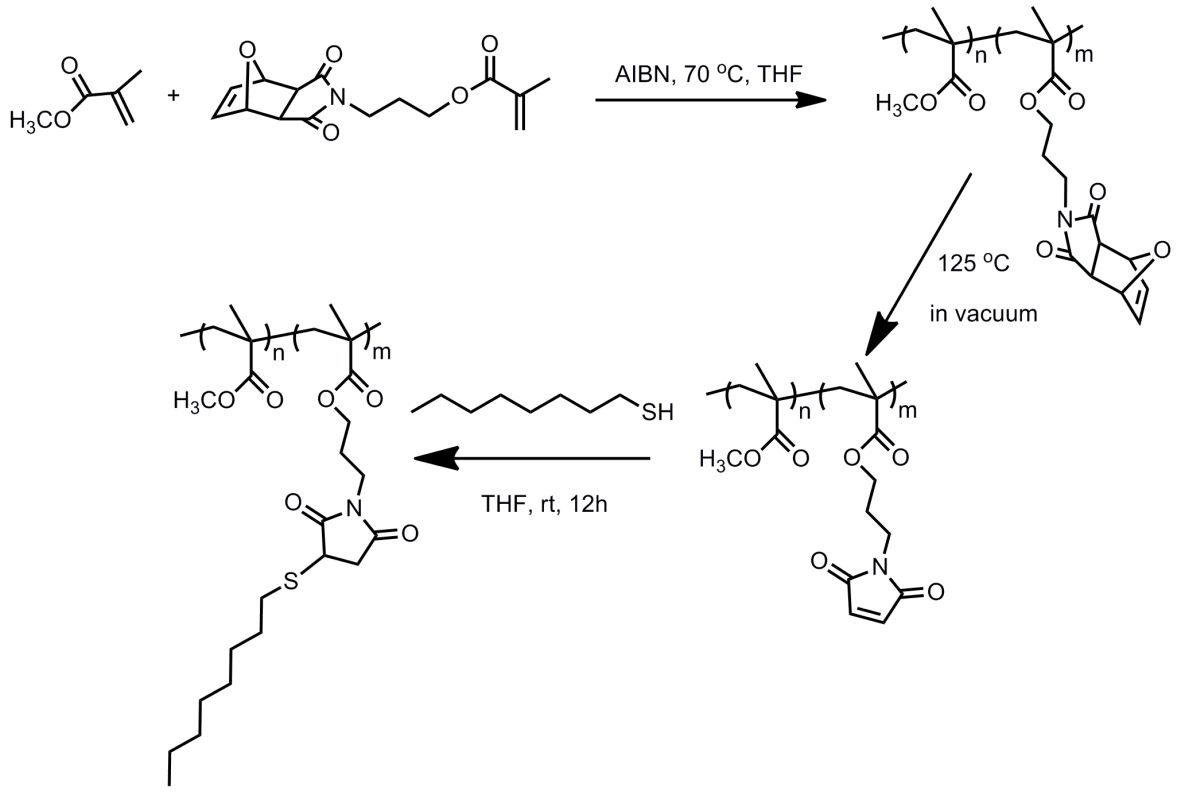

Figure 1.9. Synthesis and functionalization of a reactive copolymer via DA/rDA strategy.

1.4 Hydrogels

Hydrogels have gained a lot of attention in recent years due to their wide range of application areas including tissue engineering, biosensors, implant materials, bioimmobilization studies and drug delivery systems [25-26]. They are crosslinked polymeric networks and three dimensional structures with high swelling ability. A wide range of polymeric backbones such as poly (ethylene glycol), poly (glycolic acid), poly (lactide), poly (caprolactone) and chitosan can be considered as ideal materials for crosslinked systems [27]. However, among these PEG-based hydrogels have been extensively used thanks to the highly water-swellable, non-immunogenic and antibiofouling characteristics [28]. Hawker and his coworkers firstly synthesized well-

defined hydrogels by utilizing click reaction. Four armed PEG azide crosslinkers were prepared and reacted with PEG dialkyne via Huisgen type ‘Click’ reaction. Unreacted azide groups remained available for further functionalizations [29] (Figure 1.10).

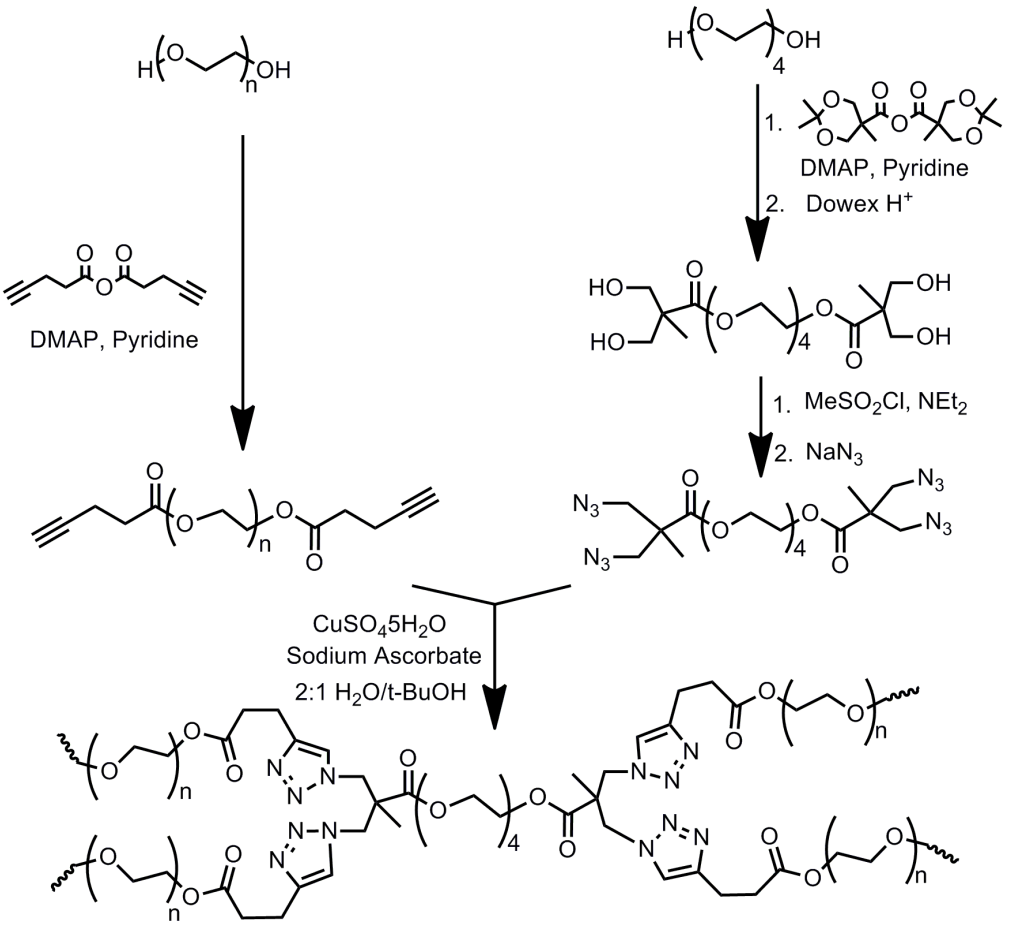

Figure 1.10. Synthesis of PEG based hydrogels via Huisgen ‘Click’ reaction.

Our research group also used ‘click’ reaction between polyester dendrons and PEG bisazides to form dendron-polymer-dendron conjugates. Hydroxyl groups at the surface of dendron were functionalized again with alkyne groups and that copolymer was reacted with TEG bisazide to form the hydrogel. Then, some of the remaining alkyne groups allow further functionalization of this gel with different biomolecules. By changing copolymer to TEG crosslinker ratio, number of remaining free functionalities after the gelation can be calculated. Functionalization studies were performed according to this correlation between the gels [30] (Figure 1.11).

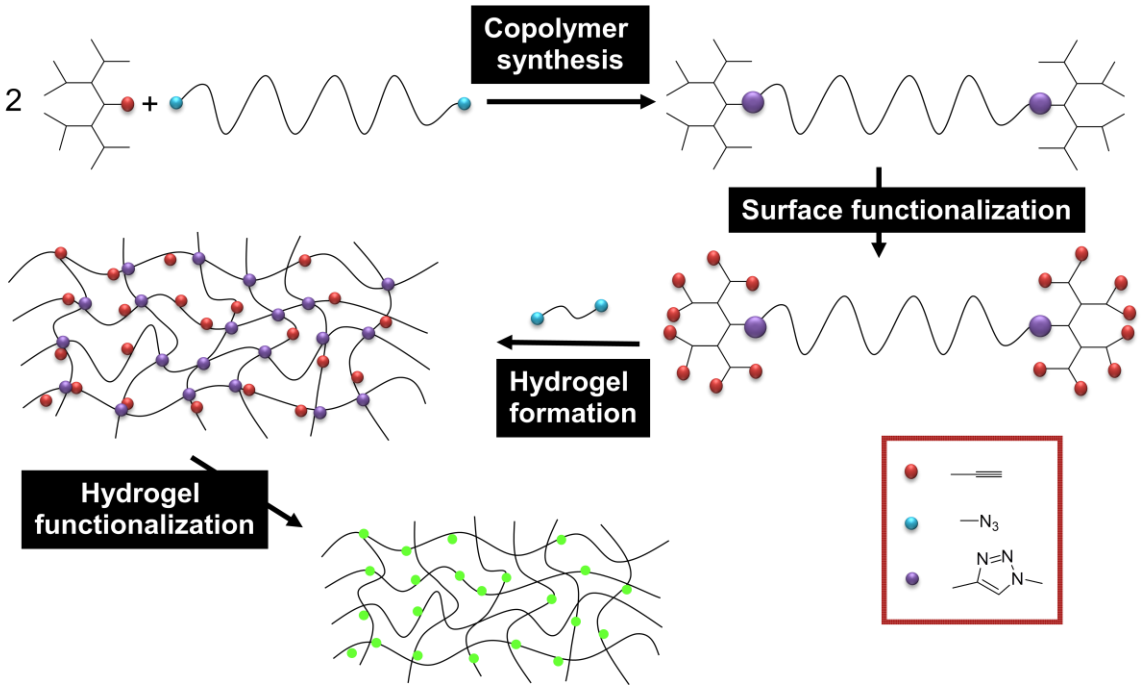

Figure 1.11. Hydrogel formation via 'Click' reaction of Dendron-Polymer Conjugates.

Functionalization of hydrogel is achieved via covalent or non-covalent attachment. For applications like bioimmobilization, controlled drug delivery and protein delivery for tissue engineering, covalent attachment techniques are preferred to ensure control over attachment [31]. Hydrogels can be utilized in such applications due to their capability of encapsulating various biomolecules in the interior matrix. They can exhibit controlled interactions between cells and proteins and slow release of drug molecules from the hydrogel matrix becomes possible in tissue engineering scaffolds. For immobilization of biomolecules, maleimide-thiol coupling chemistry is an attractive methodology since many biomolecules contain thiol containing cysteine residues or they can bind to cysteine residues at specific sites. Due to the thiol functionalities on these residues, they can undergo facile conjugations with maleimides, vinyl sulfones, acetamides, disulfides etc. Especially, maleimide containing macromolecules is widely used in biomolecular immobilizations due to its latent reactive character. With Diels-Alder protection of this unit, active double bond does not participate to the polymerization or gelation process but lately can be activated for further conjugations. Recently, our group shows the fabrication of maleimide containing anti-biofouling hydrogels and these hydrogels are amenable to site-specific thiol conjugations. In this work, novel hydrogels were synthesized via

copolymerizing a furan protected maleimide based methacrylate monomer with PEGMA. Some of the maleimides undergo retro Diels-Alder reaction and acts as a crosslinker for gelation. After that, remaining free maleimides were activated and functionalized with thiol containing dyes and enzymes. Effect of temperature and feed ratio on these gels were investigated [32] (Figure 1.12).

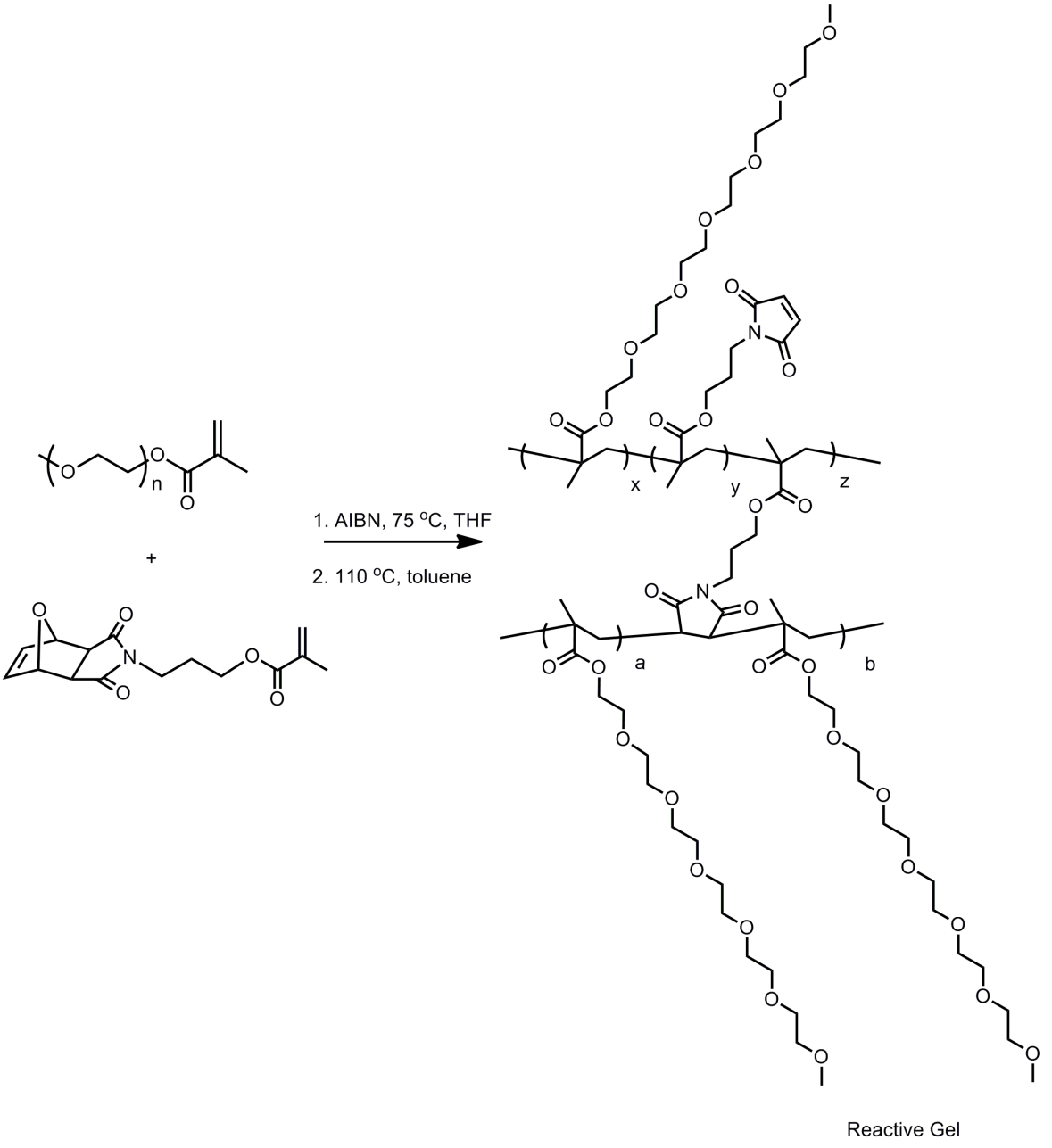

Figure 1.12. Synthesis of thiol reactive hydrogels.

1.5. Biodegradable Polymers

Conventional polymers such as polyethylene and polypropylene persist for many years after their disposal. However, biodegradable polymers can degrade in bioactive environments by the enzymatic action of microorganisms such as bacteria, fungi, and algae. Their polymer chains may also be broken down by nonenzymatic processes such as chemical hydrolysis (Figure 1.13). Biodegradation converts them to CO_2, CH_4, water and other natural substances so that environmental damage is completely removed [33].

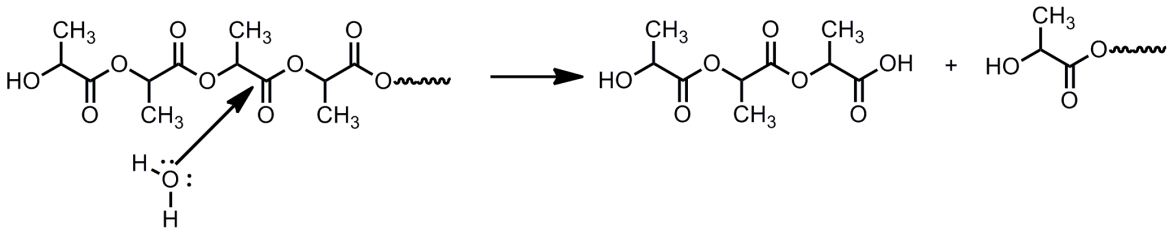

Figure 1.13. Hydrolysis and cleavage of ester linkage.

Natural and synthetic polymers can be classified as biodegradable polymers. Natural biodegradable polymers are produced from renewable resources such as plants, microorganisms and animals. They can be synthesized by chain growth polymerization catalyzed by various enzymes. Activated monomers are mostly produced by complicated metabolic processes in cells. Microorganisms are able to produce the more widespread natural biodegradable polymers such as polyesters, polysaccharides, proteins. Hydrolysis and enzymatic cleavage are most predominant degradation pathways. In case of synthetic biodegradable polymers, the attractive feature of them is the ability to modify their properties by tailoring appropriate monomers and altering synthetic protocols. Novel biodegradable polymers can be obtained by controlling specific properties and functionalities. These adaptable properties such as hydrophobicity, crystallinity, degradability, solubility and mechanical- thermal features extend application areas of synthetic biodegradable polymers (Figure 1.14) [34] .

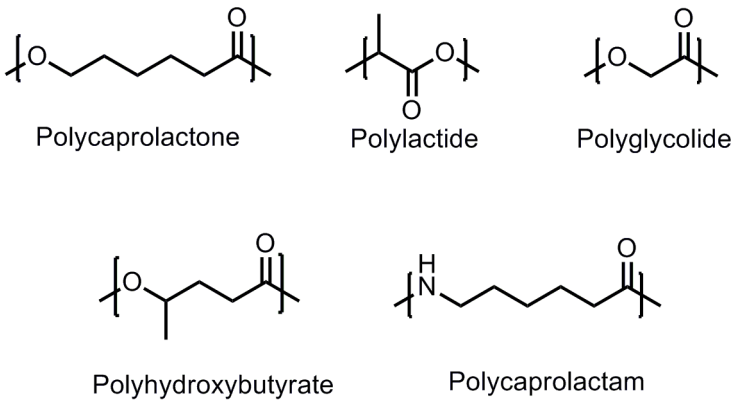

Figure 1.14. Common synthetic biodegradable polymers.

These types of synthetic polymers are environmental friendly alternatives to chemical industry when compared with other polymeric systems. Moreover, non-toxic degradation byproducts allow the use of biodegradable polymers towards several applications. For instance, in tissue engineering scaffolds, this type of polymers can be used for the attachment of the drug molecule. It encourages growth of the regenerated tissue and then slowly degrades. Also for drug delivery systems, biodegradable materials will allow the material to stay in the body and then be degraded slowly over time without needing a second surgery to remove them, when they are used as sutures and vascular stents (Figure 1.15) [35].

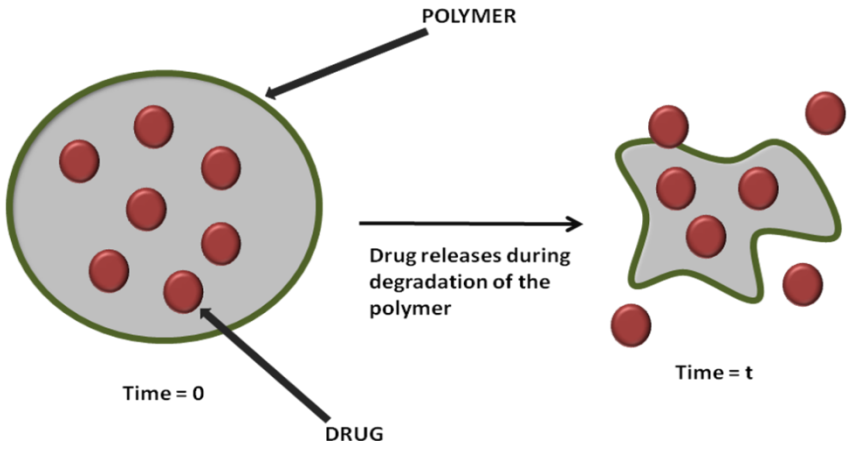

Figure 1.15. Schematic representation of drug delivery via biodegradable polymers.

1.6. Ring Opening Polymerization (ROP)

For the design of nanotechnological materials used in microelectronics or drug delivery systems, control over the macromolecular architecture of a polymer is necessary. Ring-opening polymerization (ROP) of cyclic esters is a common method to synthesize polyesters with controlled properties. Predictable molecular weights, low polydispersity indices and high end group fidelity can be achieved by ring opening polymerization (ROP) technique [36]. Cyclic esters such as caprolactone, lactide, lactam etc. are most common monomers utilized in ring opening polymerization (Figure 1.16).

The polymerizability of a cyclic monomer depends on both thermodynamic and kinetic factors. Kinetically, polymerization requires that there will be a possible mechanism for the ring to open. In the presence of a heteroatom in the ring, it provides a site for nucleophilic or electrophilic attack by the initiator which results in an initiation and then, a propogation step. However, the most important factor of a ring opening mechanism to occur is the thermodynamic factor which depends on the relative stability of the cyclic monomer. 3- and 4-membered rings are highly strained and have a large exothermic enthalpy. In these cases, enthalpy is the major factor in determining the free energy of polymerization. The large enthalpy (negative) ensures that the equilibrium between monomer and product and favors the product [37].

A suitable catalyst system is needed to obtain polymers with controlled properties via ROP technique. These catalytic systems are named as organometallic and organocatalytic ROP systems. In organometallic catalytic system, transition metal complexes are utilized as catalysts. The most common complex in organometallic ROP is tin (II) octanoate [$Sn(Oct)_2$] which is commercially available, easy to handle, and soluble in most common organic solvents [38] (Figure 1.17).

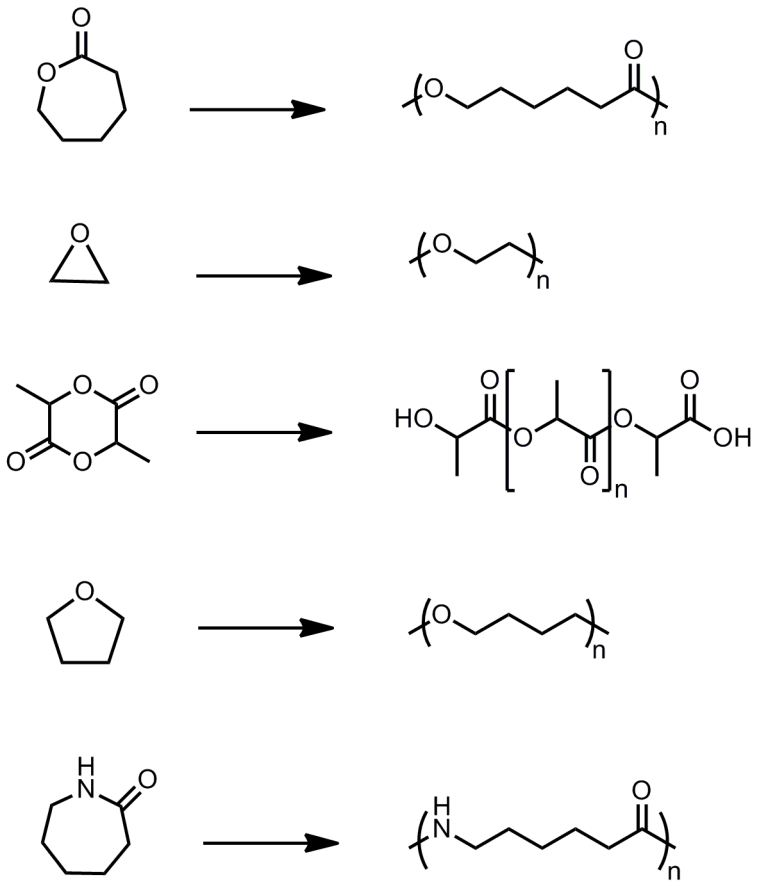

Figure 1.16. Common monomers used in ROP.

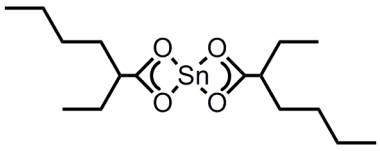

Figure 1.17. Structure of $Sn(Oct)_2$.

Although organometallic techniques polymerize cyclic monomers successfully, undesired contaminants such as toxic heavy metal ions may cause difficulties in pharmaceutical applications or environmental problems. To inhibit these kind of problems, alternative pathways have been investigated by researchers such as organocatalytic ROP systems which require organic molecules to be utilized as catalysts. Superbases, N-heterocyclic carbenes or bifunctional thiourea-amines can be used for this purpose (Figure 1.18) [39].

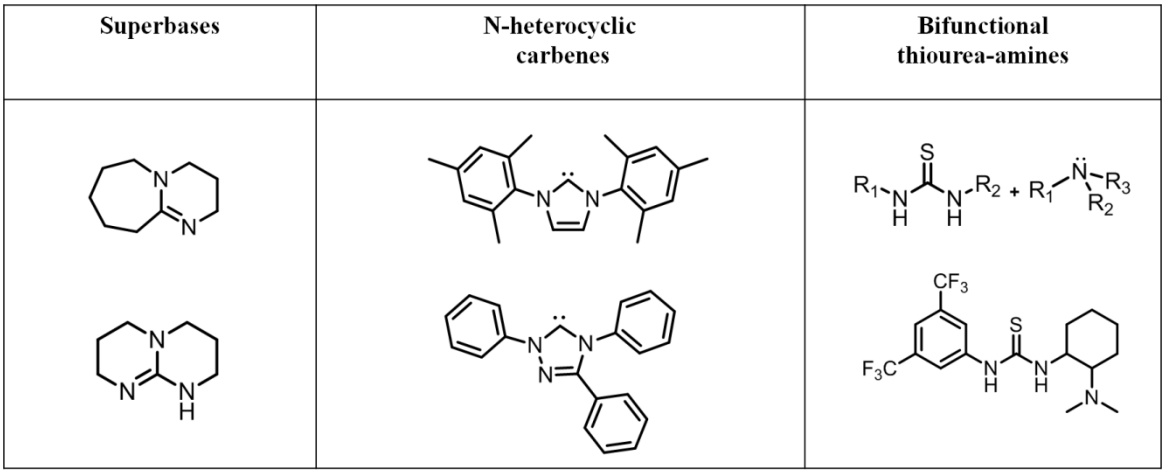

Figure 1.18 Organocatalytic ROP catalysts.

Organocatalytic System is based on the activation of monomer or initiator, or both, with the help of H-bonding. Recently, an alternative pathway has been developed for the ROP of cyclic esters through bifunctional thiourea-amines. In this system, carbonyl group of a lactide monomer is activated toward electrophilic attack by the thiourea via hydrogen bonding and the initiating/propagating alcohol is activated as nucleophiles by the tertiary amine (Figure 1.19) [40].

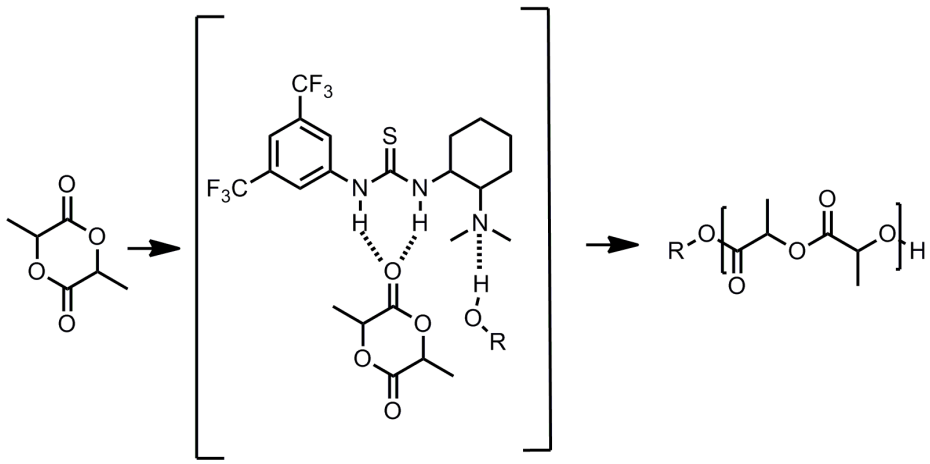

Figure 1.19. ROP of lactide via dual activation by a thiourea-tertiary amine catalyst system.

1.6.1. Reactive Polymers via organocatalytic ring opening polymerization (ROP)

Novel reactive polymers and their post-functionalization properties have been investigated by many groups and advantages of these polymers in medical applications became a reality in recent years. Especially, polymers having polyester or polycarbonate type of backbone have been studied extensively due to their excellent biodegradability. Control over the physical properties of the polymer and addition of biologically active molecules have been achieved via manipulation of pendant functionalities on these type of polymer backbones.

Aliphatic polyesters formed via ring opening polymerization (ROP) of lactide and lactone are multi-purpose polymers which have fine mechanical properties, hydrolyzability and biocompability so that they become attractive candidates for various applications such as biomedicine, microelectronics and drug delivery [41]. Ring opening polymerization of cyclic esters can simply provide these polyesters by controlling the molecular weight, polydispersity and end group fidelity [42]. Poly (lactic acid), PLA, has a leading position between these aliphatic polyesters due to its excellent biodegradability, biocompability and availibility from inexpensive and renewable sources [43]. With the help of the suitable catalyst for ROP of lactide, molecular and physical properties of PLA's can be controlled considerably [44-45]. However for further developments, creating functional group tolerant PLA polymeric systems is highly required. Also, polycarbonates are important polymeric materials which are widely used in pharmaceutical applications because of their high level of biocompatibility and biodegradability. By utilizing reactive functionalities on the polymer backbone, conjugation with different biomolecules becomes possible and physical properties can be altered. Two main strategies are mostly used in the synthesis of polycarbonates. In one of them, CO_2/epoxide copolymerization technique has been reported while in the second one; ring opening polymerization (ROP) of six membered cyclic carbonates allows to achieve polycarbonate structure [46-47].

Dove and his co-workers recently introduced well-defined allyl-functional polycarbonates via the organocatalytic ring-opening polymerization of an allyl ester-functional cyclic carbonate monomer utilizing the thiourea-sparteine catalyst system. The allyl-functional poly(carbonate)s were obtained showed low polydispersities and high end-

group fidelity. Postpolymerization functionalization were demonstrated via thiol-ene addition to the pendant allyl groups with different thiols under mild conditions [48] (Figure 1.13).

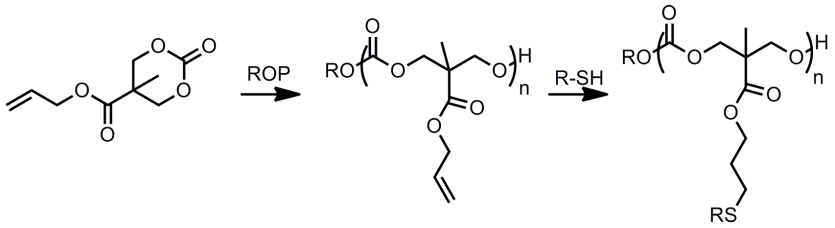

Figure 1.20. Illustration of synthesis and functionalization of allyl-functional cyclic carbonate.

In another study of Dove's group, maleimide functional polyesters were synthesized with organocatalytic ROP mechanism. These polymers can selectively target cysteine residues in proteins and enzymes. With this study, efficiency of maleimide-thiol chemistry has been proved and functionalized polymers were obtained in excellent yields without degradation of the sensitive backbone [36] (Figure 1.21).

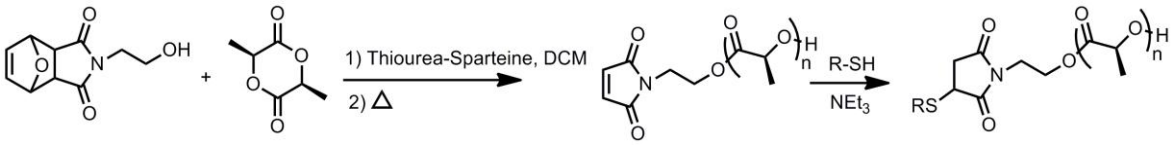

Figure 1.21. Synthesis of and Michael type thiol-ene conjugation maleimide functional PLA.

2. AIM OF THE STUDY

2.1 Thiol Reactive Hydrogels via Orthogonally Clickable Dendrons

Michael type 'Click' Chemistry is highly preferrable due to the site-specific, reagent-free binding capability of maleimide and thiol functionalities. However, a protection–deprotection strategy to the active double bond of maleimide unit using retro Diels-Alder reaction should be carried out in order to inhibit any possible side reactions. Herein, we describe a novel methodology to synthesize thiol reactive hydrogels from orthogonally reactive and biodegradable dendrons. Because of the highly monodisperse character of dendritic structure, homogeneity all over the matrix of the hydrogel is achieved. Poly(ethylene glycol) bisazide behaves like a crosslinker and an antibiofouling agent which forms the hydrogel via Huisgen type 'Click' cycloaddition. Masked maleimide functional hydrogel is activated via retro Diels-Alder strategy. Conjugation and bioimmobilization studies were carried out utilizing various thiol containing molecules (Figure 2.1). Degree of bioimmobilization is investigated by controlling the density of maleimide functionality within the gel matrix.

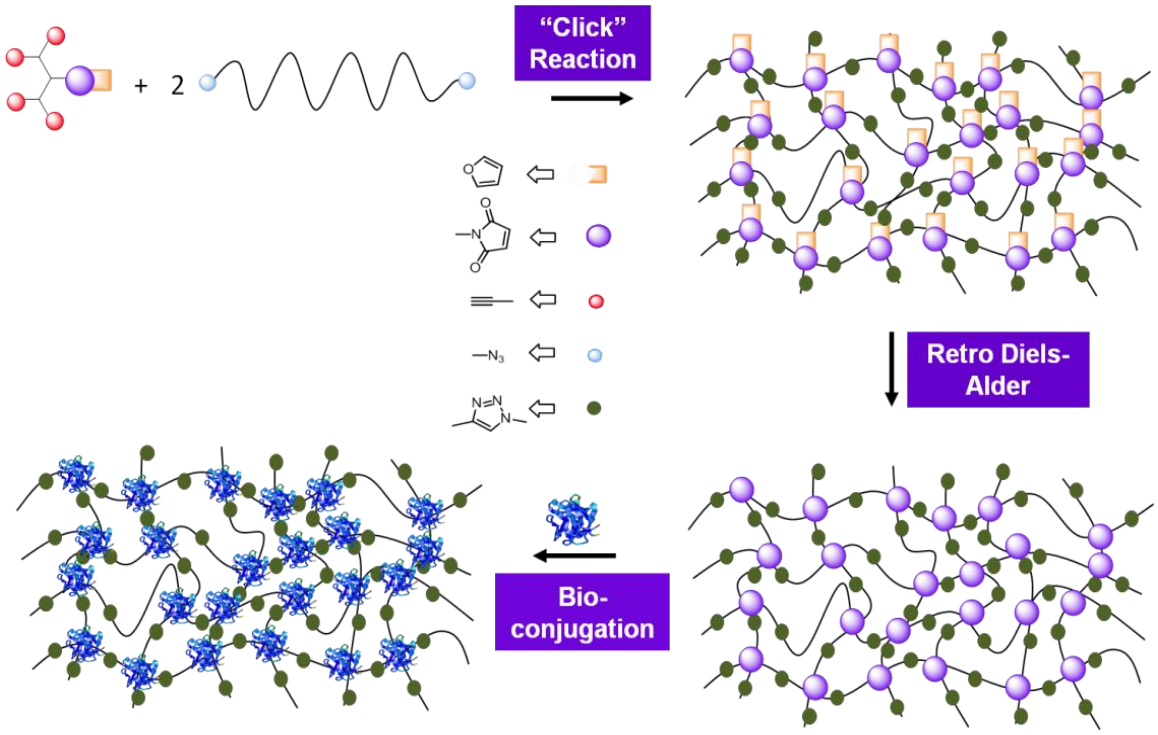

Figure 2.1. Synthetic approach towards reactive hydrogels using dendritic constructs.

2.2. Biodegradable and Thiol Reactive Polymers

Many polymers having maleimide unit as a core or side-chain functionality have been synthesized due to its effective conjugation facility for biological applications. In this study, we describe a novel strategy to synthesize thiol reactive biodegradable polyesters via utilization of a masked maleimide containing carbonate monomer. Different homo-and copolymers having maleimide groups at their side chains were synthesized by ring opening mechanism of this novel cyclic carbonate monomer and L-lactide. The polymers obtained were heated to unmask the furan protected maleimide groups to their reactive forms by the elimination of furan via the retro Diels-Alder reaction. Thereafter, biodegradable polymers containing maleimide pendant groups were subjected to conjugation by thiol containing molecules.

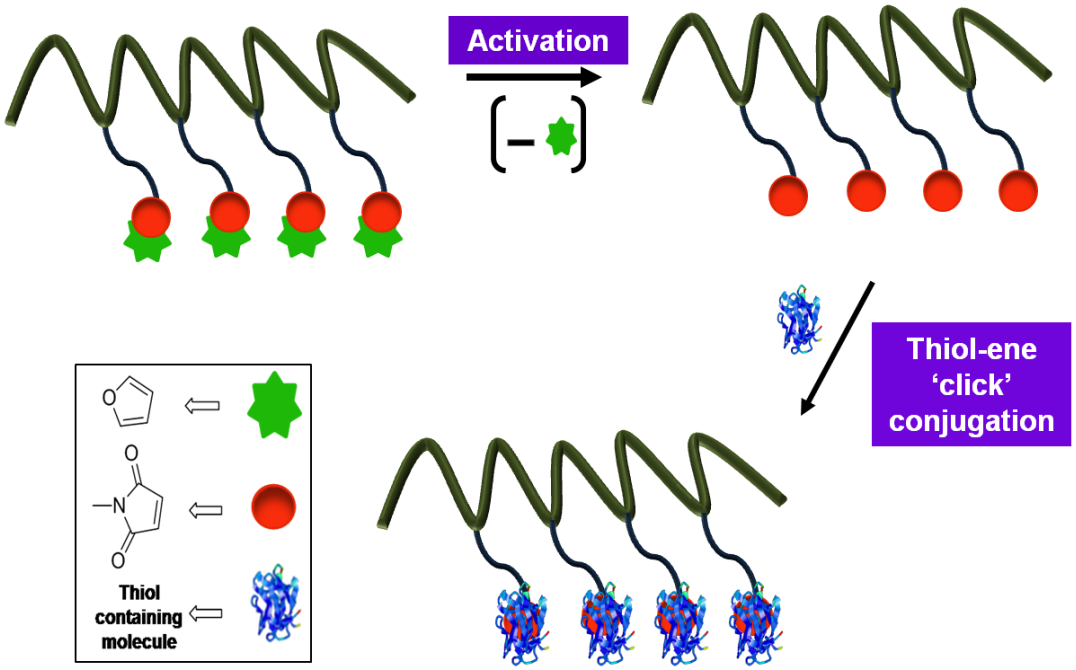

Figure 2.2. Synthetic approach towards biodegradable and multifunctional polymers via Michel type 'Click' conjugation.

3. RESULTS AND DISCUSSION

3.1 Thiol Reactive Hydrogels via Orthogonally Clickable Dendrons

3.1.1. Synthesis and Characterization

Masked maleimide functional and biodegradable G2 alkyne polyester dendron 3 was synthesized according to our previously reported procedure [49] (Figure 3.1).

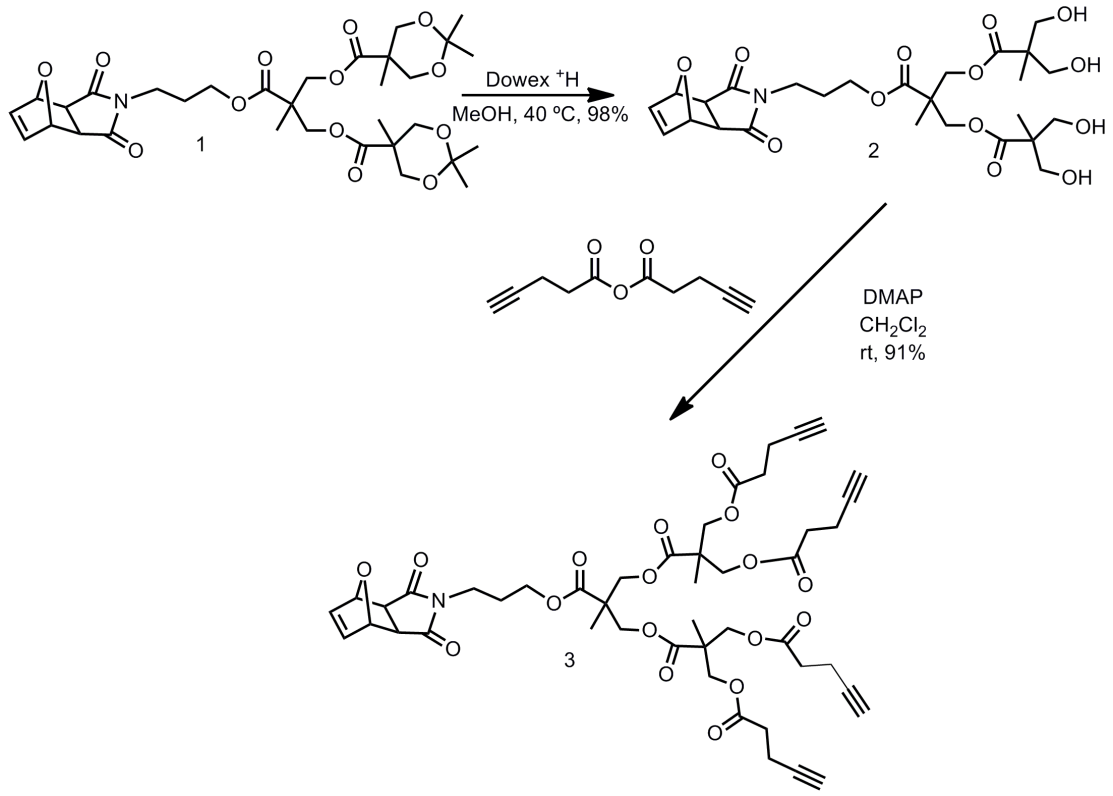

Figure 3.1. Overall Synthesis masked maleimide functional G2 alkyne dendron.

Dendron 3 has a unique character due to the multiple alkyne functionalities at its periphery and a latent reactive maleimide functionality as its core. Orthogonal reactivity of this dendron has been demonstrated via hydrogel formation from its end groups with the help of Huisgen type ‘click’ cycloaddition with azide functionalized linear PEGs. Unmasking of maleimide groups were achieved via retro Diels-Alder (Figure 3.2).

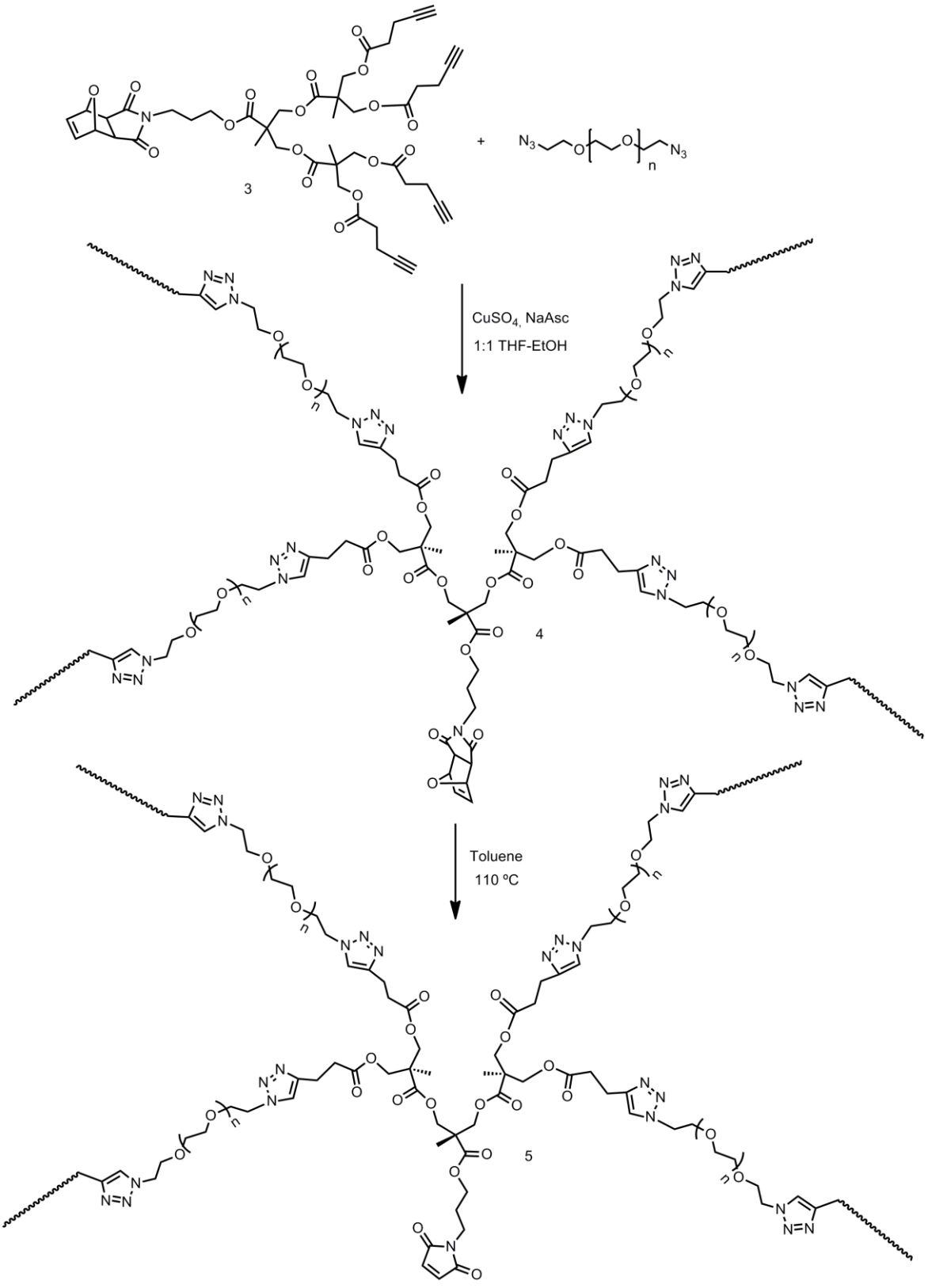

Figure 3.2. Synthesis of hydrogels.

After retro Diels-Alder reaction, reactive maleimide units were derivatized with thiol containing molecules under reagent-free and mild conditions of Michael addition reaction. The extent of functionalization can be tailored due to the varying maleimide densities in different hydrogels. Thanks to the monodispersity of dendritic structure, more homogeneous hydrogel matrixes were obtained. To prevent [3+2] dipolar cycloaddition reaction between active double bond of maleimide and azide unit under appropriate temperatures, masked maleimide units of dendron 3 was not activated prior to gelations. Five series of hydrogels were synthesized in order to investigate properties of hydrogels with variations in PEG chain length and temperature. These properties were summarized in Table 3.1 and observations are discussed thereafter.

Table 3.1. Properties of hydrogels with variations in PEG lengths and Temperature.

Item	Hydrogels[a]	Mwt of PEG	Furan (%) observed[b]	Furan (%) theoretical[c]	% Gel Conversion[d] (50 °C)	% Gel Conversion[d] (25 °C)
1	H1	10 000	0.39	0.34	96	62
2	H2	8000	0.43	0.44	91	70
3	H3	6000	0.51	0.63	84	71
4	H4	4000	0.66	0.87	86	73
5	H5	2000	1.43	1.59	85	72

[a]Reaction conditions: 1:1 alkyne:azide ratio

[b]Calculated from the amount of furan released as observed in TGA thermograms (wt %)

[c]Calculated based upon mole ratio of furan unit present in the dry and purified hydrogel

[d]Gel conversion = (dry gel weight/total weight of all monomers) / 100.

3.1.2. Effect of temperature on gelation

A temperature increase during gelation results an increase in the rate of reaction and also in conversion. Gelations occurred faster at 50 ºC and higher gel contents were obtained. From Table 1, it can be seen that 96% conversion was achieved for H1 after 3 h only. However, at 25 ºC, last conversion obtained was still 62% after 24 h of reaction time.

3.1.3. Effect of masked maleimide density within the gel

Furan amount in an hydrogel matrix can be calculated by using thermogravimetric analysis (TGA). Due to the removal of furan moieties, between 60 °C - 180 °C, a remarkable weight loss can be observed in the thermogram. However, after the retro Diels-Alder step, because all the furan moieties were already removed, no significant weight loss was investigated in the thermogram between previously mentioned temperatures (Figure 3.3).

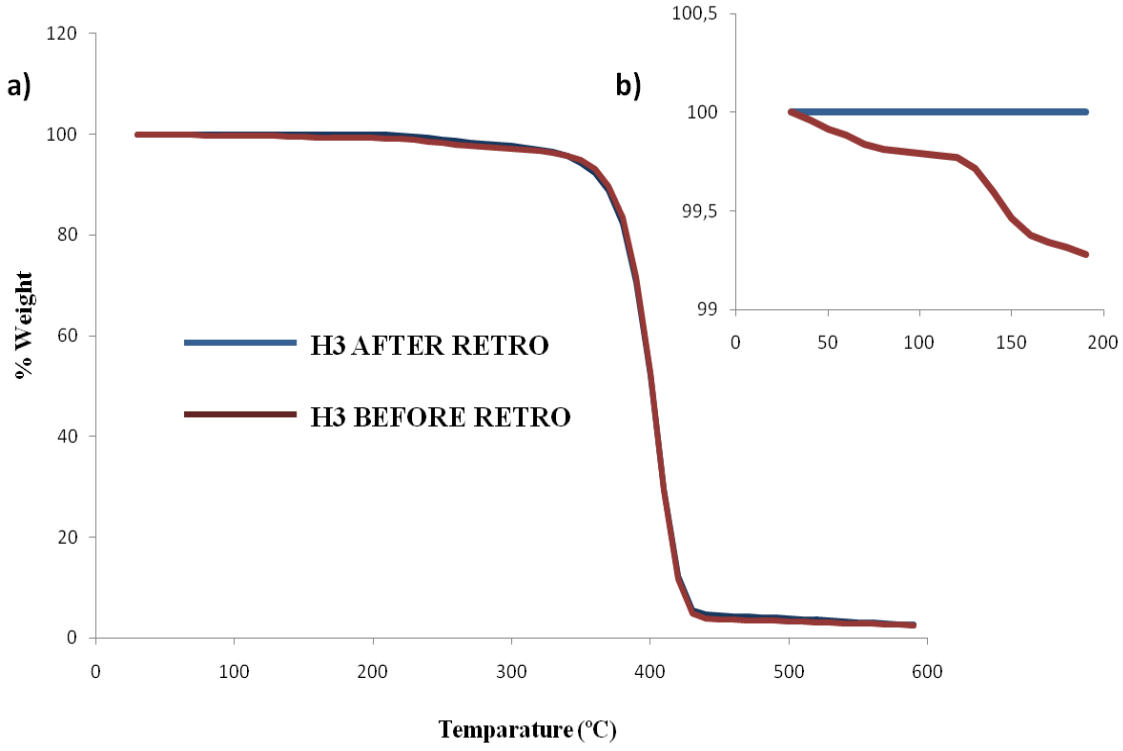

Figure 3.3. TGA thermograms of the hydrogel H3 before and after retro Diels-Alder step between (a) 0 ºC – 600 ºC. (b) 0 ºC – 180 ºC.

The amount of maleimide units within the gels can be probed also using TGA instrument. PEG2K hydrogel H5 has the largest weight loss between 60 °C - 180 °C due to the highest maleimide density in its structure (1.43%). A reasonable trend can be observed

between maleimide percentage and weight loss of different hydrogels. This thermogram illustrates various amounts of incorporated maleimide functionality into the hydrogels (Figure 3.4).

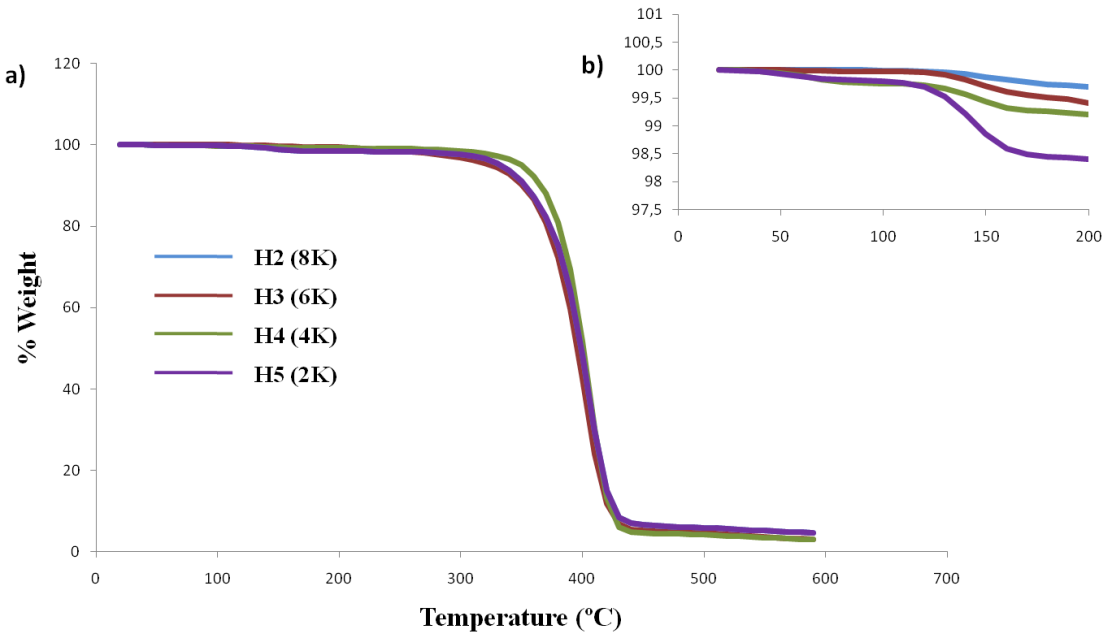

Figure 3.4. TGA thermograms of the hydrogels (H2 - H5) containing different maleimide percentages between (a) 0 ºC – 600 ºC. (b) 0 ºC – 200 ºC.

3.1.4. Swelling Studies

Swelling behavior of the hydrogels were investigated by calculating water uptake percentage as a function of time until an equilibrium condition is observed. It has been demonstrated that water uptake of the hydrogel increases as hydrophilic PEG chain length increases. As demonstrared in Figure 3.5, H5 has the least swelling ability due to the shorter hydrophilic polymer matrix which results in more compact structure. Percentage of water uptake increases as polymer length increses from 2000 Da to 10 000 Da and an expected trend is obtained. (Figure 3.5).

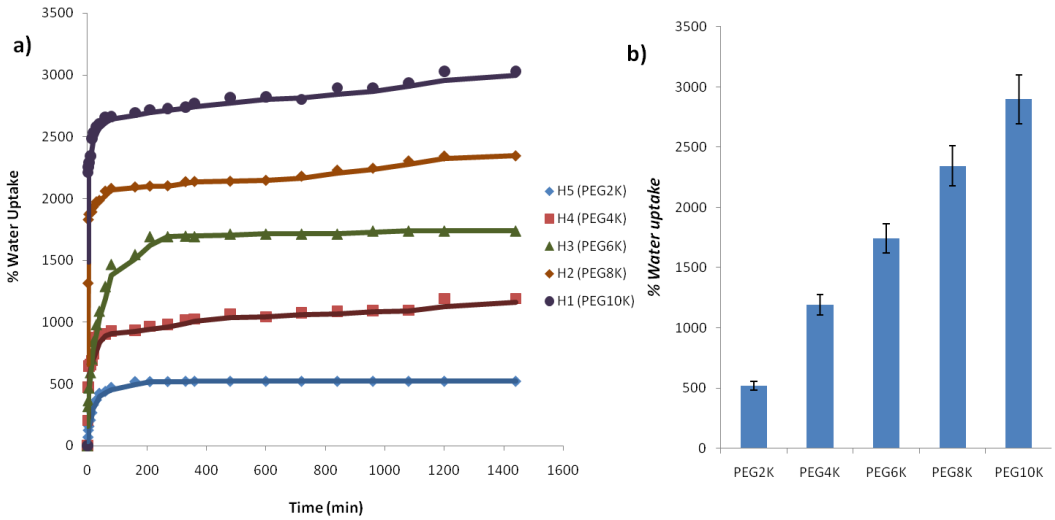

Figure 3.5. (a) Effect of PEG chain length on degree of swelling. (b)Relative swelling capacities of hydrogels.

3.1.5. Scanning electron microscopy

All hydrogelations were done by using different PEG diazides having various molecular weights. Surface morphology of these hydrogels were investigated via Scanning Electron Microscopy (SEM). Poly (ethylene glycol) polymers which have smaller molecular weights and shorter chain lengths give densely crosslinked and compact structures. Smaller pores and densely packed image of PEG2K hydrogel H5 demonstrates the proof of this assumption. In the same manner, PEG8K hydrogel H2 shows larger pores and less densely packed structure in its ESEM image (Figure 3.6). This result agrees with the previously mentioned swelling characteristics of hydrogels. Hydrogels having large pores in their morphology show higher swelling capacities.

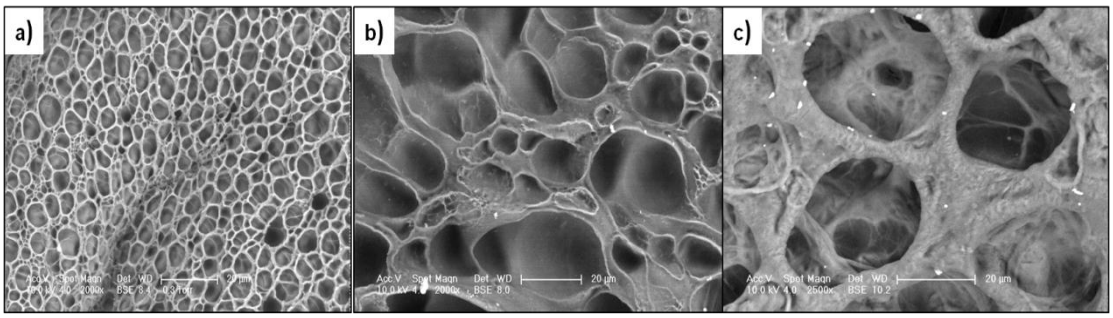

Figure 3.6. Representative SEM micrographs of hydrogels (a) H5, (b) H3 and (c) H2. Image scale bars = 20 μm.

3.1.6. Functionalization of Hydrogels

The functionalization efficiency of hydrogels were first investigated through functionalization of a thiol containing fluorescent dye, BodipyC10SH. Hydrogel H1 was left in BodipyC10SH solution and then washed with excess THF to remove unbound dye from the surface of the hydrogel. Efficiency of the functionalization and Michael type addition of thiol to the active maleimide unit was proved with highly green fluorescent image of hydrogel-dye conjugate (Figure 3.7). Five series of hydrogels containing different maleimide densities were reacted with biotin thiol. After washing with methanol to get rid of unbound biotin, hydrogels were incubated with Flourescein isothiocynate labeled Streptavidin which gives the green color on fluorescent images. Extent of the immobilization was examined after washing off physiabsorbed Streptavidin with water.

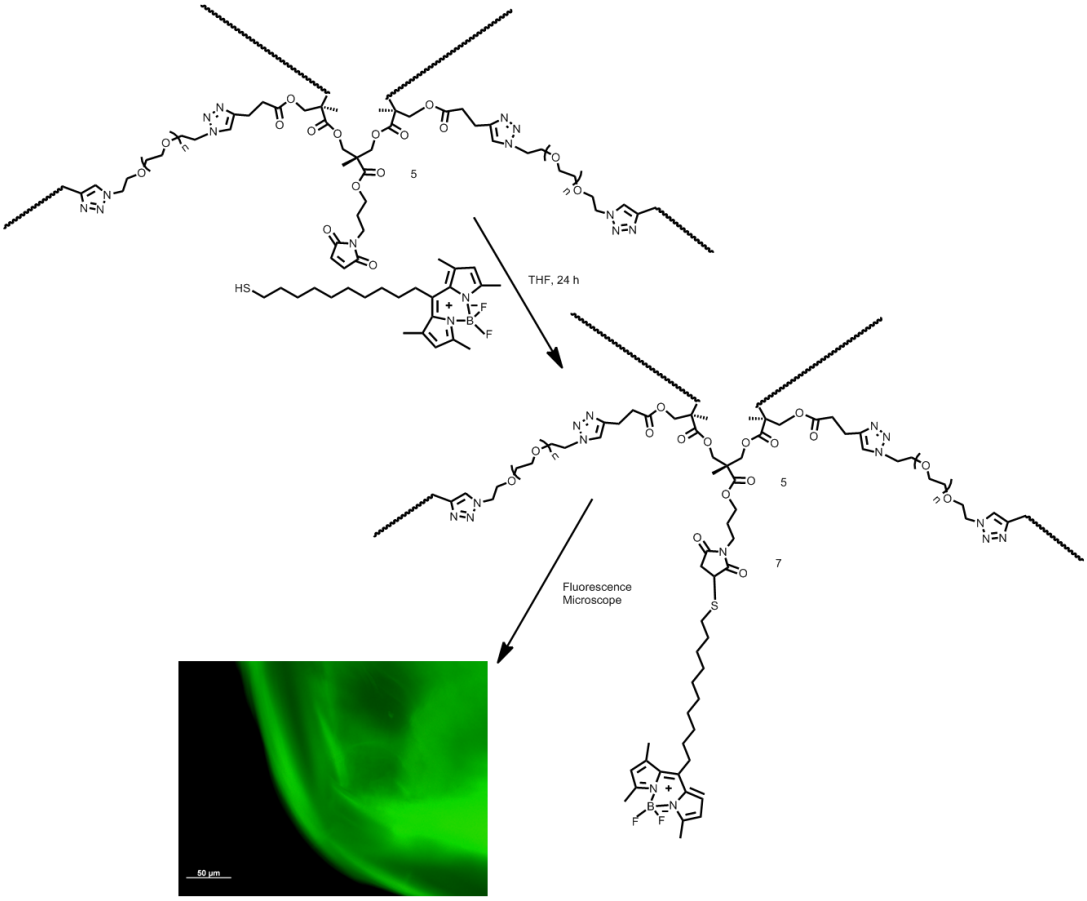

Figure 3.7. Functionalization of the hydrogel with fluorescent dye BODIPYC10SH and Fluorescence Microscopy Image of hydrogel - dye conjugate.

Bioimmobilization capability of hydrogels with enzymes was examined by utilizing a thiol containing biotin derivative (biotinylated (triethylene glycol) undecene thiol) for covalent attachment and Streptavidin as an enzyme for immobilization (Figure 3.8).

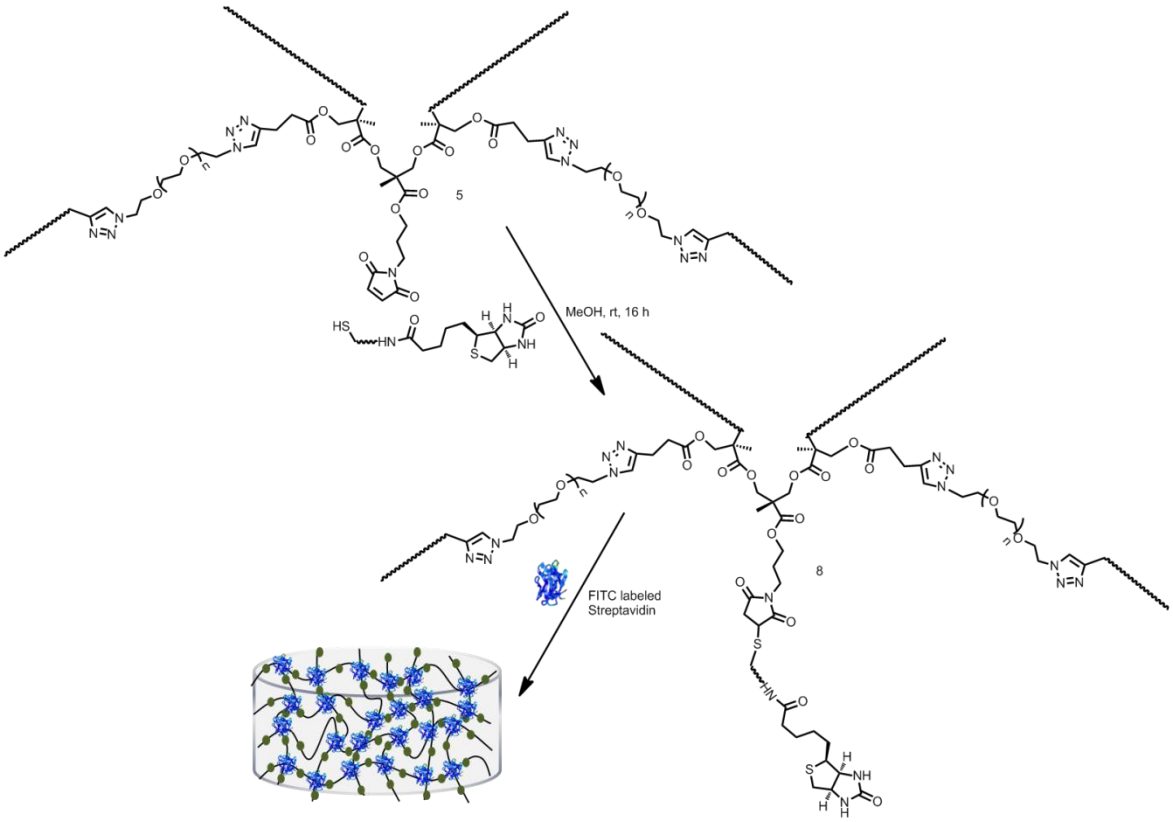

Figure 3.8. Covalent biotinylation and FITC-labeled Streptavidin immobilization on hydrogels.

Fluorescence images demonstrate that hydrogels having higher maleimide amount, have more intense fluorescence profile. Higher maleimide density in gel matrix indicates higher amount of covalently bound biotin ligand and also, more efficient immobilization of streptavidin. So, with lower immobilization of Streptavidin as in the case of H1, hydrogels give less intense fluorescence. As a control, gels which are not biotinylated were used. These controls were exposed to FITC-labeled Streptavidin and washed exactly like biotinylated gels. As expected, gels which are not biotinylated show any significant fluorescence unlike the biotinylated ones. This result indicates that streptavidin is immobilized to the gel through covalently bound ligand biotin and PEG chains serve as an antibiofouling matrix that inhibits non-specific adsorption of the enzyme to some extent.

Intensity profiles of the gels give an expected trend and proves the correlation between the maleimide density and extent of immobilization (Figure 3.9).

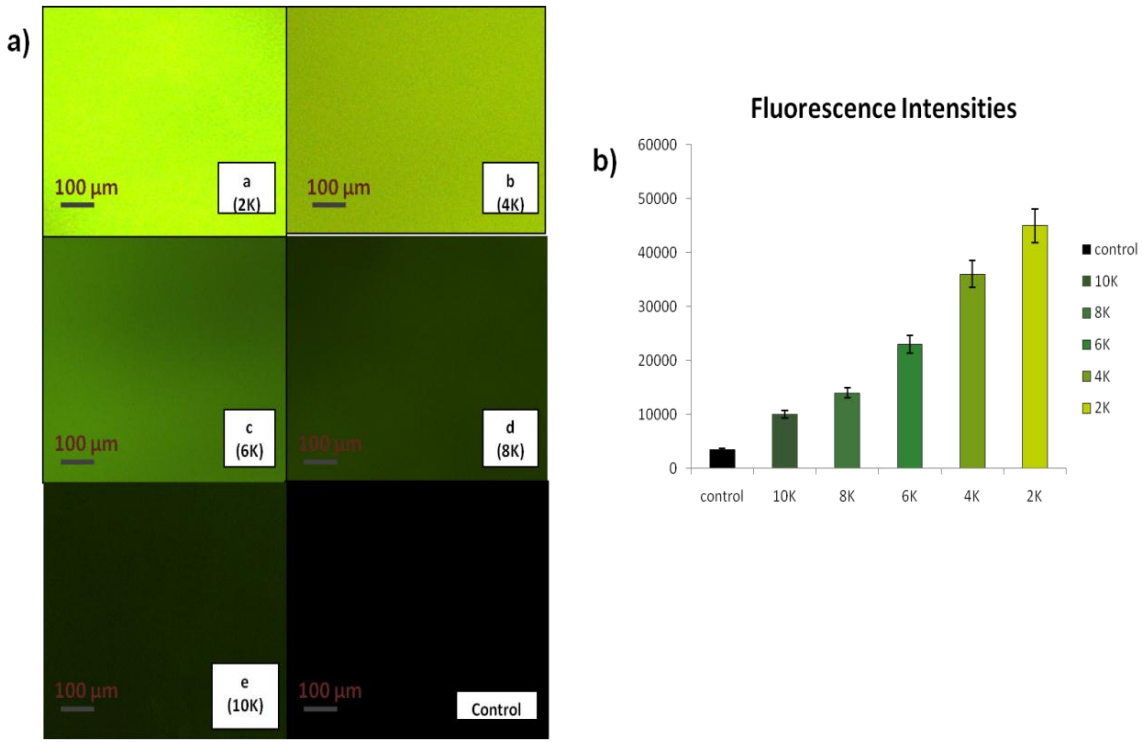

Figure 3.9. (a) Fluorescence microscope images after functionalization with Streptavidin a) H5, b) H4, c) H3, d) H2, e) H1 and control (gel without biotinylation). (b) Fluorescence intensity graph of enzyme immobilized gels and control gel without biotinylation.

3.1.7. Reason for using a masked maleimide group prior to gelation

Protection of maleimide unit with Diels-Alder strategy prior to gelation is necessary in order to prevent a possible cycloaddition of azide functionality to the reactive double bond of maleimide at the focal point of the dendron around 50 ^{o}C. To support this assumption, a control experiment was carried out in which N-Ethylmaleimide reacts with $PEG_{750}N_3$ at 50 ºC (Figure 3.10). From the ^{1}H NMR results, two doublets coming from bridge protons of triazole ring are easily assignable. These peaks appear nearly 4.60 and 5.50 ppm and have exactly 11 Hz coupling constant which agrees with the literature [50] (Figure 3.11).

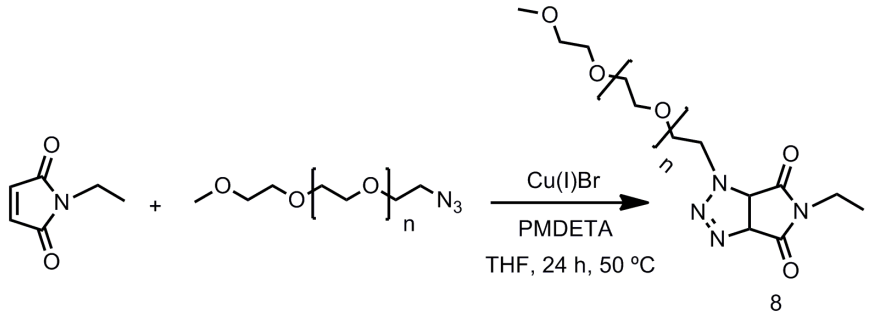

Figure 3.10. Azide cycloaddition to N-Ethylmaleimide.

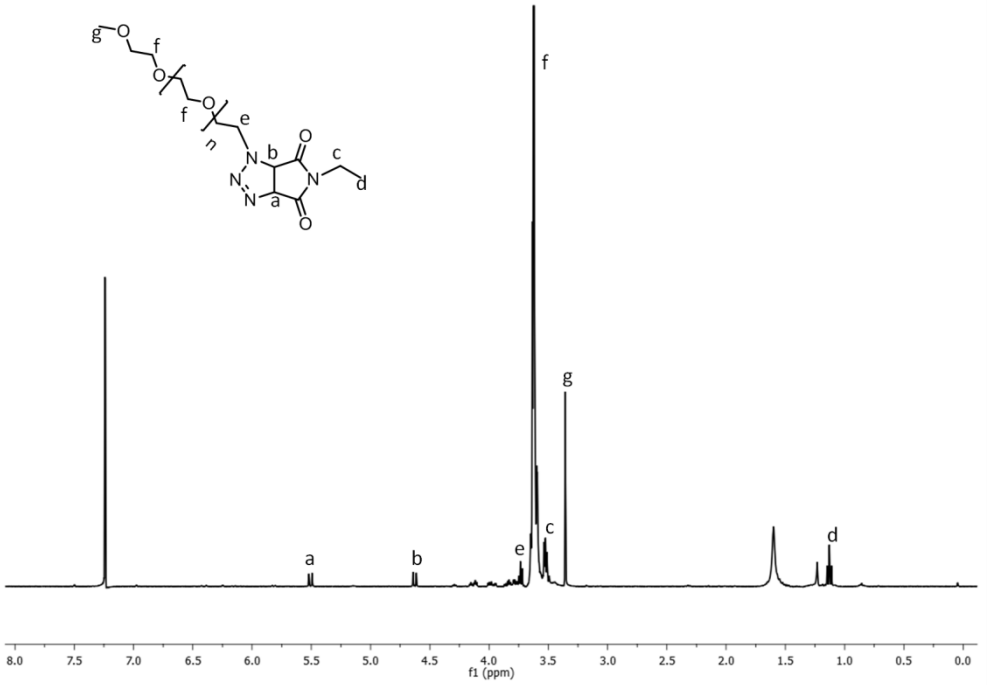

Figure 3.11. ^{1}H NMR in $CDCl_3$ of Ethylmaleimide-PEG azide 'Click' cycloadduct.

To demonstrate further proof to maleimide-azide cycloaddition, another reaction was carried out using active maleimide functional G2 alkyne dendron and $PEG_{750}N_3$ (Figure 3.12). From ^{1}H NMR results, it has been observed that azide functionalities react with not only alkyne moieties at the periphery of the dendron but also active maleimide unit at the core under 50 ºC. From the integrations, maleimide to triazole ratio was found as decreasing when we increase PEG azide amount in the reaction. This indicates loss of some maleimide double bonds that reacted with azide units. Also, small doublets appearing near 4.60 and 5.50 ppm come from bridge protons formed between triazole and

succinimide ring which proves the cycloaddition of azide unit to the maleimide moiety (Table 3.2).

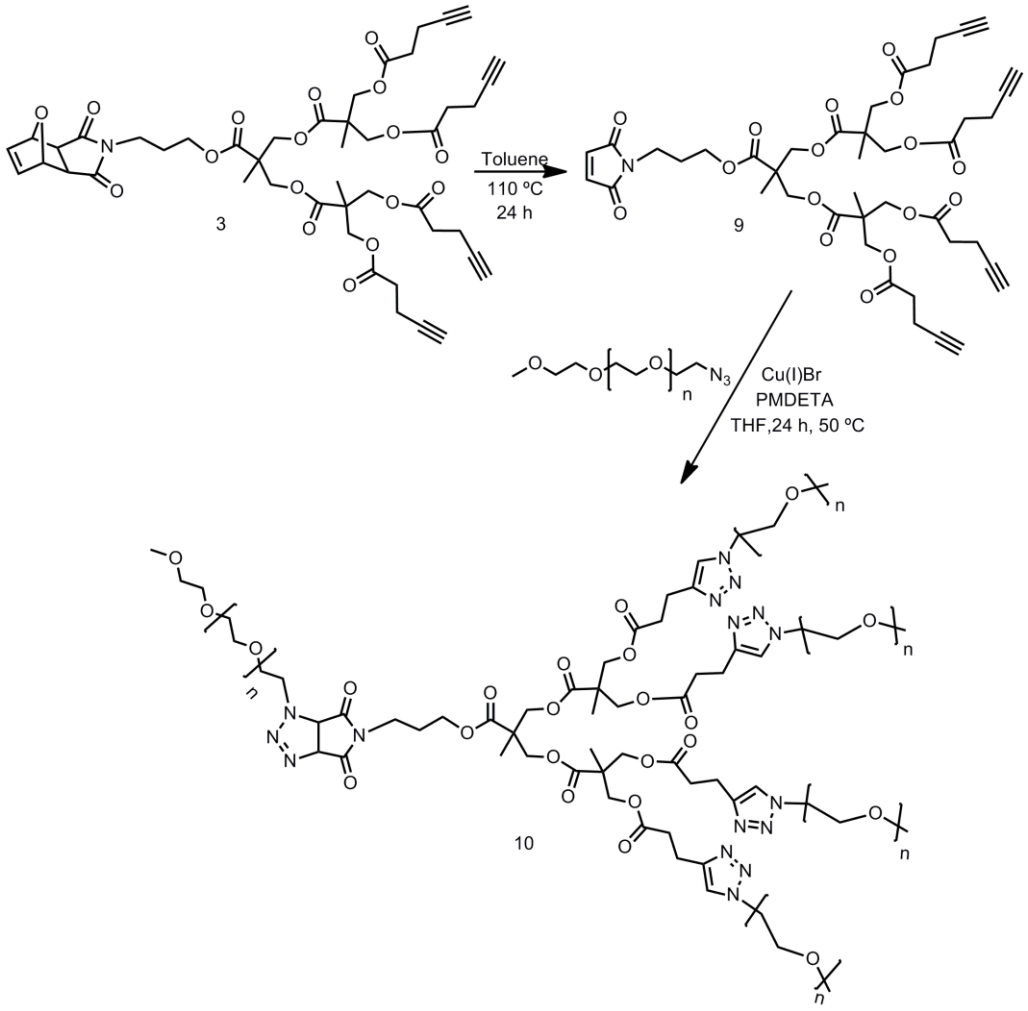

Figure 3.12. Synthesis of PEG-polymer conjugates via cycloaddition of PEG-azide to the maleimide functional dendron.

Table 3.2. Properties of synthesized PEG-polymer conjugates with activated dendron.

Item[a]	G2 Dendron : PEG Azide[b]	Alkyne : Azide[c]	Remaining Maleimide : Triazole calculated from ^{1}H NMR[d]	% Maleimide-Azide cycloadduct[e]	% Remaining free Malemide[f]
1	1 :4	1 : 1	2 : 5	22 %	78 %
2	1 : 8	1 : 2	2 : 14	39 %	61 %

[a]Reaction conditions: All reactions were performed at 50 ºC for 24 hours using Cu(I)Br/PMDETA catalyst system and THF as a solvent. G2 dendron was activated prior to reactions.

[b]Activated G2 dendron to PEG azide mole ratio in the reaction vessel.

[c]Alkyne to azide functionality mole ratio in the reaction vessel.

[d]Remaining free maleimide to formed triazole ratio according to ^{1}H NMR integrations after 24 h of reaction time.

[e]Amount of formed Maleimide-Azide cycloadduct as calculated from ^{1}H NMR.

[f]Amount of free maleimide unit which did not participate to azide cycloaddition reaction according to ^{1}H NMR calculations.

As a 3rd control experiment, a hydrogelation was performed between this active G2 dendron and PEG10K diazide at 50 ºC to obtain a new gel. Biotinylation and enzyme immobilization studies were done exactly under the same conditions with hydrogel H1 in which maleimide unit was protected prior to gelation. Then, fluorescence intensities were compared. Less fluorescence for the new gel indicates that some of the active maleimide units were lost and react with azide functionality during gelation so that the amount of immobilized enzyme decreased significantly (Figure 3.13).

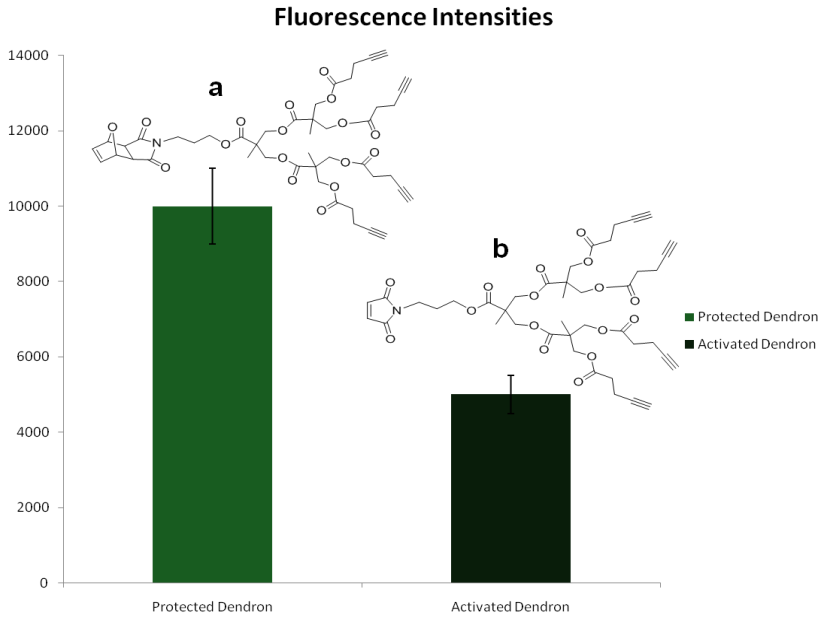

Figure 3.13. Obtained Fluorescence intensities of (a) Gel formed by using masked maleimide functional dendron at 50 ºC, (b) Gel formed by using active maleimide functional dendron at 50 ºC.

3.2. Biodegradable and Thiol Reactive Polymers

3.2.1. Synthesis of Cyclic Carbonate Monomer

Furan protected maleimide containing protected diol 1 was synthesized according to literature [43]. Acetal groups were hydrolyzed via DOWEX 50W-X2 acidic resin to generate diol containing precursor 2. Subsequently, triphosgene was used for ring closure of the free hydroxyl groups of the diol to obtain carbonate monomer 3 (Figure 3.15).

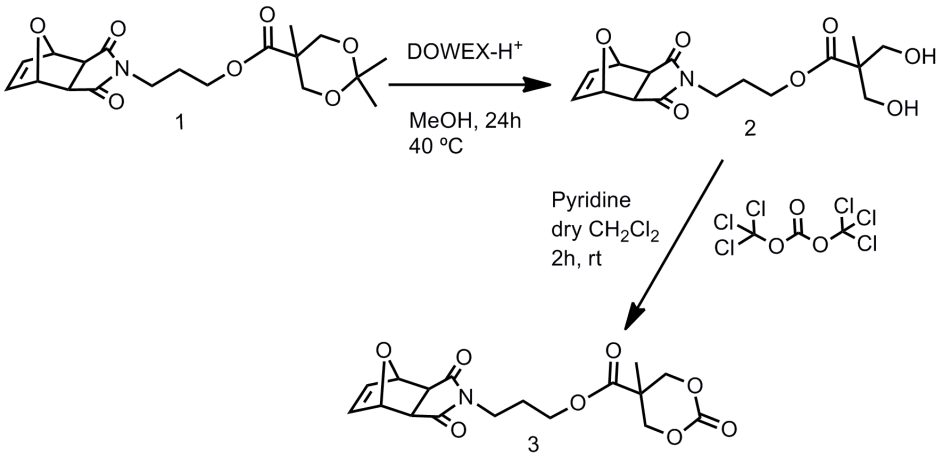

Figure 3.14. Synthesis of maleimide functional carbonate monomer 3.

The desired carbonate monomer 3 was obtained in pure form either via simple precipitation in diethyl ether or column chromatography using SiO_2. From the ^{1}H NMR spectrum, the presence of the bicyclic unit composed of the furan protected maleimide unit was evident from the proton resonances at 2.84, 5.25, and 6.50 ppm. Also, OCH_2 protons of the six membered carbonate ring appear as two doublets at 4.73 and 4.20 ppm which will be seen as one singlet after the ring opens. The ^{13}C NMR spectrum provides further support of the monomer structure due to the presence of three distinct carbonyl peaks. The peaks at 175.2, 169.8 and 146.6 ppm correspond to the carbonyl carbons of ester, amide and carbonate groups, respectively. (Figure 3.16).

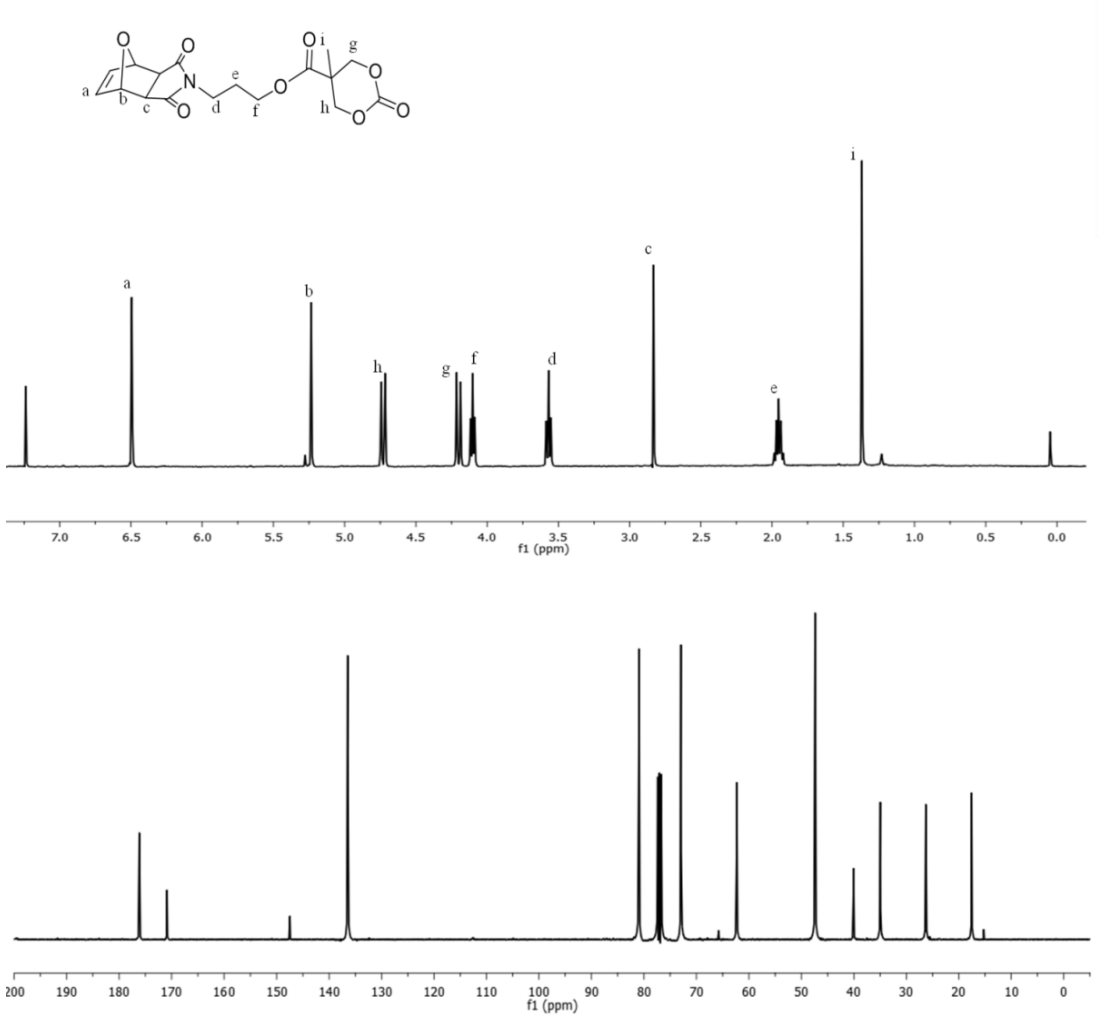

Figure 3.15. ^{1}H-NMR (top) and ^{13}C-NMR (bottom) in $CDCl_3$ of maleimide functional carbonate monomer 3.

3.2.2. Synthesis and Characterization of Homopolymers

Synthesis of biodegradable homo-and copolymers bearing reactive maleimide units at their side chains were outlined in Figure 3.17. Monomer 3 was employed to obtain homopolymers via ring opening polymerization. Initial survey of organocatalysts such as 1,8-diazabicycloundec-7-ene (DBU), triazabicyclodecene (TBD) and thiourea-tertiary amine system indicated that DBU afforded the desired efficiency. Polymerizations were carried out at room temperature using benzyl alcohol as an initiator in dry $CDCl_3$. All the polymerization conditions and the data obtained from ^{1}H NMR and GPC analysis are summarized in Table 3.3.

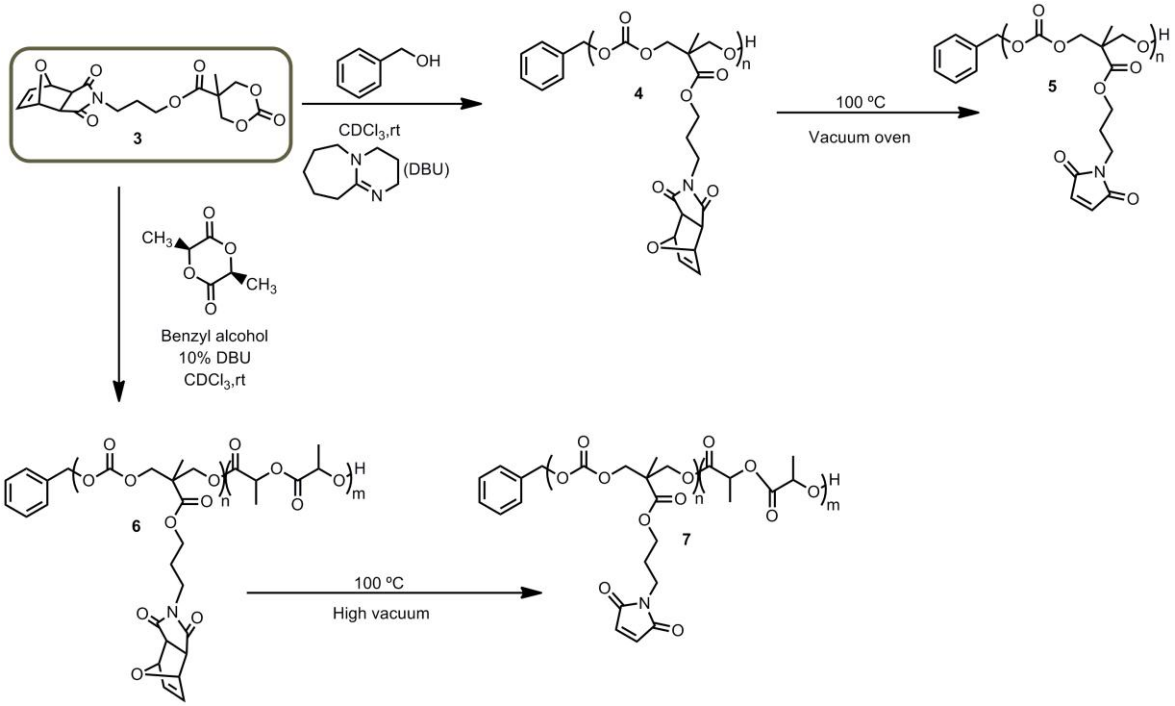

Figure 3.16. Synthesis of maleimide functional homo-and copolymers via ROP.

Table 3.3. Conditions and characterizations of homopolymers.

Item	Polymer[a]	$[M]_0/[I]_0$[b]	Time (h)	Conv (%)	$M_{n,GPC}$ (g/mol)	M_w/M_n	$M_{n,theo}$ (g/mol)	$M_{n,NMR}$ (g/mol)
1	P1	20	192	58	5725	1.13	4345	5582
2	P2	20	24	65	2767	1.11	4815	2300
3	P3	20	4	50	2803	1.07	3762	2593
4	P4	20	117	65	3443	1.24	4815	3158
5	P5	40	27	47	5039	1.11	6912	4127
6	P6	100	27	48	5585	1.13	17560	5039
7	P7	200	48	47	8181	1.14	34360	8140

[a]Reaction conditions: 2 mol % DBU for P1, 20 mol % DBU for P4 and 10 mol % DBU for all other polymers, all polymerizations were performed in $CDCl_3$ at 25 ºC, [Monomer 3] = 0.14 M using benzyl alcohol as the initiator. [b]Targeted degree of polymerization based on [Monomer]/[Initiator].

Initially homopolymerization of monomer 3 was investigated and a decrease in conversion was observed. Thereby, polymerizations were stopped at 50% conversion in order to prevent possible transesterification reactions and obtain more reliable data for further characterizations. Linear relationships between conversion and molecular weight indicated well-controlled polymerizations. Although a discrepancy between targeted and obtained molecular weights was observed due to the extremely slow incorporation of the monomer units along polymer backbone, a linear relationship between DP's and obtained molecular weights was maintained (Figure 3.18).

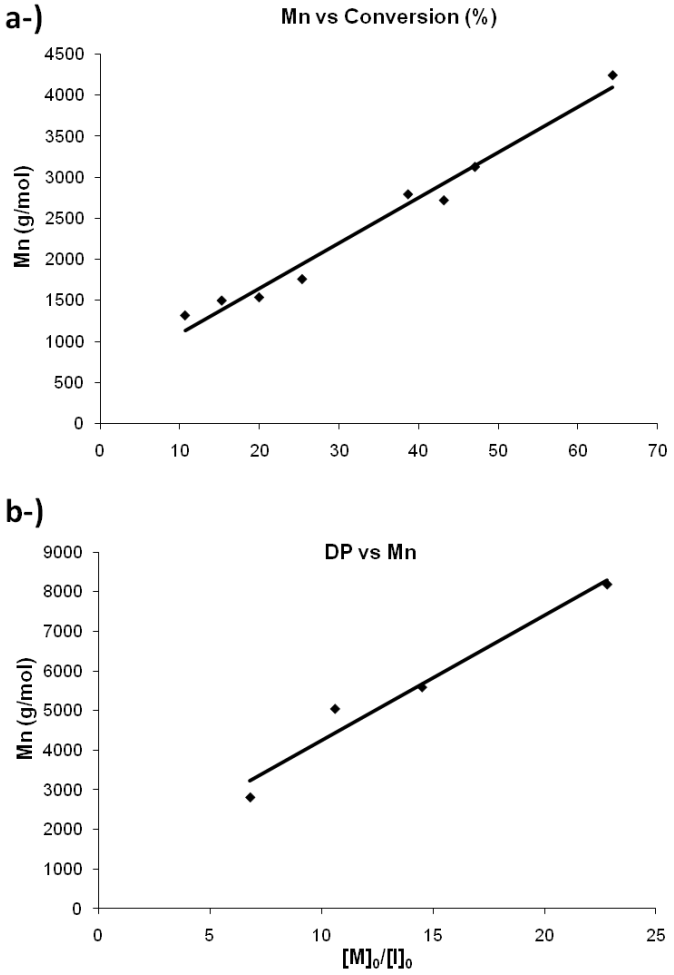

Figure 3.17. (a) Plot of number-average molecular weight (M_n) vs % monomer conversion in the ring opening polymerization of the monomer 3. Conditions: [Monomer 3] = 0.14 M $CDCl_3$ at 25 ºC, 10 mol % DBU, $[M]_0$ / $[I]_0$ = 20 using benzyl alcohol as an initiator. (b) Plot of number-average molecular weight (M_n) vs initial monomer-to-initiator ratio, $[M]_0$ / $[I]_0$, in the ring opening polymerization of the monomer 3. Conditions: [Monomer 3] = 0.14 M $CDCl_3$ at 25 ºC, 10 mol % DBU using benzyl alcohol as an initiator.

P3 homopolymer was subjected to retro Diels-Alder reaction upon heating to 100 ºC in a vacuum oven to unmask the maleimide groups to their reactive forms. Quantitative unmasking of maleimide functionalities were proved from the disapperance of the protons at 2.82, 5.23 and 6.47 ppm due to the removal of bicyclic core, and appearance of a new proton resonance at 6.65 ppm belonging to the active double bond protons of the maleimde unit (Figure 3.19).

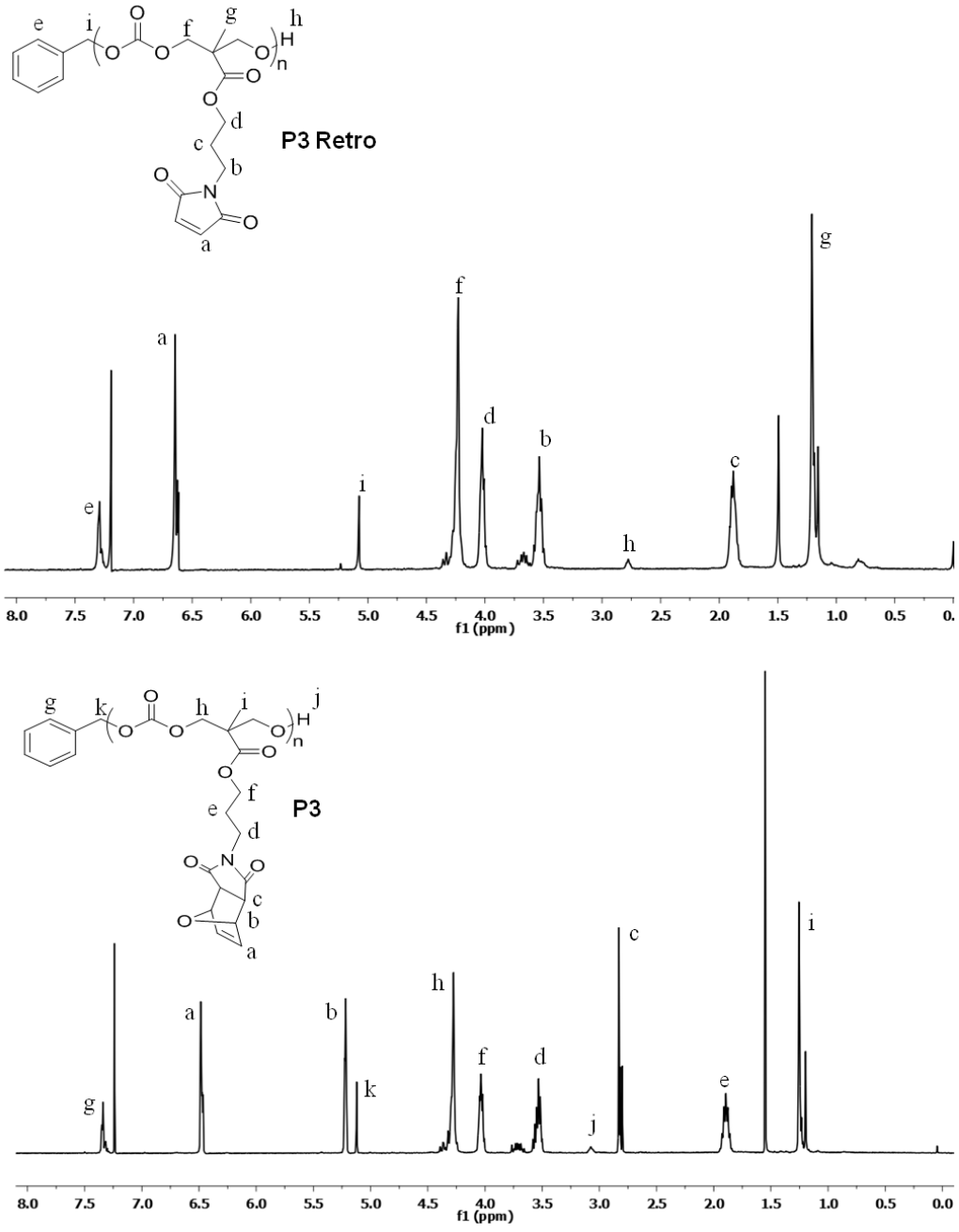

Figure 3.18. ^{1}H-NMR in $CDCl_3$ of latent reactive P3 (bottom) and reactive P3 Retro (top) homopolymers.

As expected, slight decrease in the molecular weight of the polymer P3 after the retro Diels-Alder step was observed. More importantly, no chain scission or other side reactions occurred during this activation step (Figure 3.20).

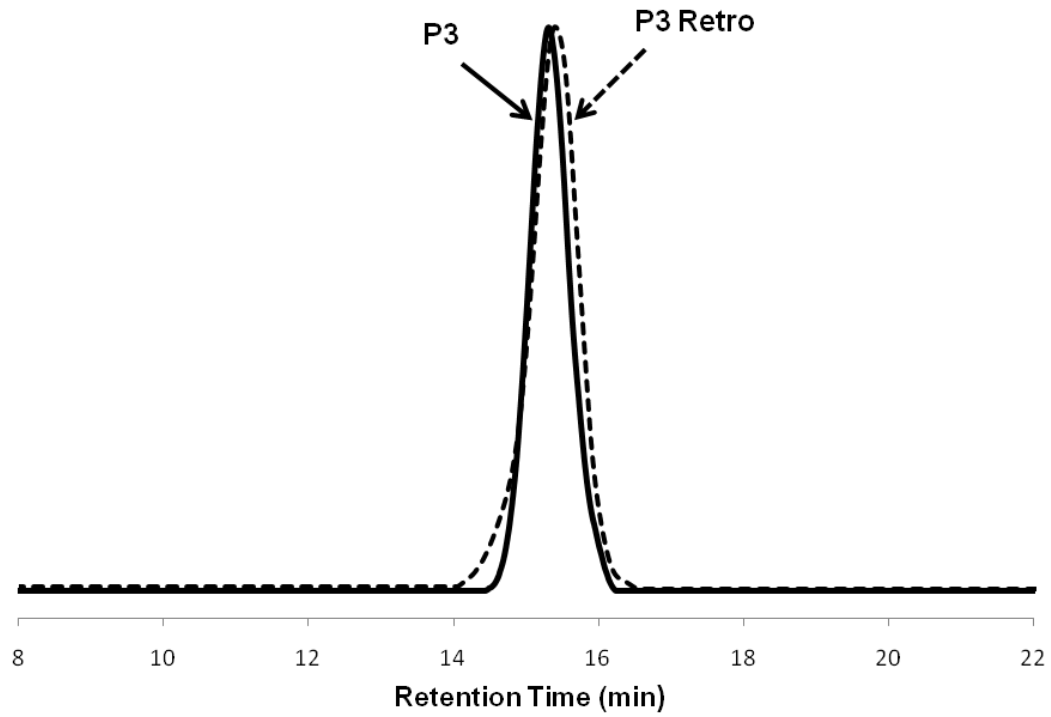

Figure 3.19. GPC traces of the homopolymer P3 ($M_{n,GPC}$ = 2803, M_w/M_n = 1.07) and homopolymer after the rDA reaction, P3 Retro, ($M_{n,GPC}$ = 2684, M_w/M_n = 1.11).

The homopolymers before and after the retro step were analyzed via MALDI-ToF instrument. In the mass spectra of the parent homopolymer P3, mass peaks corresponding to those of the polymer chains containing the unmasked maleimide functionality were detected along with the expected peaks for polymer P3 indicating that the retro Diels-Alder reaction occurs upon ionisation by the laser. The MALDI-ToF spectra of the homopolymer obtained after the retro Diels-Alder step consisted primarily of the polymer with the reactive maleimide side chains (Figure 3.21).

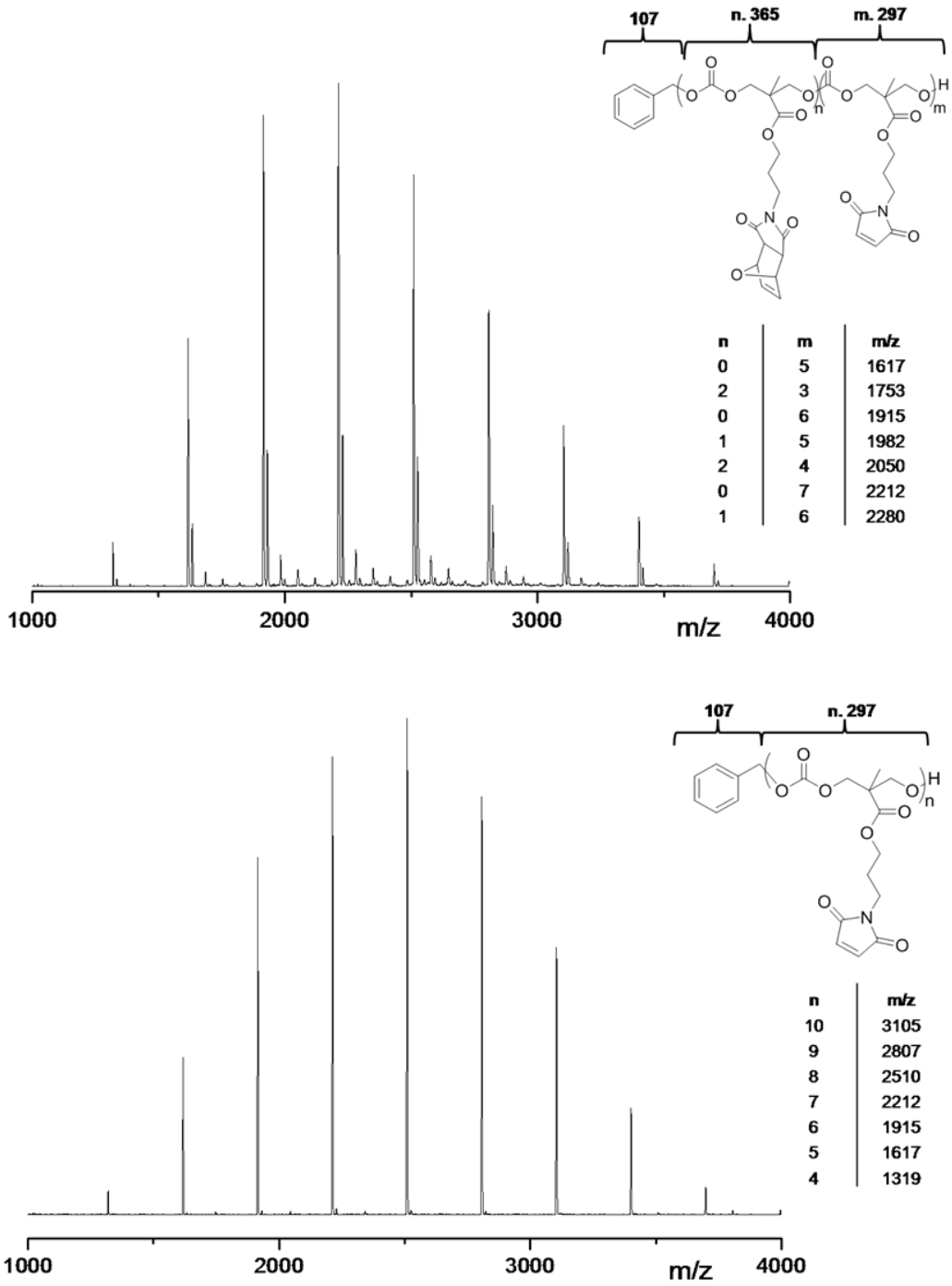

Figure 3.20. MALDI-TOF MS analysis of the polymer P3 (top) and P3 after rDA reaction (bottom).

3.2.3. Synthesis and Characterization of Copolymers

Copolymerization of L-lactide together with the monomer **3** was accomplished via ROP mechanism in the presence of DBU (%) as a catalyst for all polymers. Polymerization conditions and data analysis of copolymers were given in Table 3.4.

Table 3.4. Conditions and characterizations of carbonate monomer 3: L-lactide copolymers.

Item	Polymer[a]	Time (h)	Conv (%)	$M_{n,GPC}$ (g/mol)	M_w/M_n	$M_{n,theo}$ (g/mol)	$M_{n,NMR}$ (g/mol)	Aimed Feed Ratio (M2 :Lactide)	Obtained Feed Ratio (^{1}H-NMR)
1	P8	120	90	18 452	1.37	17 095	14 600	20 : 80	22 : 78
2	P9	8	95	22 026	1.14	14 830	19 210	5 : 95	3 : 97
3	P10	8	72	12 339	1.21	12 040	14 470	10 : 90	9 : 91
4	P11	24	70	9798	1.10	13 020	8 450	25 : 75	21 : 79
5	P12	48	58	8295	1.17	14 830	11 310	50 : 50	42 : 58
6	P13	24	40	8094	1.19	12 400	11 920	75 : 25	71 : 29
7	P14	24	85	17 148	1.16	14 222	13 700	10 : 90	8 : 92

[a]All polymerizations were performed in $CDCl_3$ at 25 ºC, 2 mol % DBU, $[M]_0/[I]_0$=100 using benzyl alcohol as the initiator.

Excellent control over the polymerization was demonstrated by close matching between aimed feed ratios and obtained incorporation of the monomers from ^{1}H-NMR experiments. Efficient rDA reaction to obtain reactive polymers was evident from complete disappearance of the peaks near 6.48, 5.28 and 2.83 ppm and arousal of a new peak at 6.69 ppm from the ^{1}H-NMR measurements. (Figure 3.22). From the GPC traces, it can be observed that higher retention time of P13 Retro indicates the decrease in the molecular weight after the removal of furan moieties (Figure 3.23).

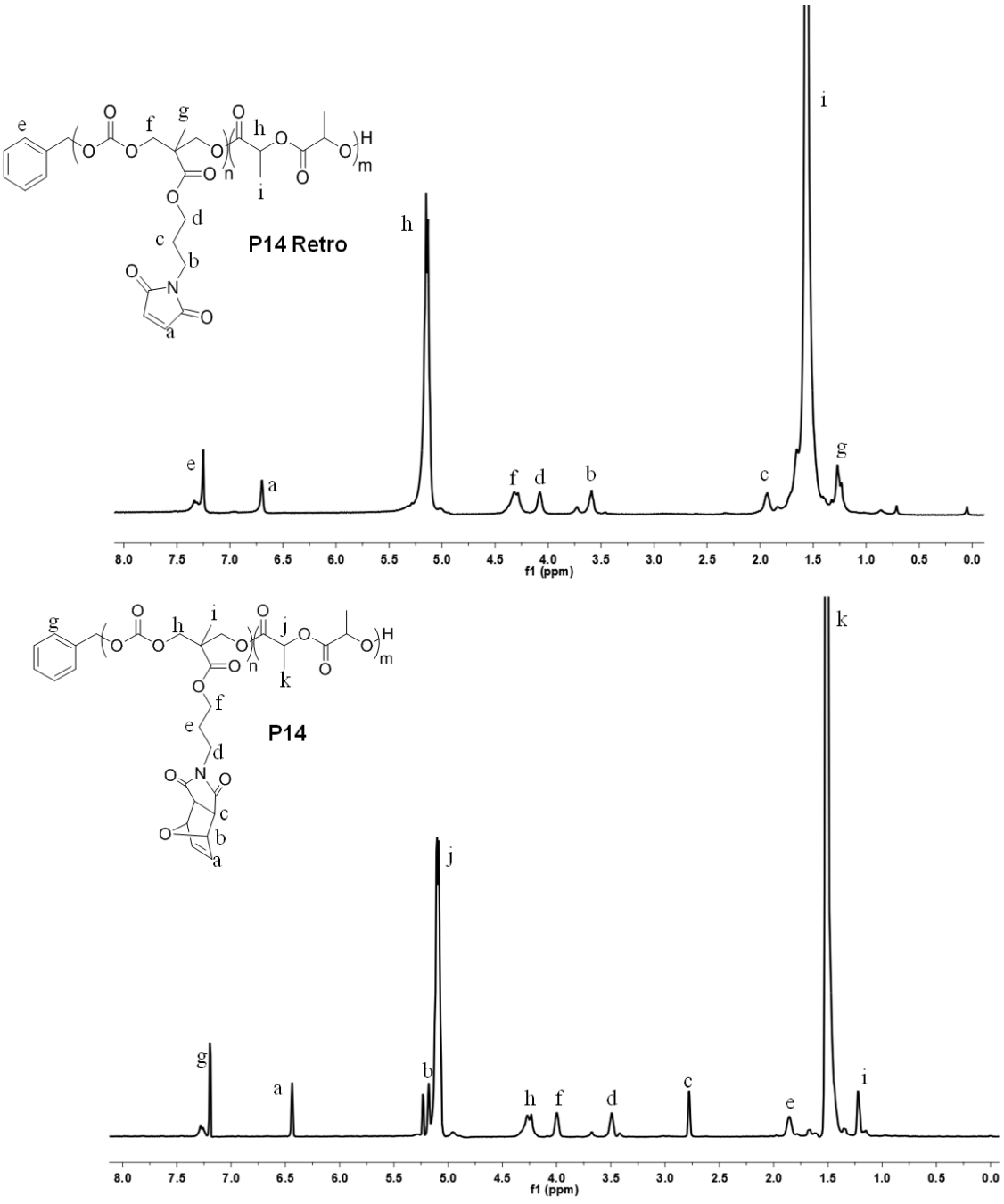

Figure 3.21. ^{1}H-NMR in $CDCl_3$ of polymer P14 (bottom) and P14 after rDA (top).

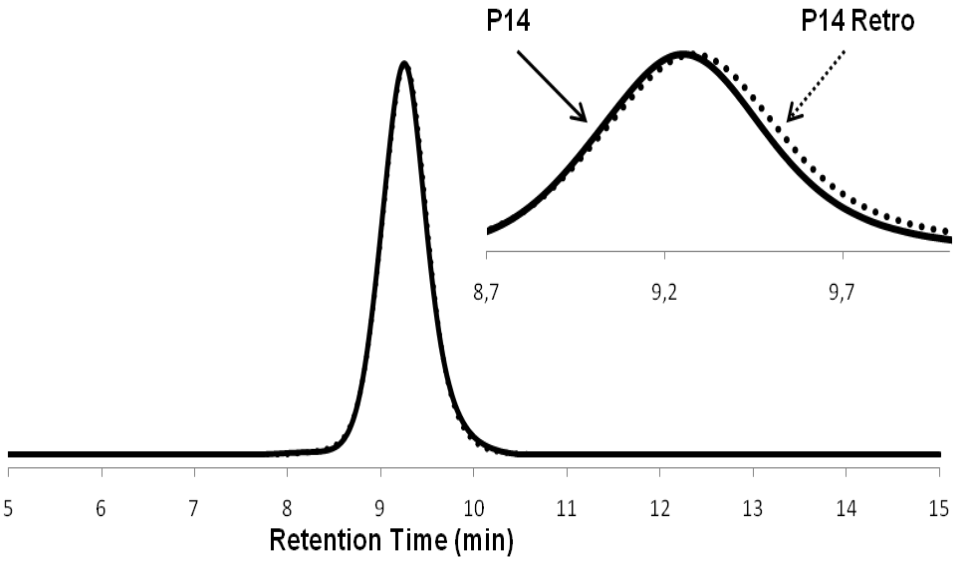

Figure 3.22. GPC traces of copolymer P14 ($M_{n,GPC}$ = 17 148, M_w/M_n = 1.16) and copolymer after the rDA reaction, P14 Retro, ($M_{n,GPC}$ = 17 000, M_w/M_n = 1.18).

Thermogravimetric analysis (TGA) was also performed for characterization of the polymer P14. From TGA analysis, due to the removal of the furan units between 60-180 ºC, one can expect that a remarkable weight loss should be observed for P14. In the same manner, when rDA reaction was applied to the same polymer (P14 Retro), no significant weight loss between these temperatures was detected (Figure 3.24).

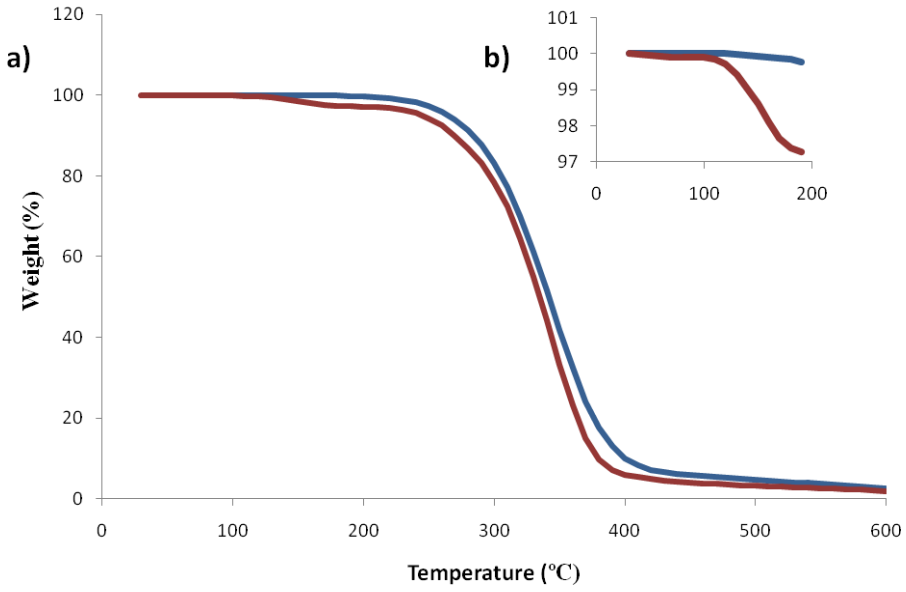

Figure 3.23. TGA thermograms of the polymer P14 and P14 after rDA between (a) 0 ºC – 600 ºC. (b) 0 ºC – 180 ºC.

Different polymers containing different maleimide amounts were also investigated by TGA analysis. As expected, an increase in the amount of maleimide functional monomer in the feed ratio results in higher weight loss (Figure 3.25).

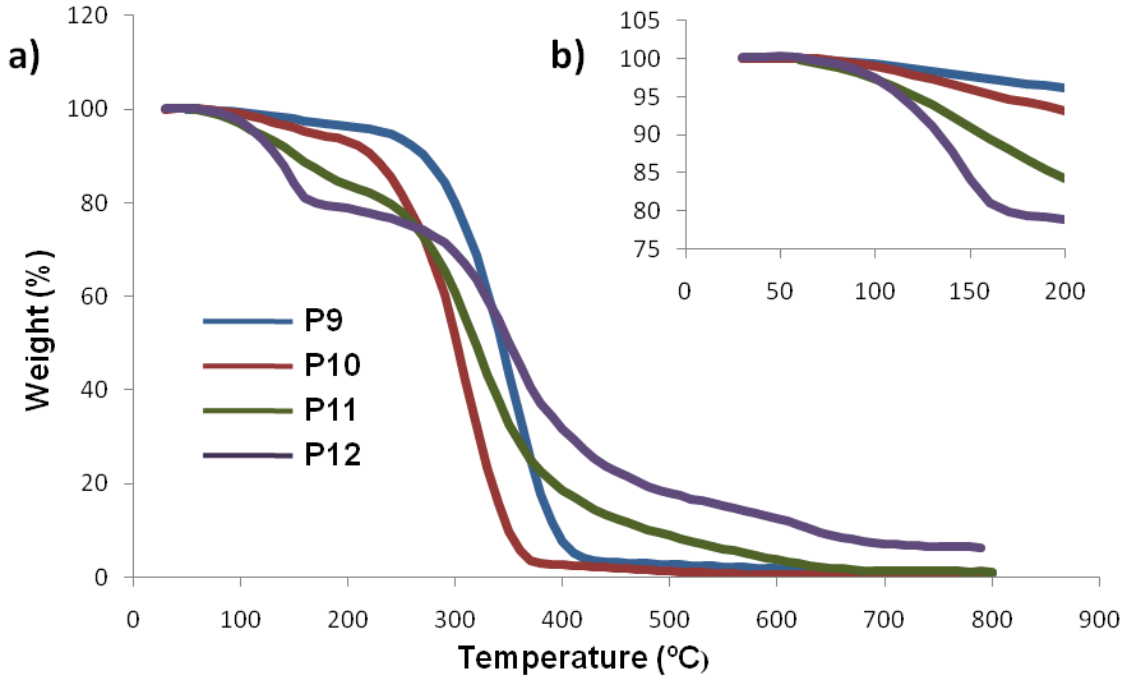

Figure 3.24. TGA thermograms of copolymers with different maleimide percentages. between (a) 0 ºC – 600 ºC. (b) 0 ºC – 200 ºC.

3.2.4. Functionalization of PLLA Copolymers

To evaluate the efficiency of Michael type addition of maleimide to thiols, functionalization studies were performed with two different thiols namely 6-(ferrocenyl)hexanethiol and 1-hexanethiol and with the polymer P14 (Figure 3.26). Quantitative conjugation of thiol containing small molecules to the maleimide side chains was achieved at room temperature by using two fold excess of thiols per maleimide group. This ratio was used for both conjugations in order to eliminate uncertainty of the exact maleimide percentage determined by ^{1}H-NMR spectroscopy.

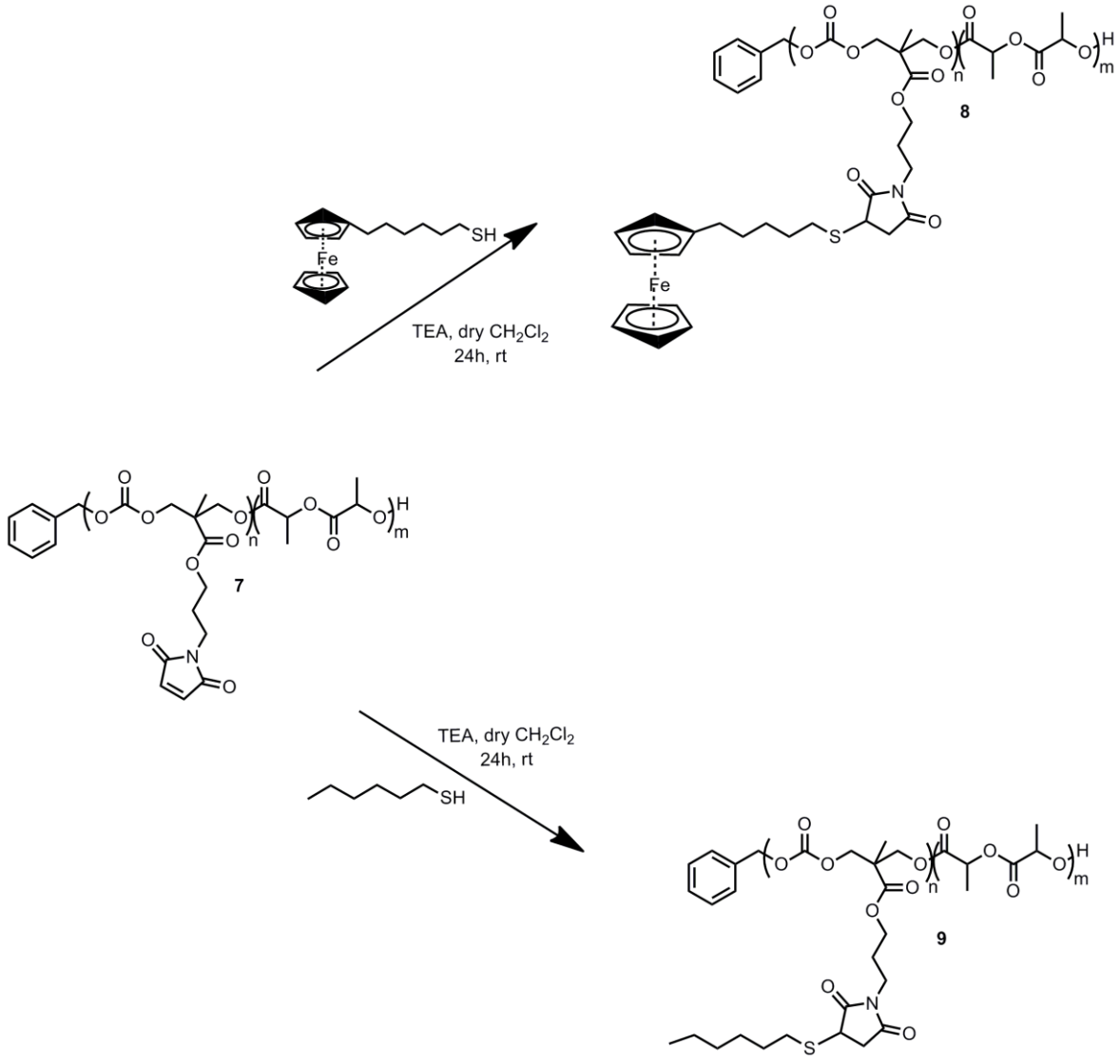

Figure 3.25. Synthesis of functionalized polymers via Michael Addition of thiols to the polymer P14.

^{1}H-NMR data of 6-(ferrocenyl) hexanethiol conjugation was examined, characteristic maleimide double bond peak at 6.69 ppm disappeared and protons of ferrocene rings appeared 4.01 and 4.08 ppm. The proton resonances from the nearly formed succinimide ring and the alkyl chain are clearly assignable. From the GPC results, the peak which has a low retention time belongs to the functionalized polymer which has higher molecular weight in comparison to P14 Retro (Figure 3.27).

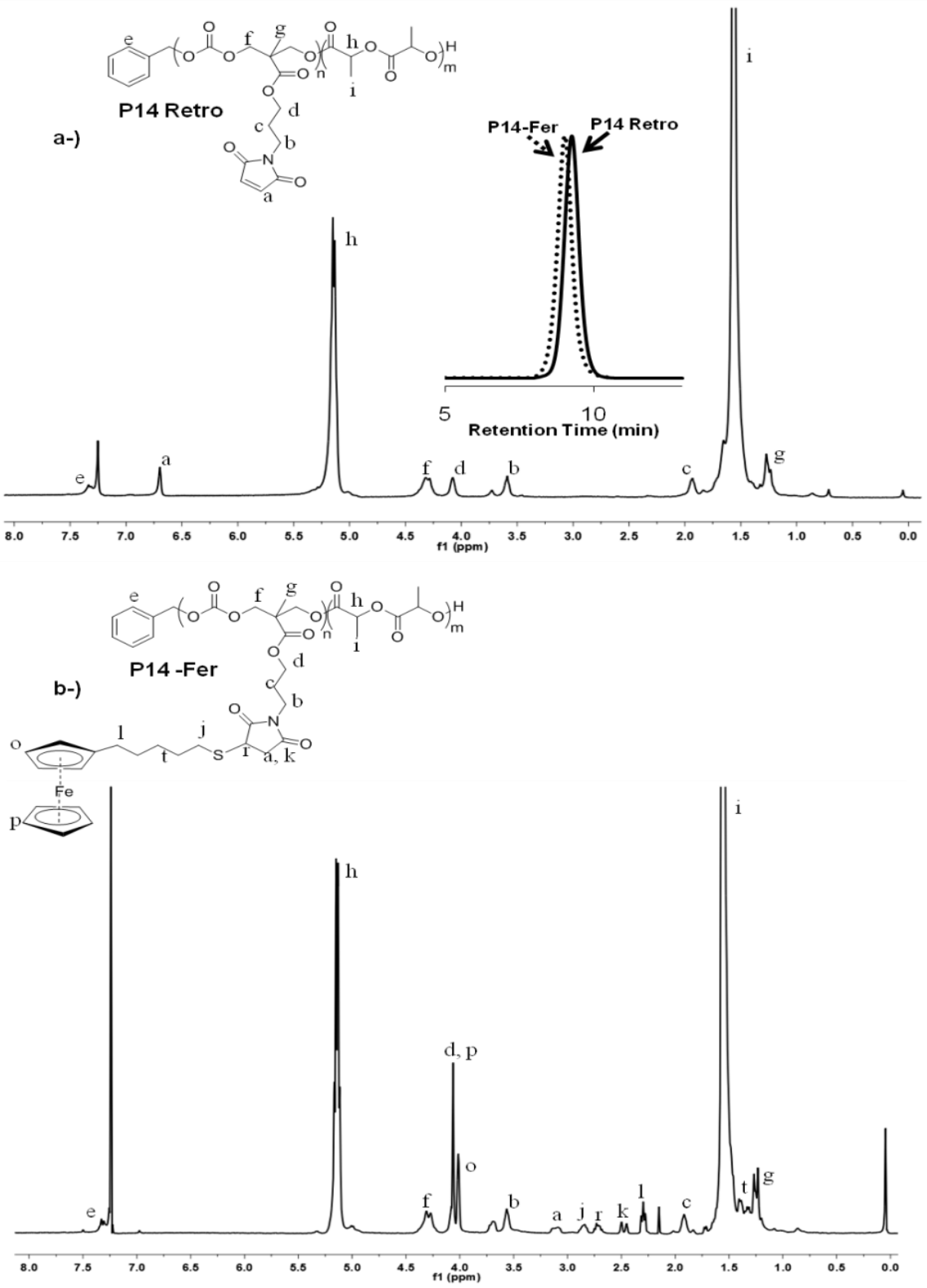

Figure 3.26. ^{1}H-NMR in $CDCl_3$ of (a) P14 Retro (b) ^{1}H-NMR of in $CDCl_3$ 6-(ferrocenyl)hexanethiol functionalized polymer (P14-Fer) and GPC traces before ($M_{n,GPC}$ = 17 000, M_w/M_n = 1.18) and after thiol functionalization ($M_{n,GPC}$ = 18 400, M_w/M_n = 1.20).

Similarly, disappearance of maleimide proton resonances and appearance of expected proton resonances were observed for the 1-hexanethiol conjugation (Figure 3.28). With these conjugation studies, it has been demonstrated that maleimide-thiol type click chemistry is a efficient method for functionalization of the copolymers without degradation of the polymer backbone.

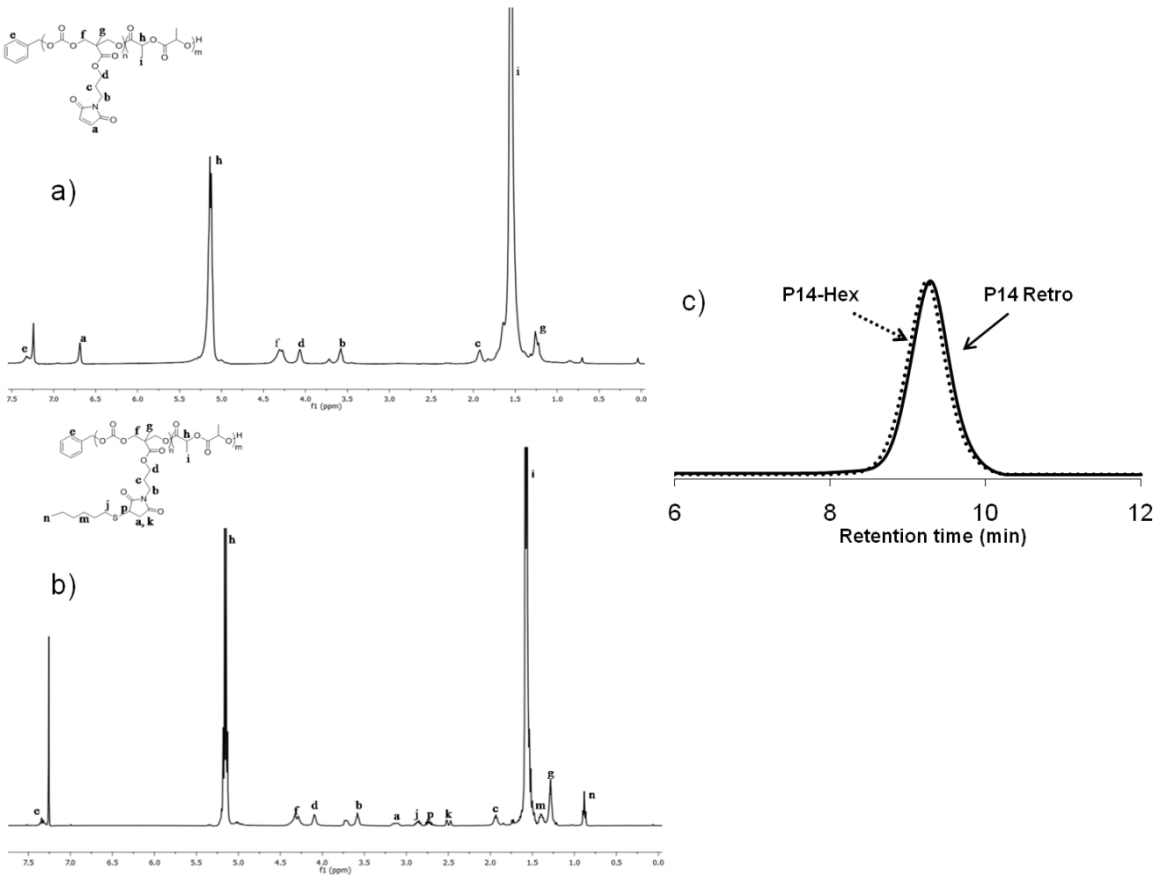

Figure 3.27. ^{1}H-NMR spectra of (a) P14 Retro, (b) 1-hexanethiol functionalized polymer (P14-Hex) and (c) GPC traces before ($M_{n,GPC}$ = 17 000, M_w/M_n = 1.18) and after functionalization ($M_{n,GPC}$ = 17 761, M_w/M_n = 1.19).

4. EXPERIMENTAL

4.1 Materials and Methods

2,2-Bis(hydroxymethyl)propionic acid (BMPA), Dowex X50WX2 and 4-pentynoic acid were obtained from Alfa Aesar. All poly(ethylene glycol) were purchased from Fluka. *L*-Lactide was purchased from Aldrich and purified by recrystallisation from dry dichloromethane. Azide-functionalized PEGs were synthesized according to the literature [51]. All solvents were obtained from Aldrich or Merck. THF is obtained from J.T. Baker prior to functionalizations. Dichloromethane was dried over CaH_2, distilled and degassed before polymerizations or was used after distillation over P_2O_5 (J. T. Baker) prior to functionalizations. Biotinylated (triethylene glycol) undecanethiol was purchased from Nanoscience Instruments (Phoenix, AZ). Fluorescein (FITC) conjugated streptavidin is obtained from Pierce and used as received. BodipyC10SH was synthesized according to literature procedure [52]. Fourier transform infrared (ATR-FTIR) spectroscopy (Thermo Fisher Scientific Inc. Nicolet 380) was used for both dendron and hydrogel characterizations. The dry surfaces of the hydrogels were observed with an ESEM-FEG/EDAX Philips XL-30 (Philips, Eindhoven, The Netherlands) instrument using an accelerating voltage of 10kV. Functionalized hydrogels were visualized with Zeiss Observer. Z1 inverted fluorescent microscope. Polymerizations and monomer drying were performed under moisture and oxygen free conditions in either a nitrogen filled glove box or by standard Schlenk techniques. The gel-permeation chromatography (GPC) measurements of the homopolymers were carried out with a Polymer Laboratories Midas autosampler and LC1120 HPLC pump equipped with a guard column (Polymer Laboratories PLGel 5 μM,50×7.5 mm), two mixed D columns (Polymer Laboratories PLGel 5 μM, 300×7.5 mm) and a Polymer Laboratories ERC-7515A differential refractive index (DRI) detector. The mobile phase was chloroform/triethyl amine (95/5) eluent at a flow rate of 1.0 $mL.min^{-1}$ and samples were calibrated against linear poly(styrene) standards (540 to 2.9×104 $g.mol^{-1}$) using Cirrus v3.0; elution time was standardized against that of toluene. The second GPC was used for the analysis of copolymers and functionalized polymers and is a TD-GPC with a Agilent 1200 model pump, four Waters

Styragel columns (guard, HR 5E, HR 4, HR 3, and HR 2), and a Viscotek TDA 302 triple detector (RI, dual laser light scattering (LS) and a differential pressure viscometer), was conducted to measure the absolute molecular weights in THF with a flow rate of 0.5 mL/min at 35 ºC. All three detectors were calibrated with a PS standard having narrow molecular weight distribution (Mn = 115 000 g/mol, M_w/M_n = 1.02) provided by Viscotek. Data analyses were performed with Omni-Sec version 4.5 software from Viscotek. ^{1}H NMR spectra was recorded on a Bruker DPX 300 MHz, DPX 400 MHz or Varian 400 MHz spectrometer at 293 K. Mass spectra were acquired by MALDI-ToF (matrix-assisted laser desorption and ionization time-of-flight) mass spectrometry using a Bruker Daltonics Ultraflex II MALDI-ToF mass spectrometer, equipped with a nitrogen laser delivering 2 ns laser pulses at 337 nm with positive ion ToF detection performed using an accelerating voltage of 25 kV. The samples were measured in reflectron ion mode and calibrated by comparison to 2 × 10^3 and 5 × 10^3 g.mol^{-1} poly(ethylene glycol) standards. Elemental analysis of the maleimide functional carbonate monomer was done on a FlashEA^R 1112 Series Elemental Analyzer (CHNS Separation Column, PTFE; 2 m; 6 x 5 mm) Thermogravimetric analysis (TGA) was performed on a TA Instruments at a heating rate of 10 º C/min under a nitrogen atmosphere.

4.2 Thiol Reactive Hydrogels via Orthogonally Clickable Dendrons

4.2.1. Synthesis of Second Generation (G2) Alkyne Dendron

Dendron 1 was synthesized according to previously recorded literature procedures [43]. G2 Dendron 1 (1.5 g, 2.3 mmol) was dissolved in MeOH (30 mL) and to this solution Dowex H^+ resin was added with a tip of spatula. The resulting mixture was stirred at 40 ºC until the consumption of the dendron was observed via TLC. The resin was then filtered off and washed with MeOH. The filtrate was concentrated in *vacuo* to give a white solid (1.27 g, 98% yield). Compound 2 (0.2 g, 0.3 mmol) was then added to a solution of DMAP (0.045 g, 0.3 mmol), pyridine (0.6 mL) and 4-pentynoic anhydride (0.39 g, 1.8 mmol) in dry CH_2Cl_2 (4.5 mL). The mixture was then stirred at room temperature for 12 h. Excess anhydride was quenched with water (2.0 mL) for 3 h. Reaction mixture was diluted with 20 mL CH_2Cl_2 and extracted with 1 M $NaHSO_4$ (3 x 20 mL), 10% Na_2CO_3 (3 x 20 mL) and then with brine (1 x 20 mL) combined organic layers were dried over anhydrous

Na_2SO_4. The residue was concentrated in *vacuo*. Crude product was purified by column chromatography to give 0.28 g of maleimide protected alkyne dendron as a colorless viscous liquid (91% yield).[69] ^{1}H NMR ($CDCl_3$,δ, ppm) 6.50 (s, 2H, C*H* = C*H*), 5.24 (s, 2H, C*H* bridgehead protons), 4.27 (s, 4H), 4.24 (d, 4H, *J* = 11.3 Hz, CH_2 ester protons), 4.21 (d, 4H, *J* = 11.2 Hz, CH_2 ester protons), 4.04 (t, 2H, *J* = 6.2 Hz, OCH_2), 3.56 (t, 2H, *J* = 6.8 Hz, NCH_2), 2.84 (s, 2H, bridge protons), 2.56 - 2.53 (m, 8H, CH_2CH_2C ≡ CH), 2.49 - 2.44 (m, 8H, CH_2CH_2C≡CH), 1.96 (t, 4H, *J* = 2.6 Hz, C ≡ C*H*), 1.92 (tt, 2H, *J* = 6.8, 6.2 Hz, NCH_2C$H_2$$CH_2$O), 1.27 (s, 3H, CC$H_3$), 1.23 (s, 6H, CC$H_3$), ^{13}C NMR ($CDCl_3$, δ, ppm) 176.1, 171.9, 171.8, 171.1, 136.4, 82.3, 80.9, 69.2, 65.6, 65.3, 61.9, 47.4, 46.6, 46.3, 35.2, 33.1, 26.5, 17.8, 17.5, 14.2, FTIR (cm^{-1}) 1732.0, 1697.8.

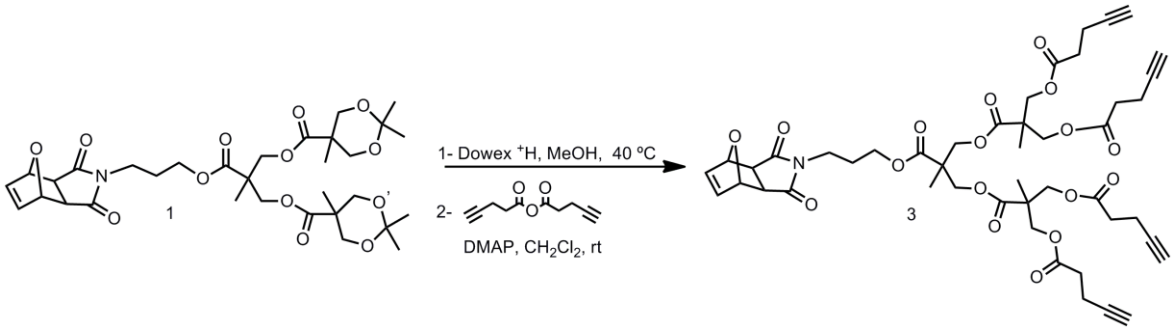

Figure 4.1. Synthesis masked maleimide functional G2 alkyne dendron 3.

4.2.2. Hydrogel Synthesis

Five series of hydrogels were synthesized at both 25 ºC and 50 ºC containing different PEG weights. As a representative synthesis, to a small vial, furan protected maleimide dendron (8.2 mg, 0.0092 mmol) and PEG6K diazide (110 mg, 0.0184 mmol) were added and dissolved in 75 µL ethanol and 75 µL THF mixture. To this solution 5 µL deionized H_2O containing sodium ascorbate (2 mg, 10.1 µmol) was added and the mixture was sonicated till a clear solution was obtained. Copper sulfate (3.7 mg, 0.015 mmol) in water (50 µL) was added and placed either at room temperature (25 ºC) or at 50 ºC in an oil bath. The formed gel was taken out from the vial and left for stir in EDTA solution (5%, pH 7-8) to get rid of trapped $CuSO_4$, ethanol to remove unreacted dendron and finally with deionized water. Then, the hydrogel was frozen and freeze-dried in vacuo. The

gel conversions were calculated as 71.1% at 25 ºC after 24 hours and 84.0% at 50 ºC after 3 hours of reaction time. Other series of hydrogels were synthesized in the same manner.

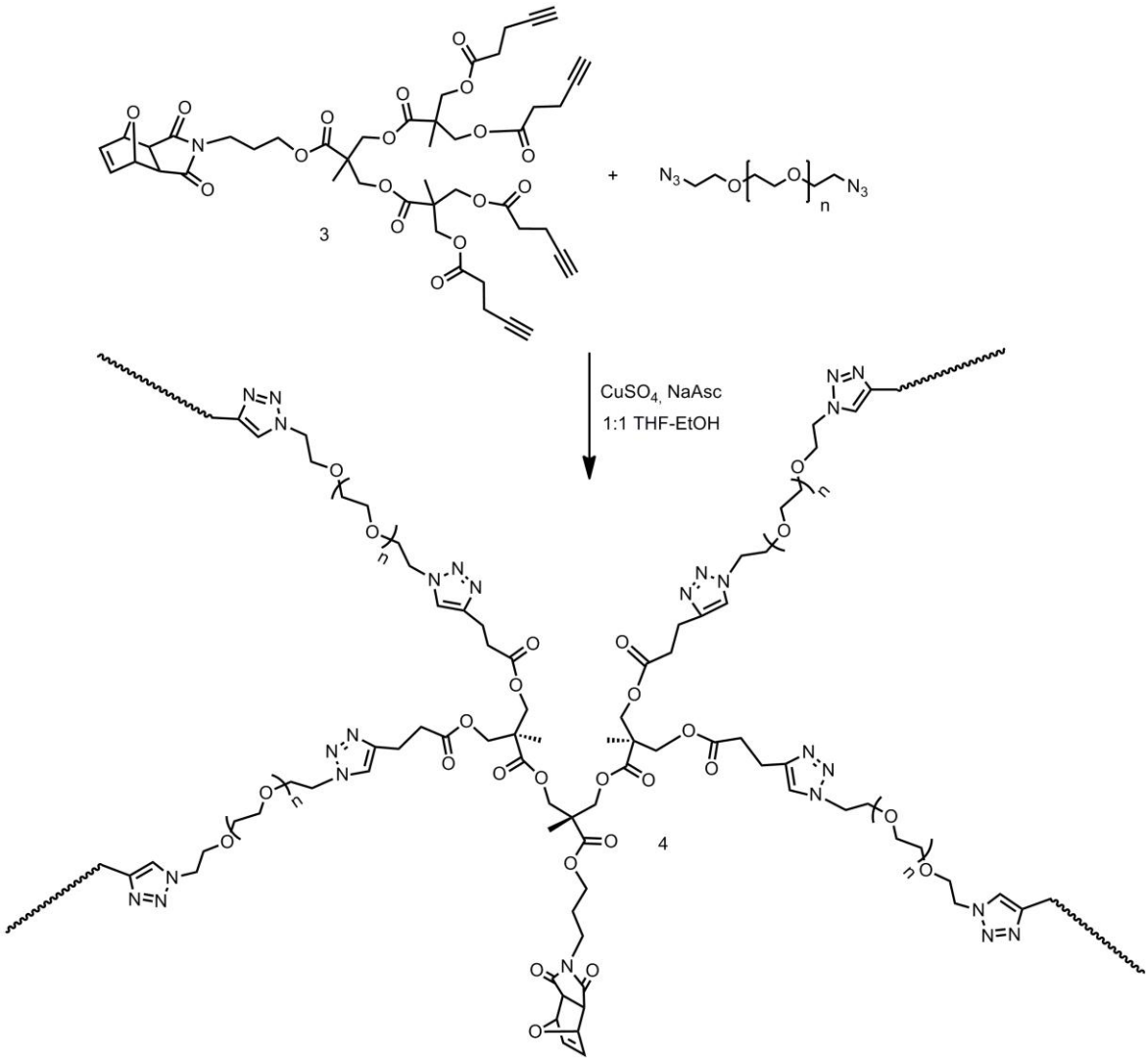

Figure 4.2. Representative Hydrogel Synthesis.

4.2.3. Hydrogel activation

Freeze-dried hydrogels were heated at 110°C in dry toluene for 3 hours. Thermogravimetric analysis (TGA) experiments demonstrated that retro Diels-Alder of the maleimide functional group was achieved. Hydrogel sample prior to activation step had a significant weight loss between 60 ^{o}C - 180 ^{o}C because of the removal of the furan

moieties. However, hydrogel after the retro Diels-Alder reaction showed no significant weight loss between these temperatures.

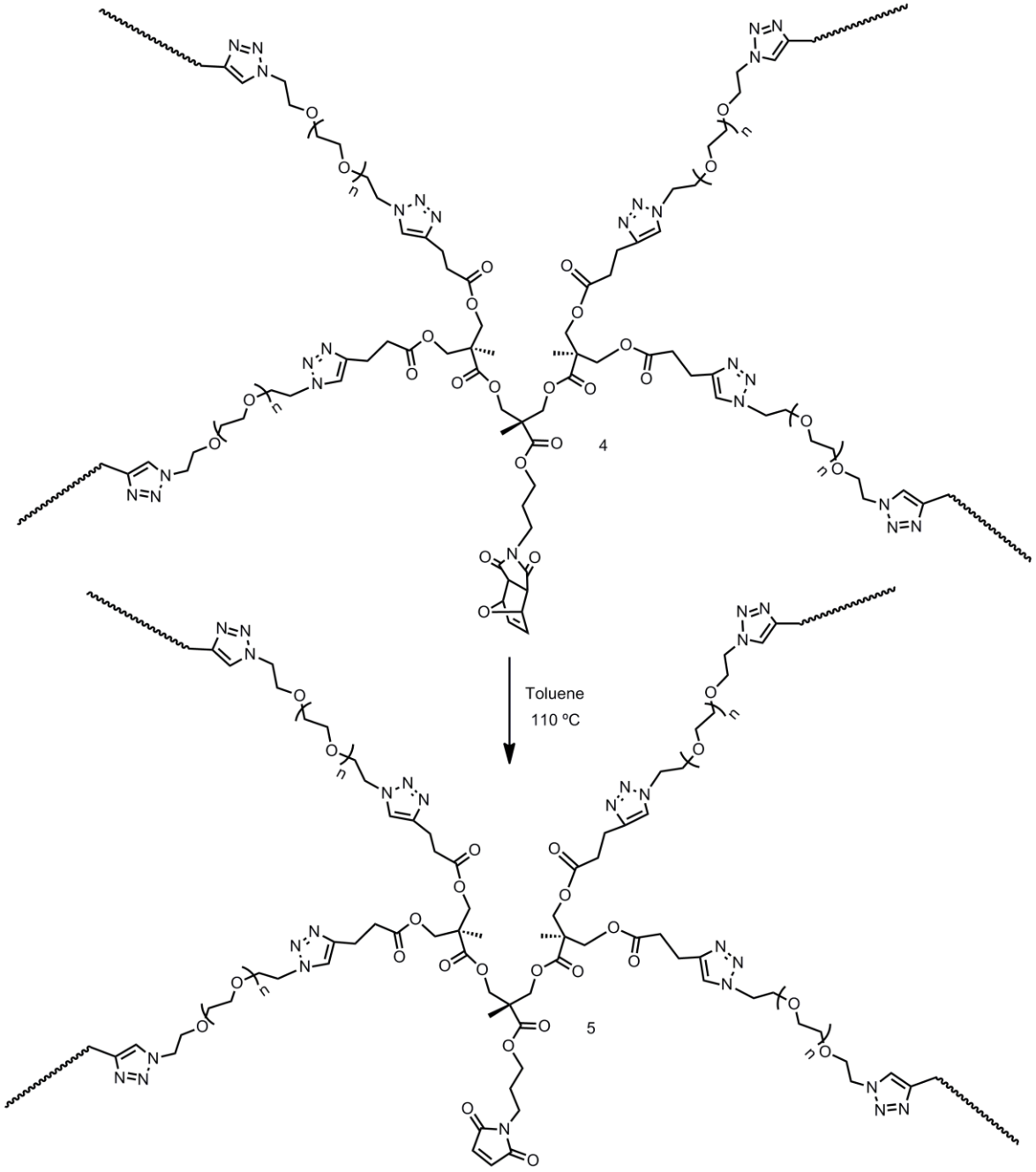

Figure 4.3. Activation of hydrogels.

4.2.4. Swelling Studies

Water uptake of the hydrogels were investigated by transferring a piece of dry and purified hydrogel to a flask containing deionized water. Increase in the weight of hydrogel

was recorded as a function of time after immersing the gel into the water for a given period of time and drying it on the surface of a filter paper. These experiments were repeated at least three times with different pieces of a particular hydrogel. The swelling ratio percent W was calculated via equation 1 where M_w and M_d are the weights of wet and dry samples.

$$W = (M_w - M_d) / M_d \times 100 \quad (1)$$

4.2.5. Scanning Electron Microscopy Studies

Hydrogel samples were placed in deionized water for one day at room temperature in order to reach to the equilibrium state. Then, swollen hydrogels were frozen and freeze-dried in lyophilizer. The morphology of the gels were examined by using scanning electron microscope. Images were taken using ESEM-FEG/EDAX Philips XL-30 (Philips, Eindhoven, The Netherlands) instrument by using an accelerating voltage of 10 kV.

4.2.6. Functionalization with fluorescent dye BodipyC10SH

After activation step of the PEG10K hydrogel H1, functionalization with a fluorescent dye, BodipyC10SH was tried. To a solution of BodipyC10SH (0.48 mg) in dry THF (1 mL), a piece of dried hydrogel H1 (6 mg, 1.43% furan) was added and reacted for 24 h. After washing the hydrogel with THF, fluorescence microscopy images were taken.

4.2.7. Functionalization with Streptavidin

After unmasking of maleimide groups with retro Diels-Alder reaction, a piece of PEG6K hydrogel H3 (6 mg, 0.51% furan) was added to a degassed solution of thiol containing Biotin (0.77mg) in MeOH (1 mL) and reacted for 16 h. Hydrogel was washed with MeOH a few times and FITC labeled Streptavidin (0.1 mg) was added onto the gel and left to react for 30 minutes. After washing with deionized water several times, fluorescent microscopy images were taken. For the control experiment, another piece of hydrogel H3 (6 mg, 0.51% furan) which was not biotinylated was placed in a vial and incubated with FITC labeled Streptavidin (0.1 mg). After washing with deionized water several times, fluorescent images were taken.

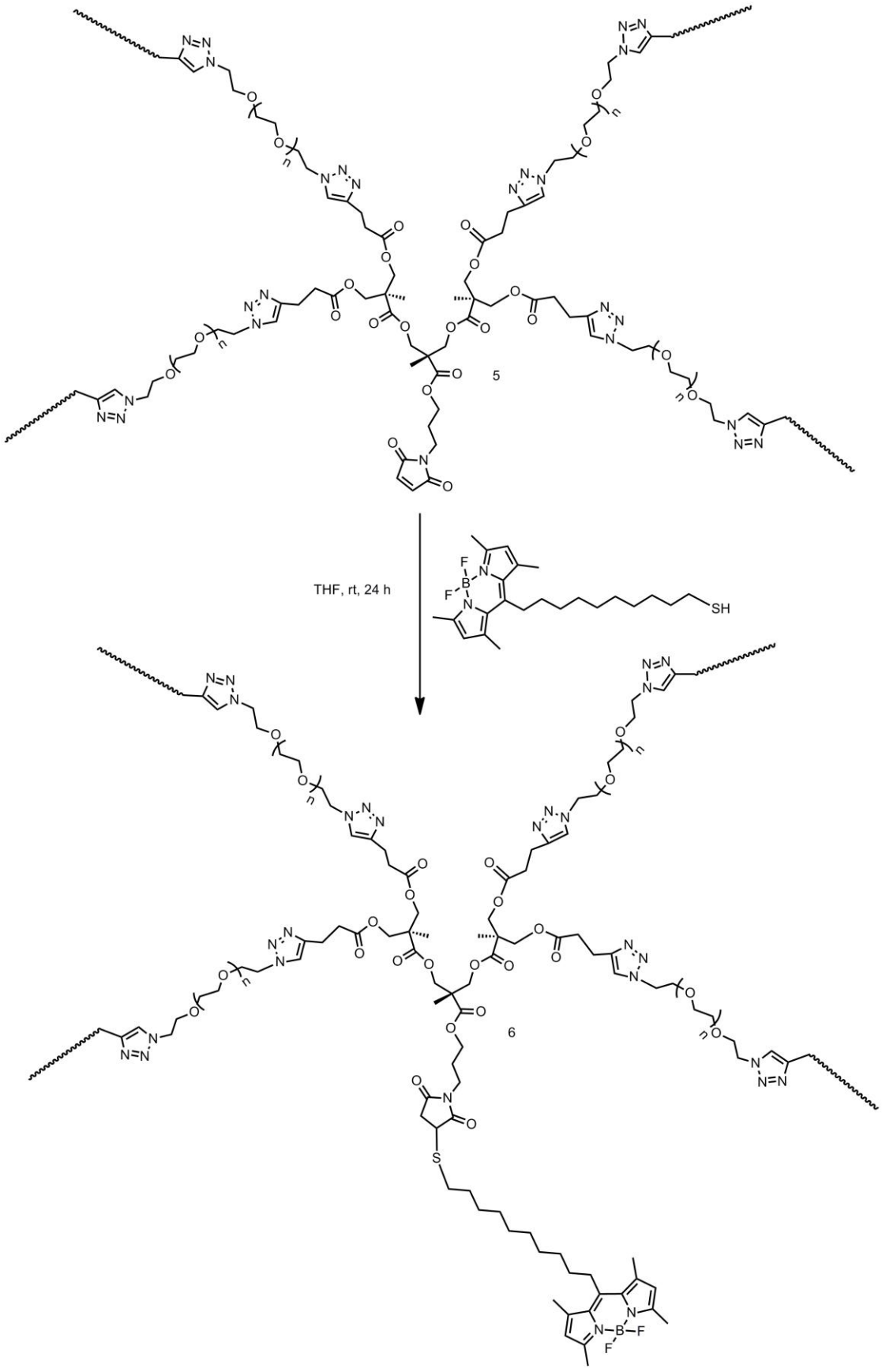

Figure 4.4. Functionalization of the hydrogel with fluorescent dye BODIPYC10SH.

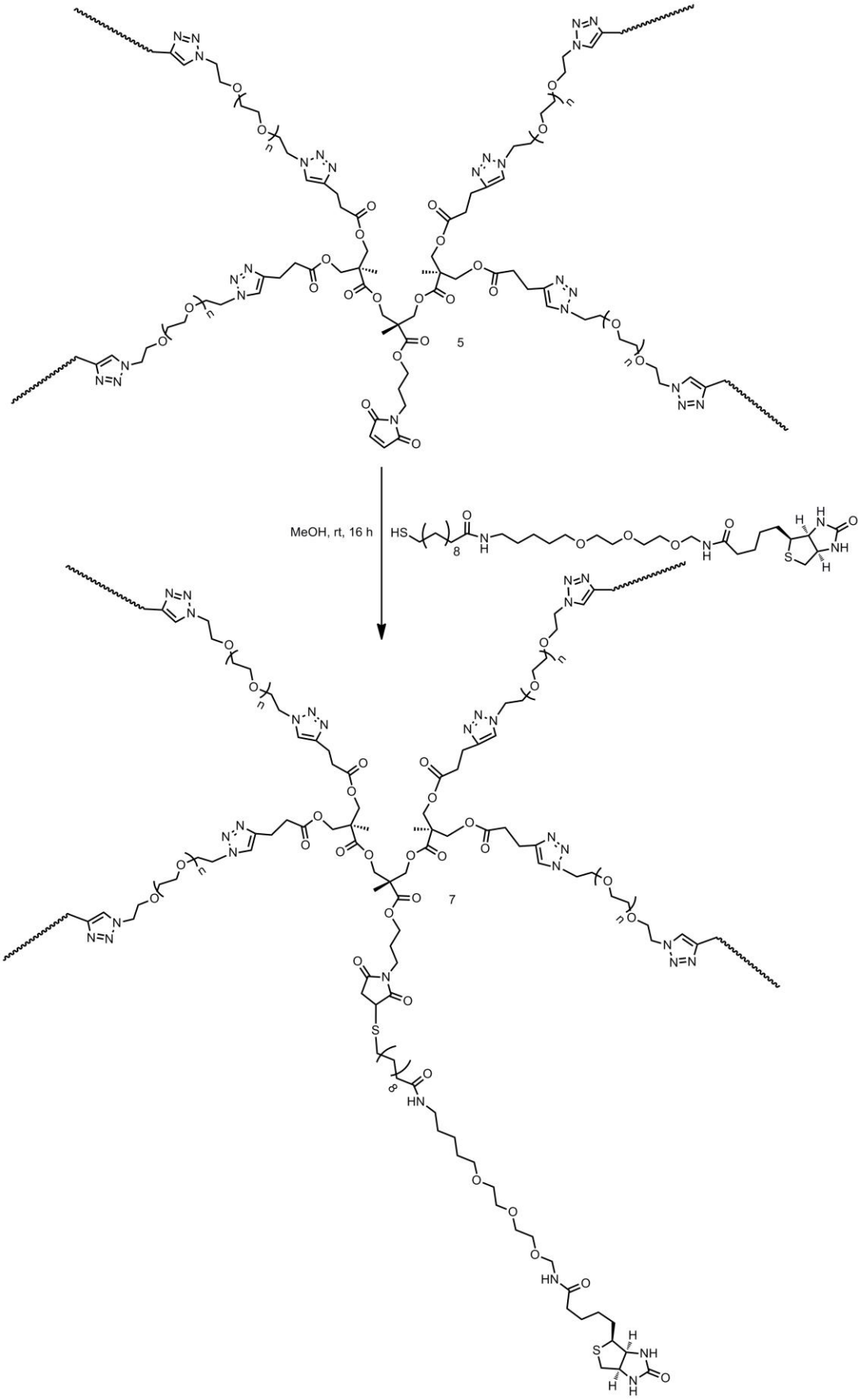

Figure 4.5. Biotinylation of hydrogel with Biotin-SH.

4.2.8. Activation of G2 alkyne dendron 3

Compound 3 (0.05 g, 0.056 mmol) was dissolved in dry toluene (4 mL) and the mixture was heated to reflux. Progress of the reaction was monitored by TLC until consumption of compound 3 is observed. The mixture was then concentrated in *vacuo* to give 8 (0.40 g , 91%) as a pale yellow viscous liquid. ^{1}H NMR ($CDCl_3$,δ, ppm) 6.70 (s, 2H), 4.26 (s, 4H), 4.25 (d, 4H, *J* = 11.2 Hz), 4.21 (d, 4H, *J* = 11.2 Hz), 4.07 (t, 2H, *J* = 6.4 Hz), 3.61 (t, 2H, *J* = 6.4 Hz), 2.56 – 2.53 (m, 8H), 2.48 – 2.44 (m, 8H), 1.98 – 1.92 (m, 6H), 1.27 (s, 3H), 1.24 (s, 6H), ^{13}C NMR ($CDCl_3$, δ, ppm) 171.6, 170.8, 170.3, 133.9, 82.1, 69.1, 65.3, 65.0, 61.9, 46.3, 46.0, 34.0, 32.8, 27.2, 17.5, 17.3, 13.9, FTIR (cm^{-1}) 1732.2, 1704.7.

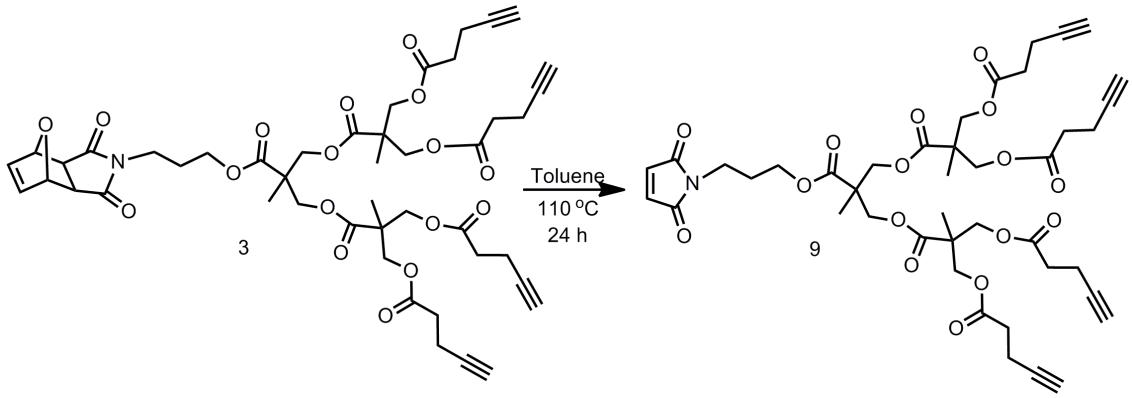

Figure 4.6. Activation of G2 alkyne dendron.

4.2.9. Synthesis of PEG Polymer Conjugates

$PEG_{750}N_3$ was synthesized according to literature procedure. $PEG_{750}N_3$ (0.222g, 0.292 mmol) was dissolved in THF (2 mL) and mixed with compound 8 (0.03g, 0.036mmol) in the presence of Cu(I)Br/PMDETA catalyst system under N_2 atmosphere. The mixture was then stirred at 50 ºC for 24 h. Product was purified by precipitation in ether to give compound 9 as a white solid.

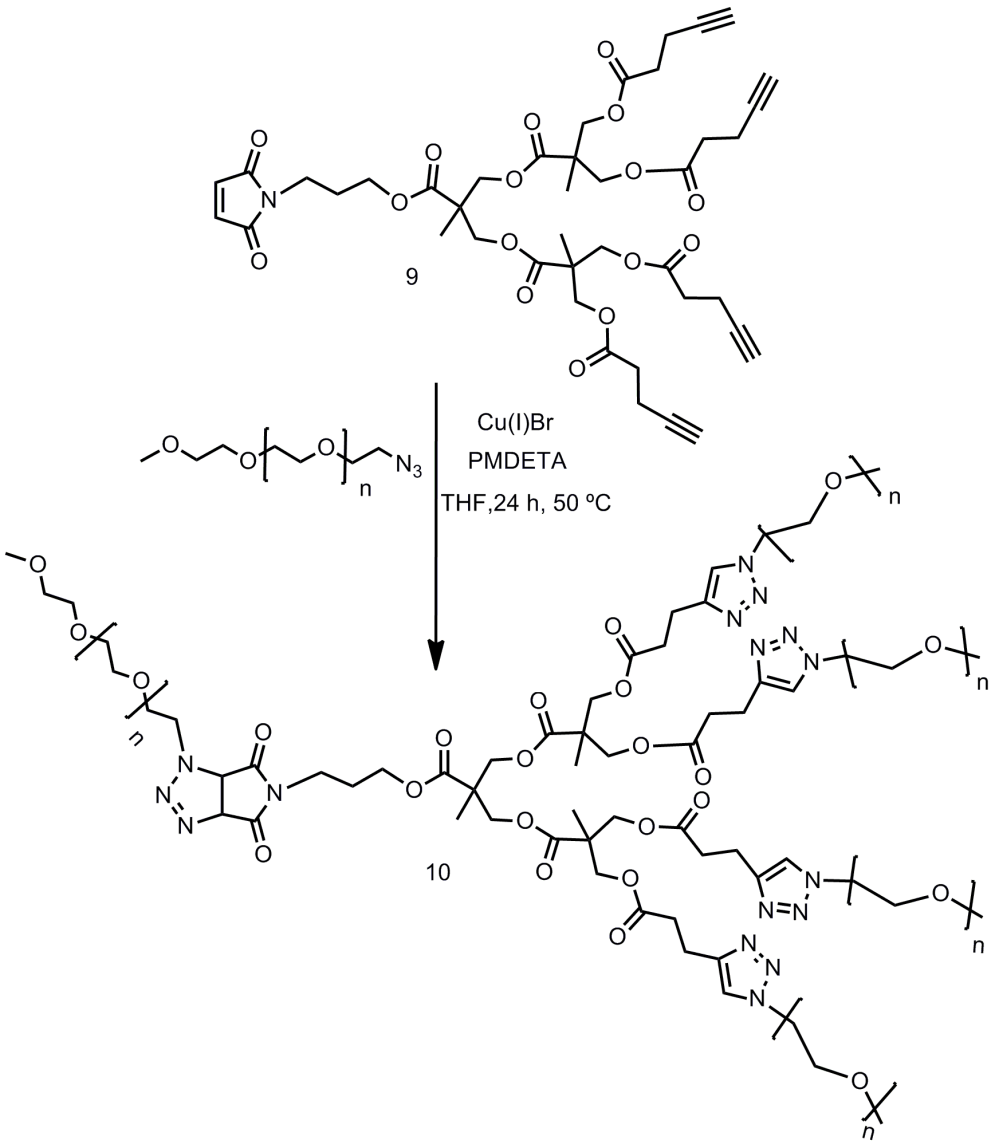

Figure 4.7. Synthesis of G2 Dendron-PEG polymer conjugate.

$PEG_{750}N_3$ (0.076g, 0.1 mmol) was dissolved in THF (3 mL) and mixed with N-Ethylmaleimide (0.025g, 0.2mmol) in the presence of Cu(I)Br/PMDETA catalyst system under N_2 atmosphere. The mixture was then stirred at 50 ºC for 24 h. Product was purified by column chromatography to give compound 10 as an orange viscous liquid. ^{1}H NMR ($CDCl_3$,δ, ppm) 5.50 (d, 1H, *J* = 11.0 Hz, N-C*H*), 4.62 (d, 1H, *J* = 11.0 Hz, N-C*H*), 3.73 (t, 2H, *J* = 5.2 Hz, N-CH_2 protons of PEG), 3.65-3.59 (m, 88H, O-CH_2 protons of PEG), 3.53 (q, 2H, N-CH_2-CH_3), 3.37(s, 3H, O-CH_3), 1.13 (t, 3H, *J* = 7.2 Hz, N-CH_2-CH_3).

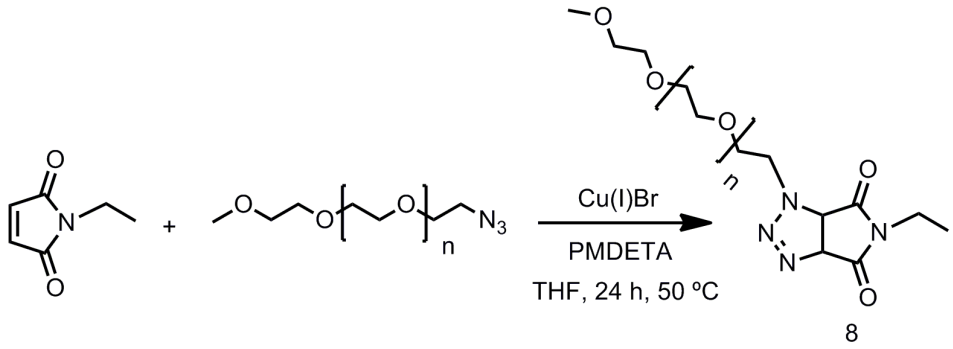

Figure 4.8. Synthesis of N-Ethylmaleimide-PEG polymer conjugate.

4.3 Biodegradable and Thiol Reactive Polymers

4.3.1 Synthesis of Cyclic Carbonate Monomer 3

Compound 1 (1.7 g, 4.5 mmol) was dissolved in MeOH (25 mL) and Dowex H^+ resin was added to this mixture with a tip of spatula. The resulting mixture was stirred at 40 ºC until complete consumption of 1 was observed via TLC. The resin was filtered off and washed with MeOH. The filtrate was then purified via precipitation from cold CH_2Cl_2 and concentrated in *vacuo* to give a white solid 2 (1.50 g, 99% yield). Compound 2 (1.50 g, 4.4 mmol) was then added to a solution of pyridine (2.08 mL, 25.8 mmol in dry CH_2Cl_2 (60 mL). To this solution, bis(trichloromethyl) carbonate (0.63 g, 2.14 mmol) in dry CH_2Cl_2 (20 mL) was added dropwise at -78 ºC. The resulting mixture was left to stir 2 hours at room temperature. Extraction was done with saturated NH_4Cl (1 x 100 mL), 1 M HCl (3 x 30 mL) and saturated $NaHCO_3$ (1 x 100 mL). Combined organic layers were dried over anhydrous Na_2SO_4 and the residue was purified via recrystallization from diethyl ether to give 1.35 g of the carbonate monomer 3 as a white solid (84% yield). ^1H NMR ($CDCl_3$, δ, ppm) 6.50 (s, 2H, C*H* = C*H*), 5.25 (s, 2H, C*H* bridgehead protons), 4.73 (d, 2H, *J* = 10.7 Hz, CH_2 ester protons), 4.20 (d, 2H, *J* = 10.7 Hz, CH_2 ester protons), 4.10 (t, 2H, J = 6.1 Hz, OCH_2), 3.57(t, 2H, *J* = 6.6 Hz, NCH_2), 2.84 (s, 2H, bridge protons), 1.99 – 1.92 (m, 2H, $NCH_2CH_2CH_2O$), 1.37 (s, 3H, CCH_3). ^{13}C NMR ($CDCl_3$, d, ppm) 175.2, 169.8, 146.6, 135.6, 80.1, 72.1, 61.5, 46.6, 39.1, 34.1, 25.5, 16.8. Anal. Calcd. for maleimide functional carbonate monomer [$C_{17}H_{19}NO_8$]: C, 55.89; H, 5.24; N, 3.83. Found: C, 55.45; H, 5.24; N, 3.84.

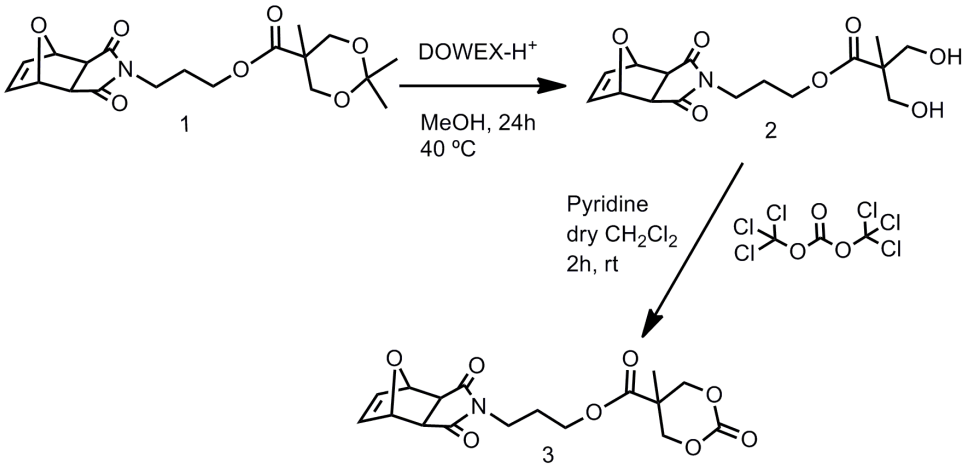

Figure 4.9. Synthesis of maleimide functional carbonate monomer 3.

4.3.2. Synthesis of maleimide functional homopolymers

Monomer 3 (50 mg, 0.14 mmol), benzyl alcohol (0.71 μL, 6.8 x 10^{-3} mmol) and 1,8-diazabicycloundec-7-ene (1.93 μL, 1.37 x 10^{-3} mmol) were placed in a vial under nitrogen atmosphere of a glove box. Degassed $CDCl_3$ (1 mL) was added to the reaction mixture and left to stir for 4 hours at room temperature. The resulting polymer was puried by precipitation from 1:3 methanol : diethyl ether mixture. The polymer was dried for 24 h in a vacuum oven at room temperature. ($[M]_0/[I]_0$ = 20, conversion = 50%, $M_{n,theo}$ = 3762, $M_{n,NMR}$ = 2593, $M_{n,GPC}$ = 2803, M_w/M_n = 1.07) ^{1}H NMR ($CDCl_3$, δ, ppm) 7.35 – 7.30 (m, 5H, aromatic C*H* = C*H*), 6.47 (s, 12H, C*H* = C*H*), 5.23 (s, 12H, C*H* bridgehead protons), 5.12 (s, 2H, benzylic protons) 4.32 (s, 24H, CH_2 ester protons), 4.04 (t, 12H, *J* = 5.0 Hz, OCH_2), 3.55 (t, 12H, J = 6.6 Hz, NCH_2), 3.07 (s, 1H, O*H*), 2.82 (s, 12H, bridge protons), 1.93 – 1.86 (m, 12H, $NCH_2CH_2CH_2CH_2O$), 1.22 (s, 18H, CCH_3).

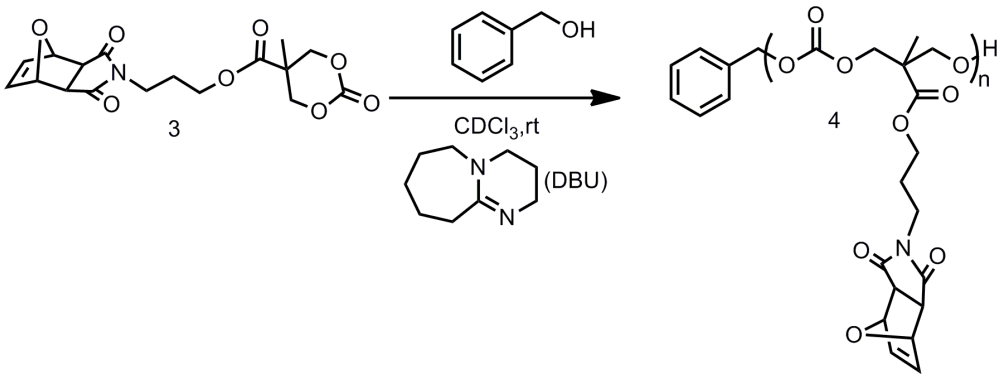

Figure 4.10. Synthesis of maleimide functional homopolymer 4.

4.3.3. Synthesis of activated homopolymer by retro Diels-Alder reaction

Polymer 4 was left at 100ºC in a vacuum oven for 24 hours. ^{1}H NMR analysis proves that oxabicyclic moiety conversion to the maleimide functional group has been achieved. ($M_{n,GPC}$ = 2684, M_w/M_n = 1.11) ^{1}H NMR ($CDCl_3$, δ, ppm) 7.29 – 7.28 (m, 5H, aromatic C*H* = C*H*), 6.69 (s, 12H, C*H* = C*H*), 5.12 (s, 2H, benzylic protons) 4.30 (s, 24H, CH_2 ester protons), 4.06 (t, 12H, *J* = 6.1 Hz, OCH_2), 3.58 (t, 12H, J = 7.3 Hz, NCH_2), 2.82 (s, 1H, O*H*), 1.94 (m, 12H, $NCH_2CH_2CH_2O$), 1.23 (s, 18H, CCH_3).

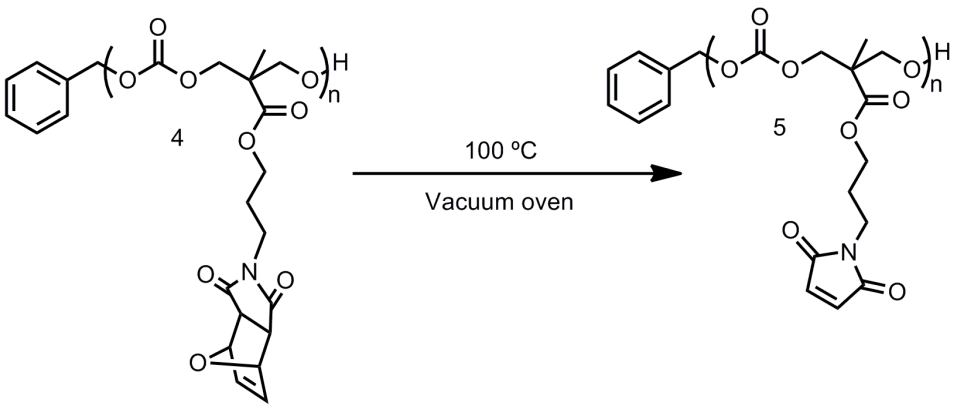

Figure 4.11. Activation of maleimide functional homopolymer 4.

4.3.4. Synthesis of maleimide functional PLLA copolymers

Monomer 3 (0.5 g, 1.37 mmol), benzyl alcohol (7.09 μL, 6.85 x 10^{-2} mmol), L-lactide (0.79 g, 5.47 mmol) and 1,8-diazabicycloundec-7-ene (3.95 μL, 2.74 x 10^{-2} mmol) were placed in a vial under nitrogen atmosphere of a glove box. Degassed $CDCl_3$ (9 mL) was added to the reaction mixture and left to stir for 24 hours at room temperature. The resulting polymer was puried by precipitation from 1:1 methanol : diethyl ether mixture. The polymer was dried for 24 h in a vacuum oven at room temperature. ($[M]_0/[I]_0$ = 100, conversion = 85%, $M_{n,theo}$ = 16 088, $M_{n,NMR}$ = 13 700, $M_{n,GPC}$ = 17 148, M_w/M_n = 1.16) ^{1}H NMR ($CDCl_3$, δ, ppm) 7.35 – 7.31 (m, 5H, aromatic C*H* = C*H*), 6.48 (s, 12H, C*H* = C*H*), 5.28 (s, 12H, C*H* bridgehead protons), 5.14 (q, 158H, C*H* protons of lactide) 4.30 (d, *J* = 5.7 Hz, 24H, CH_2 ester protons), 4.04 (t, 12H, *J* = 5.0 Hz, OCH_2), 3.54 (t, 12H, *J* = 6.5 Hz, NCH_2), 2.83 (s, 12H, bridge protons), 1.93 – 1.86 (m, 12H, $NCH_2CH_2CH_2O$), 1.56 (d, *J* = 6.4 Hz, 474H, CH_3 protons of lactide), 1.23 (s, 18H, CCH_3).

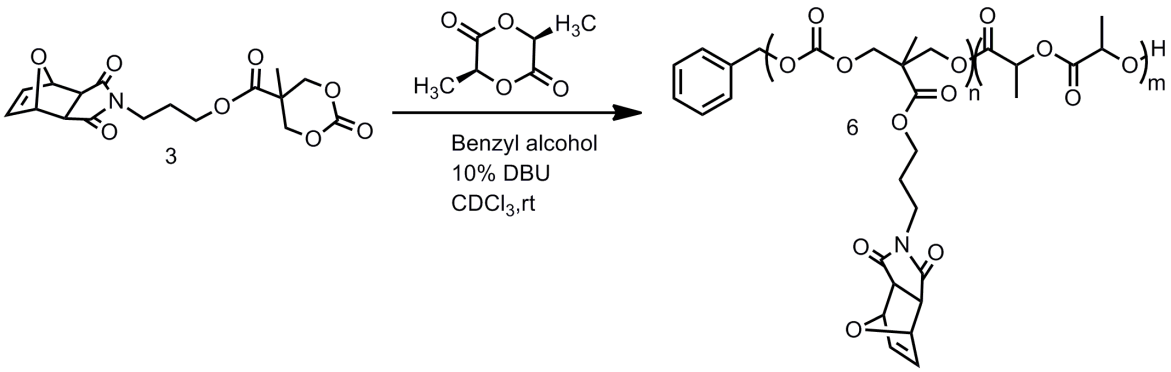

Figure 4.12. Synthesis of maleimide functional copolymer 6.

4.3.5. Synthesis of activated copolymer by retro Diels-Alder reaction

Polymer 6 was left at 100 ºC for 24 hours under high vacuum. ^{1}H NMR analysis proves that cativation of maleimide double bond has been achieved. ($M_{n,GPC}$ = 17 000, M_w/M_n = 1.18) ^{1}H NMR ($CDCl_3$,δ, ppm) 7.34 – 7.30 (m, 5H, aromatic C*H* = C*H*), 6.69 (s, 12H, C*H* = C*H*), 5.16 (q, 158H, C*H* protons of lactide) 4.29 (d, *J* = 5.7 Hz, 24H, CH_2 ester protons), 4.07 (t, 12H, *J* = 5.0 Hz, OCH_2), 3.56 (t, 12H, *J* = 6.5 Hz, NCH_2), 3.09 (1.96 – 1.89 (m, 12H, $NCH_2CH_2CH_2O$), 1.55 (d, *J* = 6.7 Hz, 474H, CH_3 protons of lactide), 1.26 (s, 18H, CCH_3).

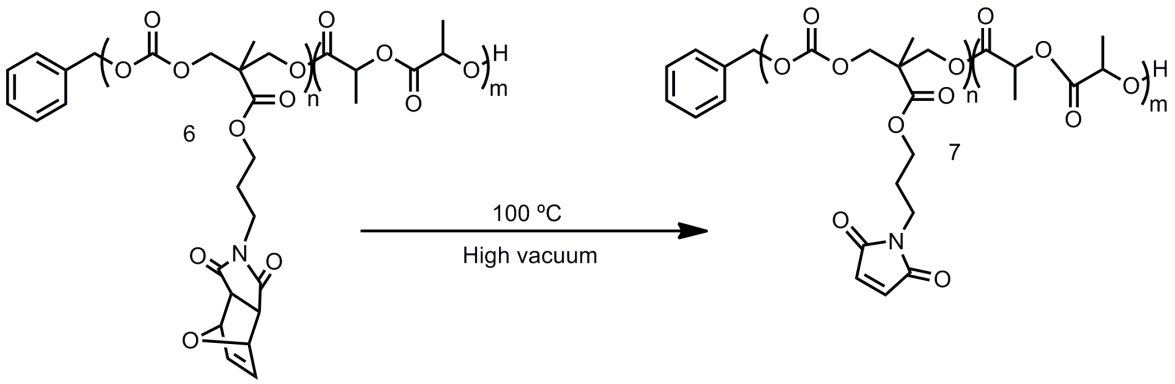

Figure 4.13. Activation of maleimide functional copolymer 6.

4.3.6. Functionalization of copolymer 7 with 6-(ferrocenyl)hexanethiol

Copolymer **7** (20 mg, 1.2 x 10^{-3} mmol), 6-(ferrocenyl)hexanethiol (7.26 mg, 2.4 x 10^{-3} mmol) and NEt_3 (3.4 μL, 2.4 x 10^{-3} mmol) were dissolved in 1 mL dry CH_2Cl_2 and left to stir at room temperature under nitrogen atmosphere for 24 hours. Obtained polymer was purified by precipitation from 1:1 methanol : diethyl ether mixture. ($M_{n,GPC}$ = 18 400, M_w/M_n = 1.20) ^{1}H NMR ($CDCl_3$,δ, ppm) 7.33 – 7.31 (m, 5H, aromatic C*H* = C*H*), 5.14 (q, 158H, C*H* protons of lactide), 4.29 (d, *J* = 5.7 Hz, 24H, CH_2 ester protons), 4.08 (s, 30H, C*H* protons of ferrocene), 4.07 (t, 12H, *J* = 5.0 Hz, OCH_2), 4.01 (s, 24H, C*H* protons of ferrocene), 3.58 (t, 12H, *J* = 6.5 Hz, NCH_2), 3.09 (br, 6H, CH_2-CH-S), 2.84 (br, 6H, C*H*-S-CH_2), 2.72 (br, 12H, CH_2-S), 2.50 (br, 6H, CH_2-CH-S), 2.28 (t, 12H, Fer-CH_2), 1.93 – 1.80 (m, 12H, $NCH_2CH_2CH_2O$), 1.55 (d, *J* = 6.7 Hz, 474H, CH_3 protons of lactide), 1.26 (s, 18H, CCH_3).

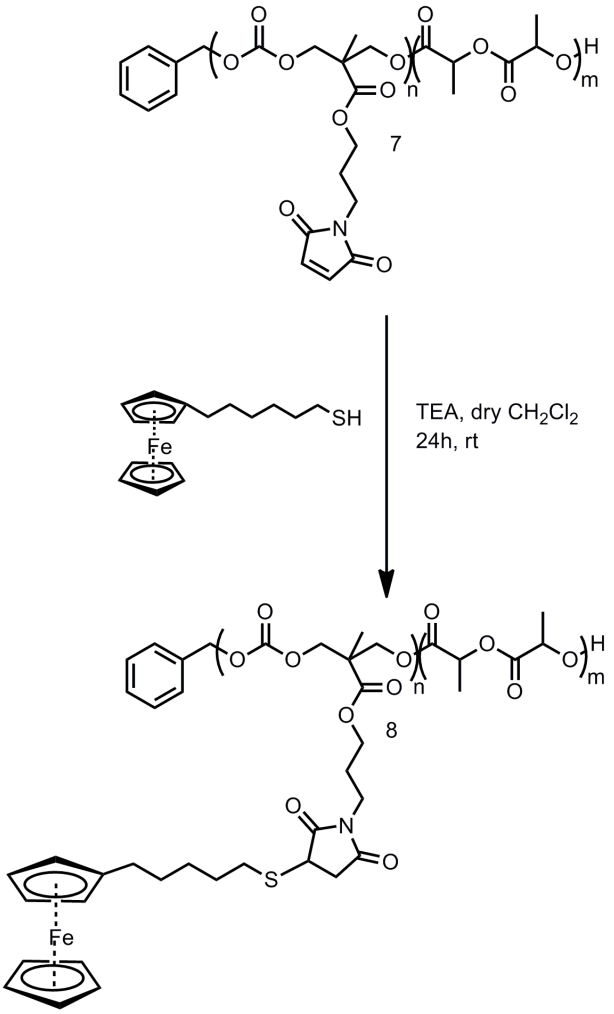

Figure 4.14. Functionalization of copolymer **7** with 6-(ferrocenyl) hexanethiol.

4.3.7. Functionalization of copolymer 7 with 1-hexanethiol

Copolymer **7** (20 mg, 1.2 x 10^{-3} mmol), 1-hexanethiol (3.4 μL, 2.4 x 10^{-3} mmol) and NEt_3 (3.4 μL, 2.4 x 10^{-3} mmol) were dissolved in 1 mL dry CH_2Cl_2 and left to stir at room temperature under nitrogen atmosphere for 24 hours. Obtained polymer was purified by precipitation from 1:1 methanol : diethyl ether mixture. ($M_{n,GPC}$ = 17 761, M_w/M_n = 1.19) ^{1}H NMR ($CDCl_3$,δ, ppm) 7.34 – 7.30 (m, 5H, aromatic C*H* = C*H*), 5.16 (q, 158H, C*H* protons of lactide) 4.29 (d, *J* = 5.7 Hz, 24H, CH_2 ester protons), 4.07 (t, 12H, *J* = 5.0 Hz, OCH_2), 3.58 (t, 12H, *J* = 6.5 Hz, NCH_2), 3.06 (br, 6H, CH_2-CH-S), 2.85 (br, 6H, C*H*-S-CH_2), 2.74 (br, 12H, CH_2-S), 2.47 (br, 6H, CH_2-CH-S), 1.96 – 1.89 (m, 12H, $NCH_2CH_2CH_2O$), 1.55 (d, *J* = 6.7 Hz, 474H, CH_3 protons of lactide), 1.26 (s, 18H, CCH_3), 0.87 (t, 18H, *J* = 6.4 Hz, CH_3 protons of hexanethiol).

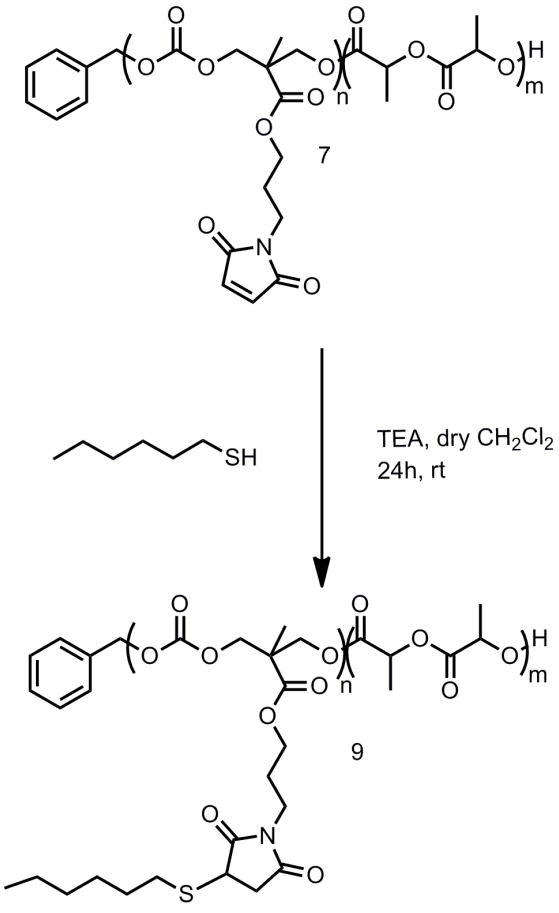

Figure 4.15. Functionalization of copolymer **7** with 1-hexanethiol.

5. CONCLUSIONS

Site-specific and highly efficient Michael type thiol-ene chemistry was utilized to obtain novel thiol reactive polymers and hydrogels. These side-chain multifunctional materials have biodegradable backbones which were prepared from polyester dendrons. They gain an increased interest in recent years due to the broadening applications in the fields like biomolecular immobilization, drug-delivery and enzyme modifications.

In the first part of the study, a special type of biodegradable and orthogonally functionalizable G2 alkyne dendron was utilized to form thiol reactive hydrogels utilizing Diels – Alder / retro Diels – Alder strategy. Alkyne units of this dendron were crosslinked with azide containing PEG chains via copper catalyzed Huisgen type of [3+2] cycloaddition. Unmasking of maleimide groups into their reactive forms was monitored by thermogravimetric analysis. Functional hydrogels were derivatized with thiol containing molecules via Michael type thiol-ene addition. Efficient bioconjugation was achieved with the fluorescent dye BODIPY-SH and extent of bioimmobilization was tailored with FITC labeled Streptavidin after covalent attachment of biotin ligand to the hydrogels. Effect of varying maleimide density on immobilization efficiency was investigated from fluorescence profiles of functionalized gels. As an extension, necessity of using Diels-Alder strategy for the maleimide protection was proved with a series of control experiments.

In the second part, a new class of maleimide containing cyclic carbonate monomer has been synthesized and its self polymerization and copolymerization character with L-lactide has been investigated via organocatalytic ring opening mechanism. Obtained polymers have narrow molecular weight distributions. The side chains of these polymers were activated by retro Diels-Alder reaction to obtain reactive maleimide groups for further conjugations.

APPENDIX

^{1}H NMR, ^{13}C NMR and IR data of the newly synthesized compounds are included.

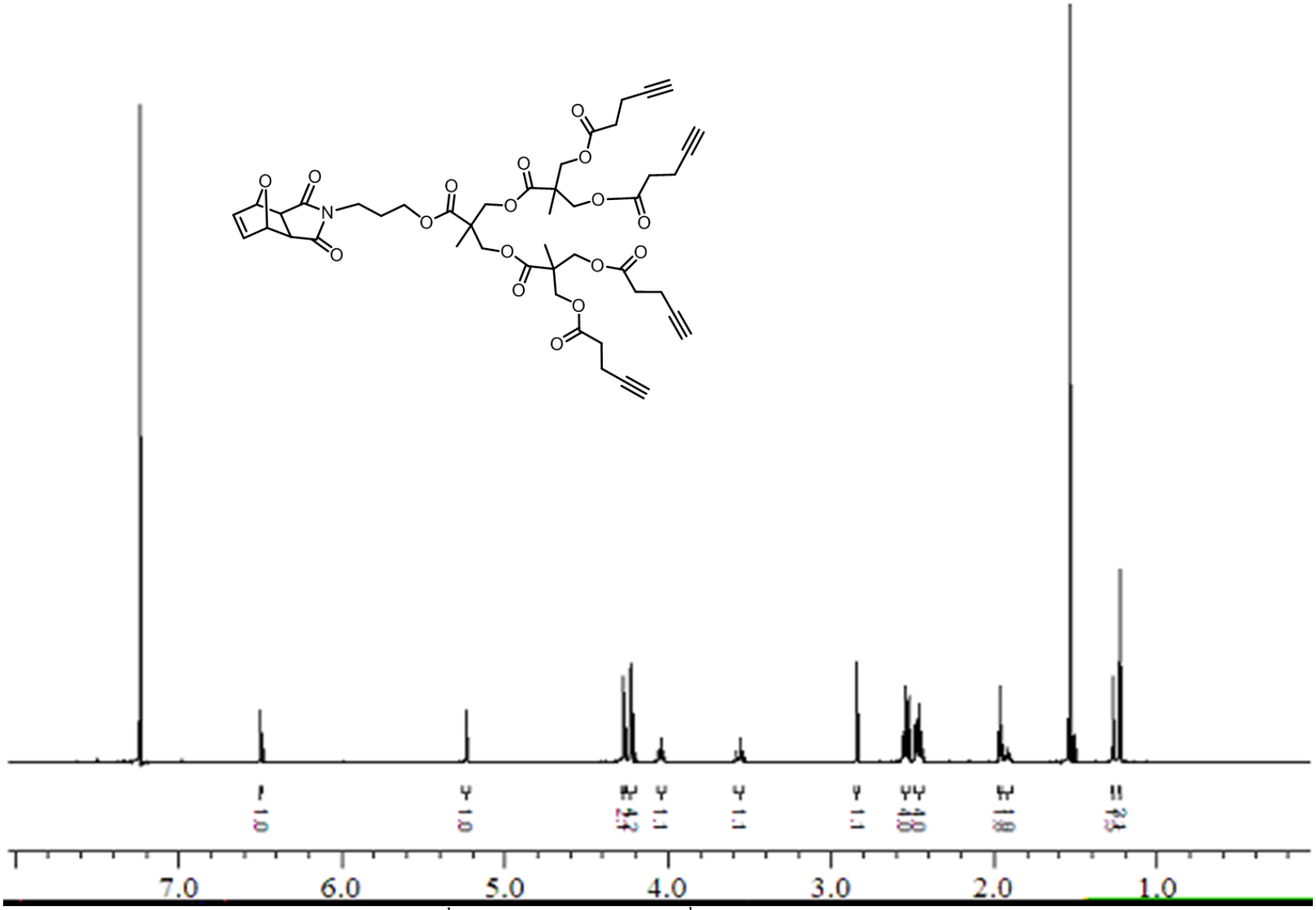

Figure A.1. ^{1}H NMR spectrum of 2nd generation alkyne dendron 3.

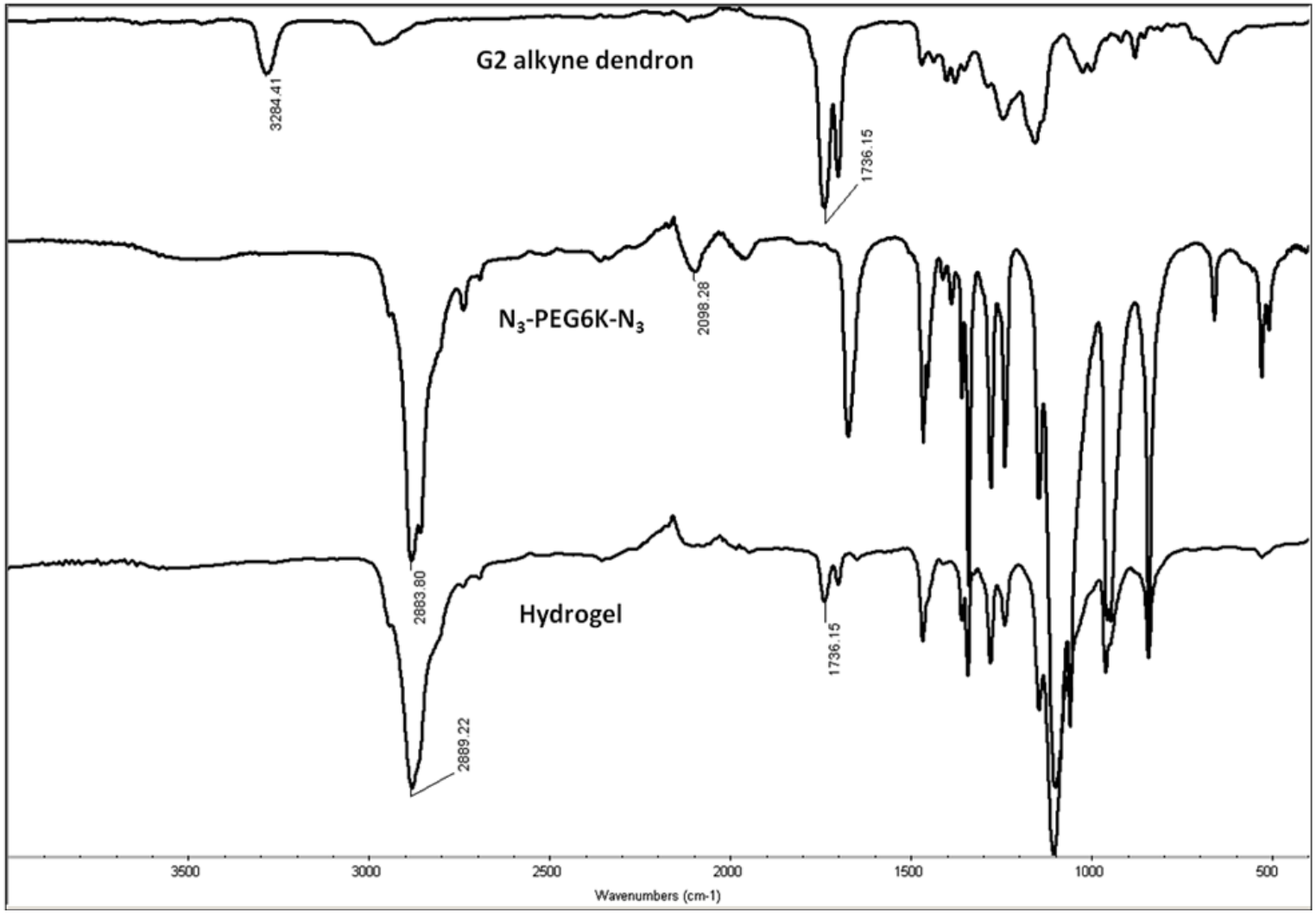

Figure A.2. FTIR traces of G2 alkyne dendron 3, PEG6K bisazide and the hydrogel 4.

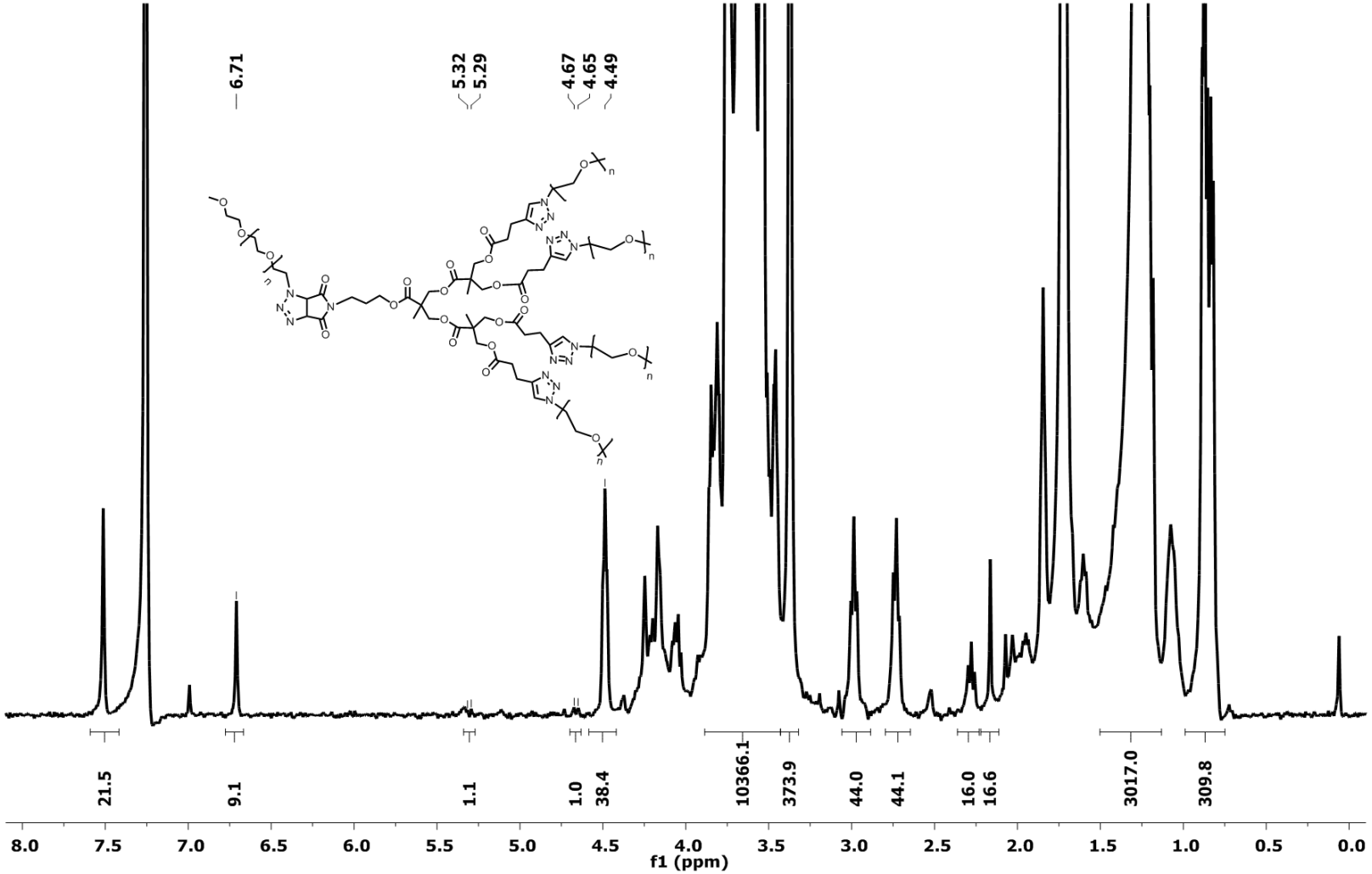

Figure A.3. ^{1}H NMR spectrum of Dendron-PEG polymer conjugate 9 (1:1 Alkyne:Azide ratio).

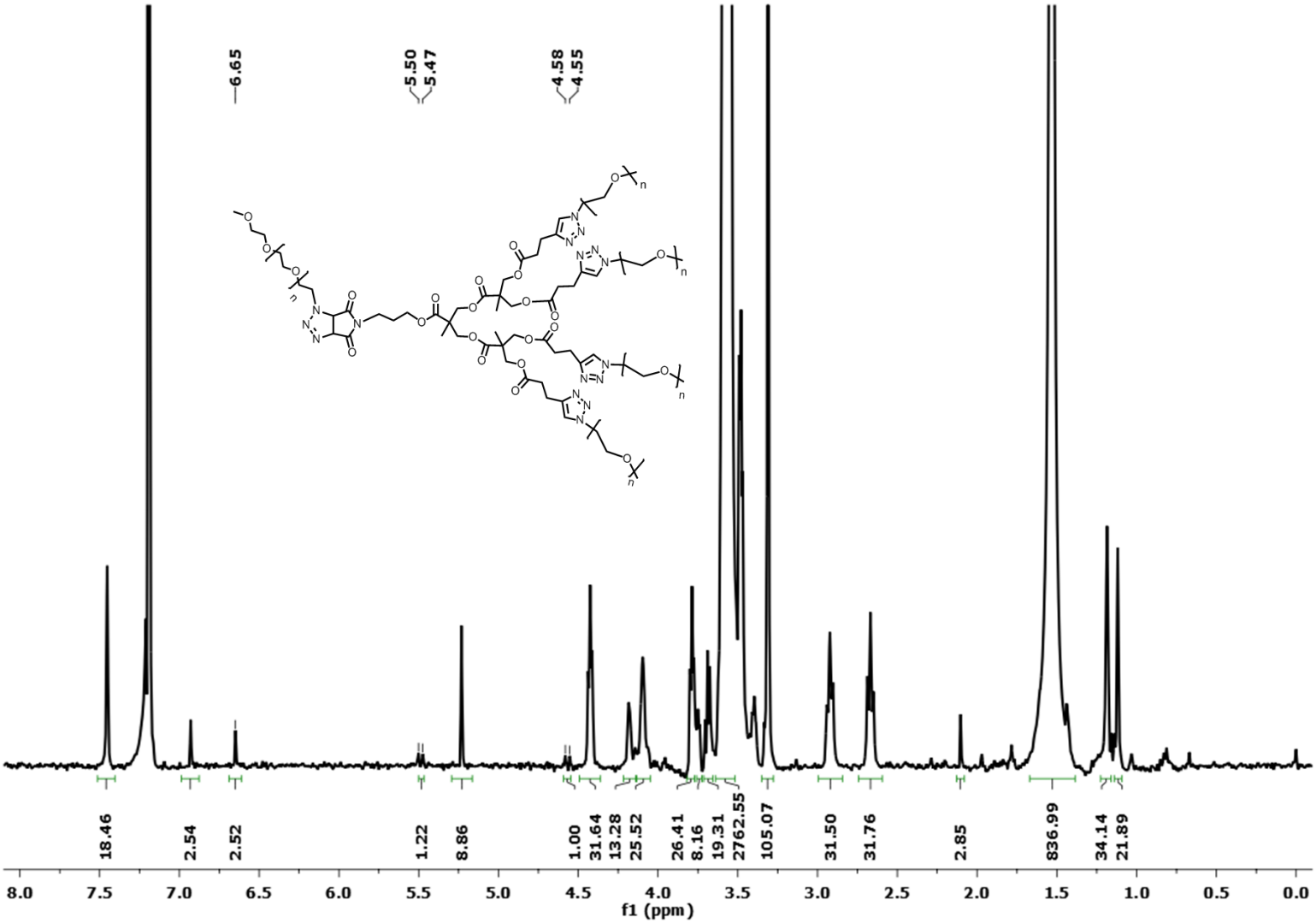

Figure A.4. ^{1}H NMR spectrum of Dendron-PEG polymer conjugate (1:2 Alkyne:Azide ratio).

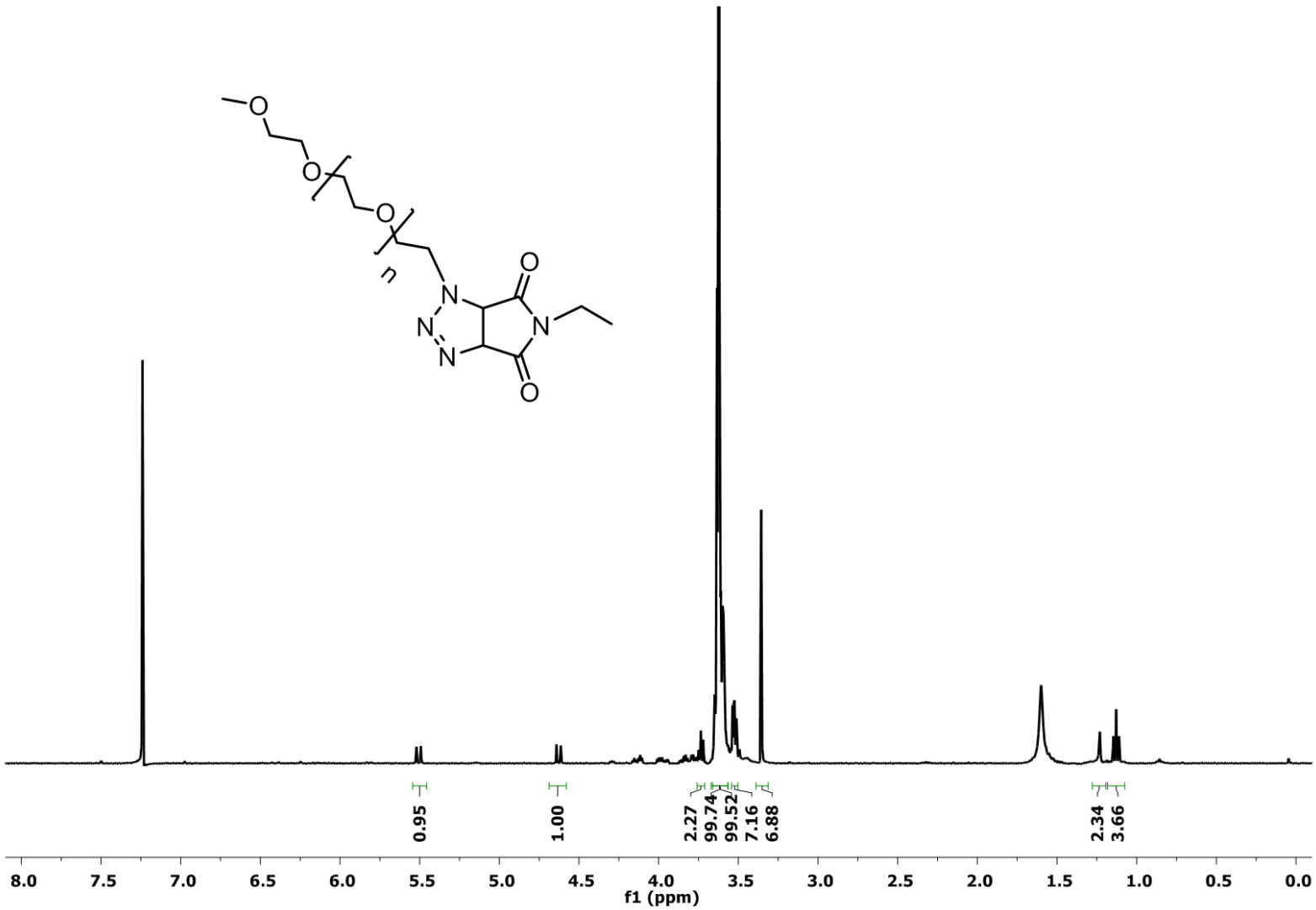

Figure A.5. ^{1}H NMR spectrum of N-Ethylmaleimide-PEG polymer conjugate 10.

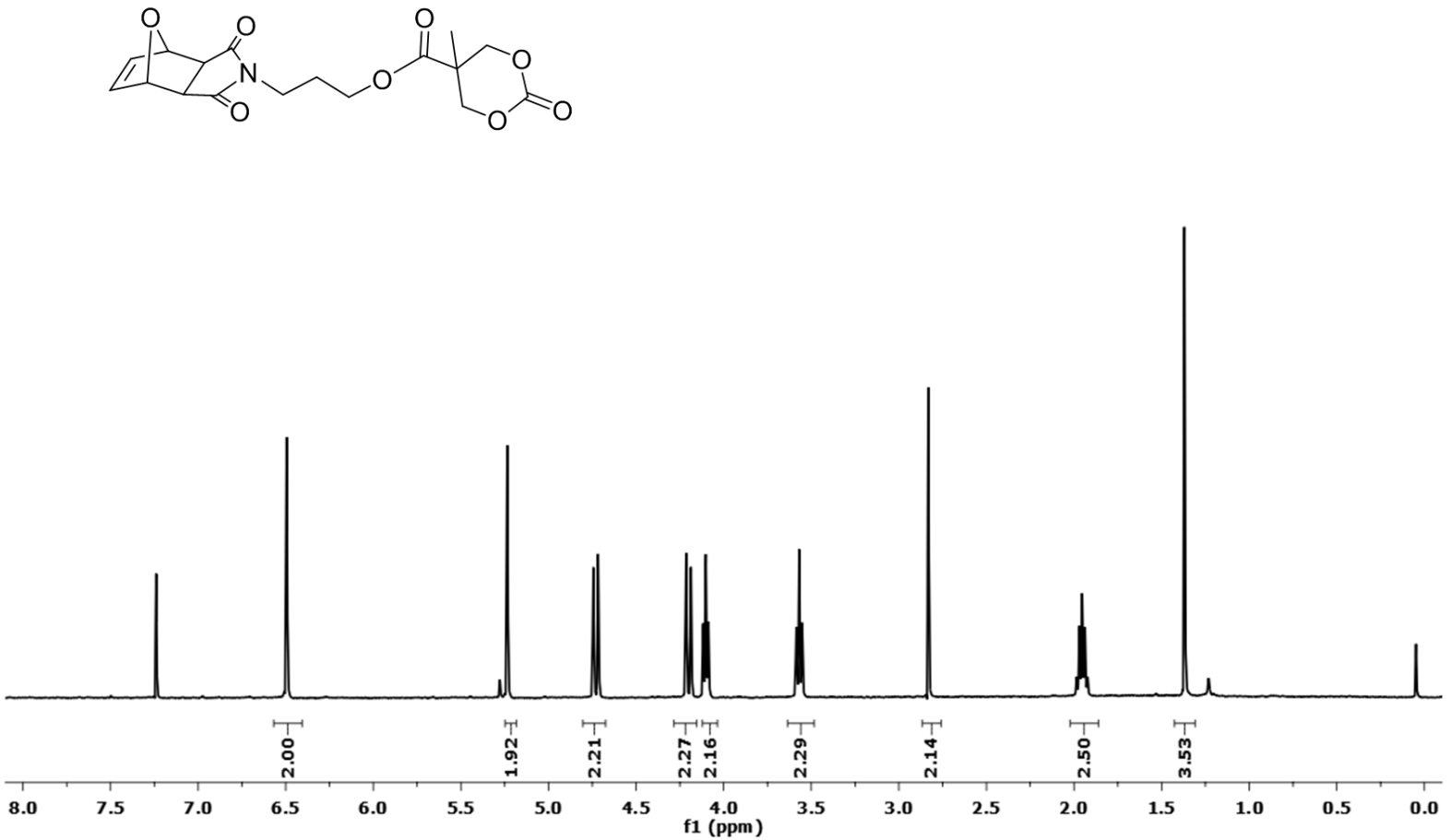

Figure A.6. ^{1}H NMR spectrum of maleimide functional carbonate monomer 3.

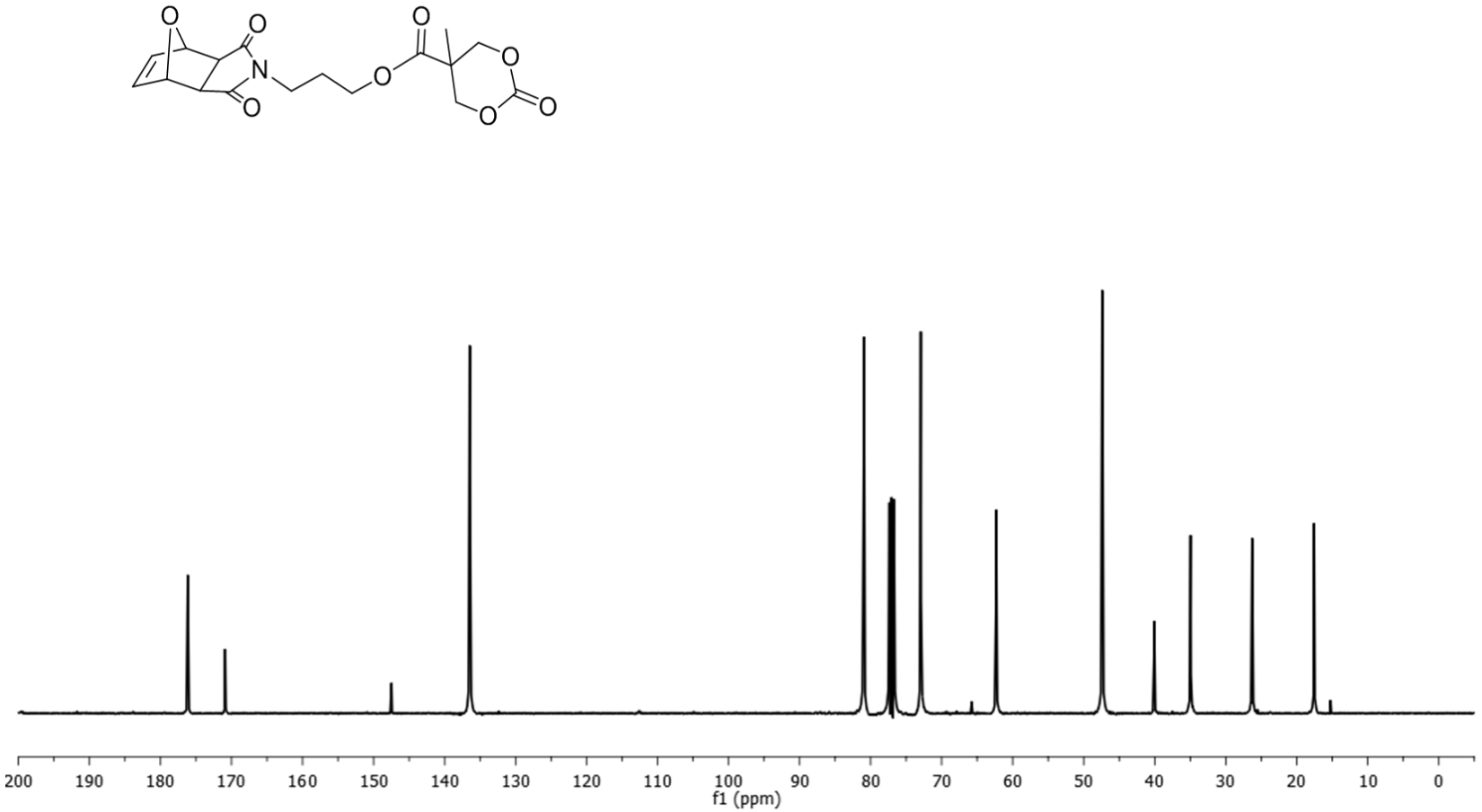

Figure A.7. ^{13}C NMR spectrum of maleimide functional carbonate monomer 3.

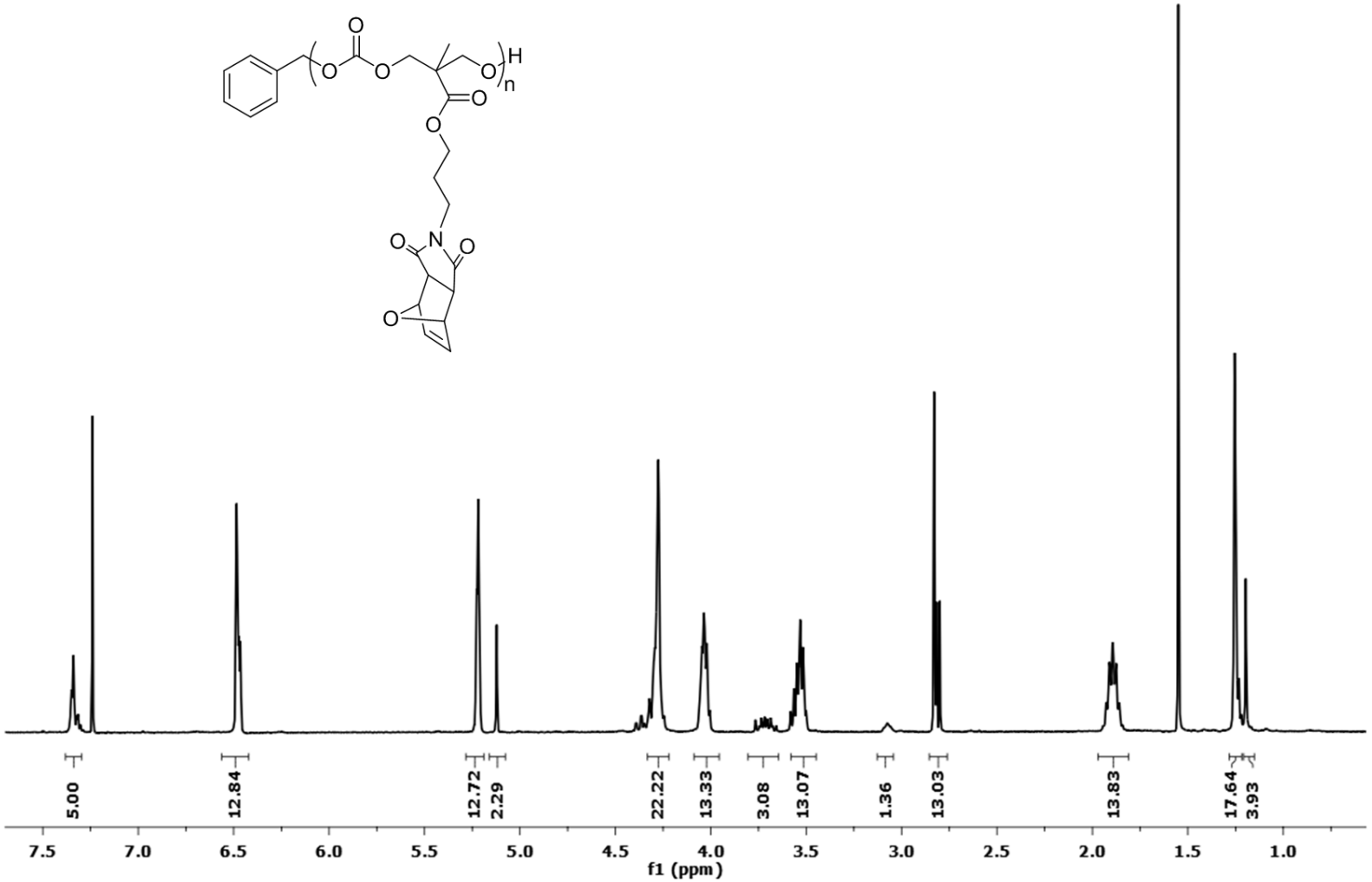

Figure A.8. ^{1}H NMR spectrum of maleimide functional homopolymer 4.

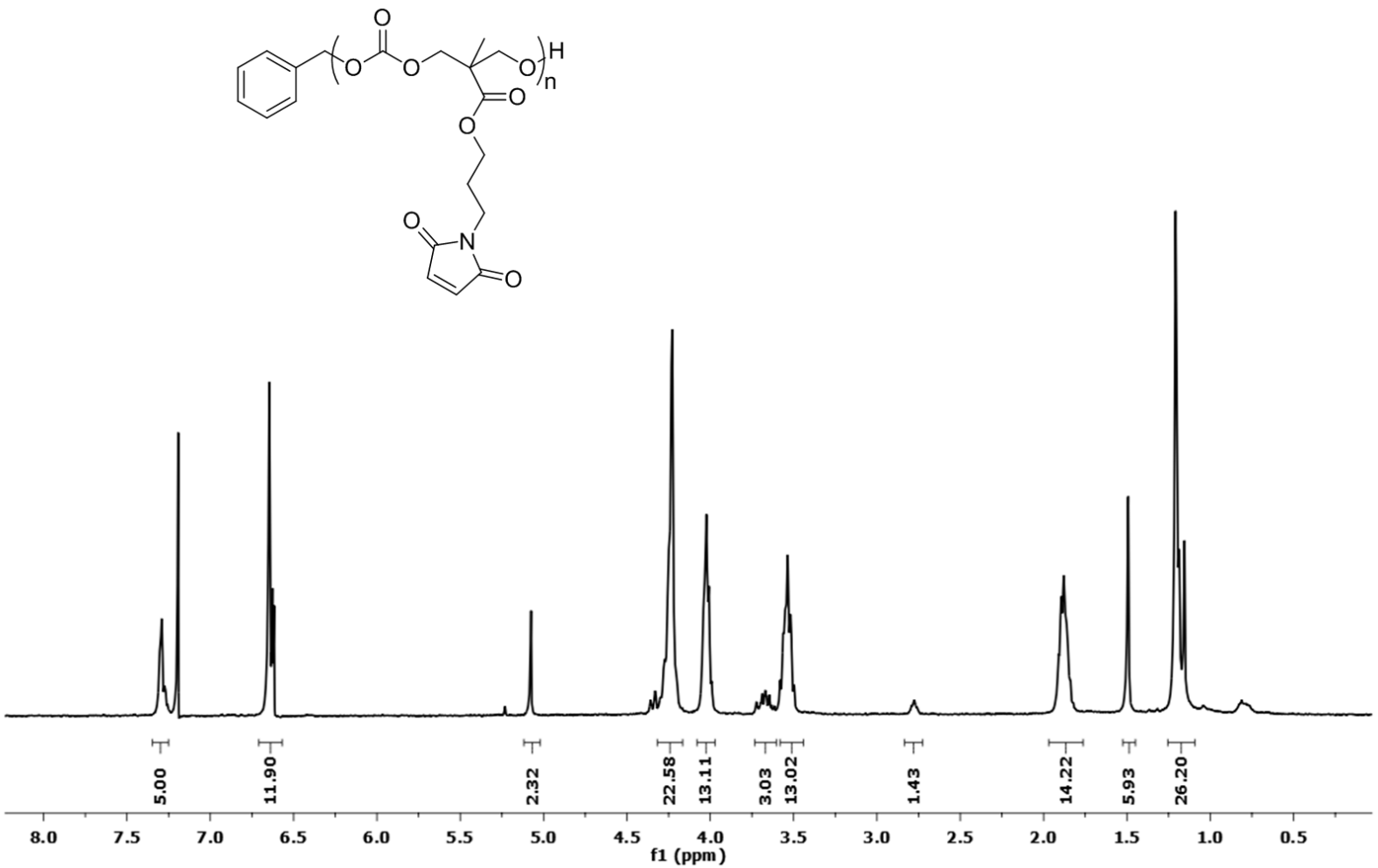

Figure A.9. ^{1}H NMR spectrum of activated homopolymer 5.

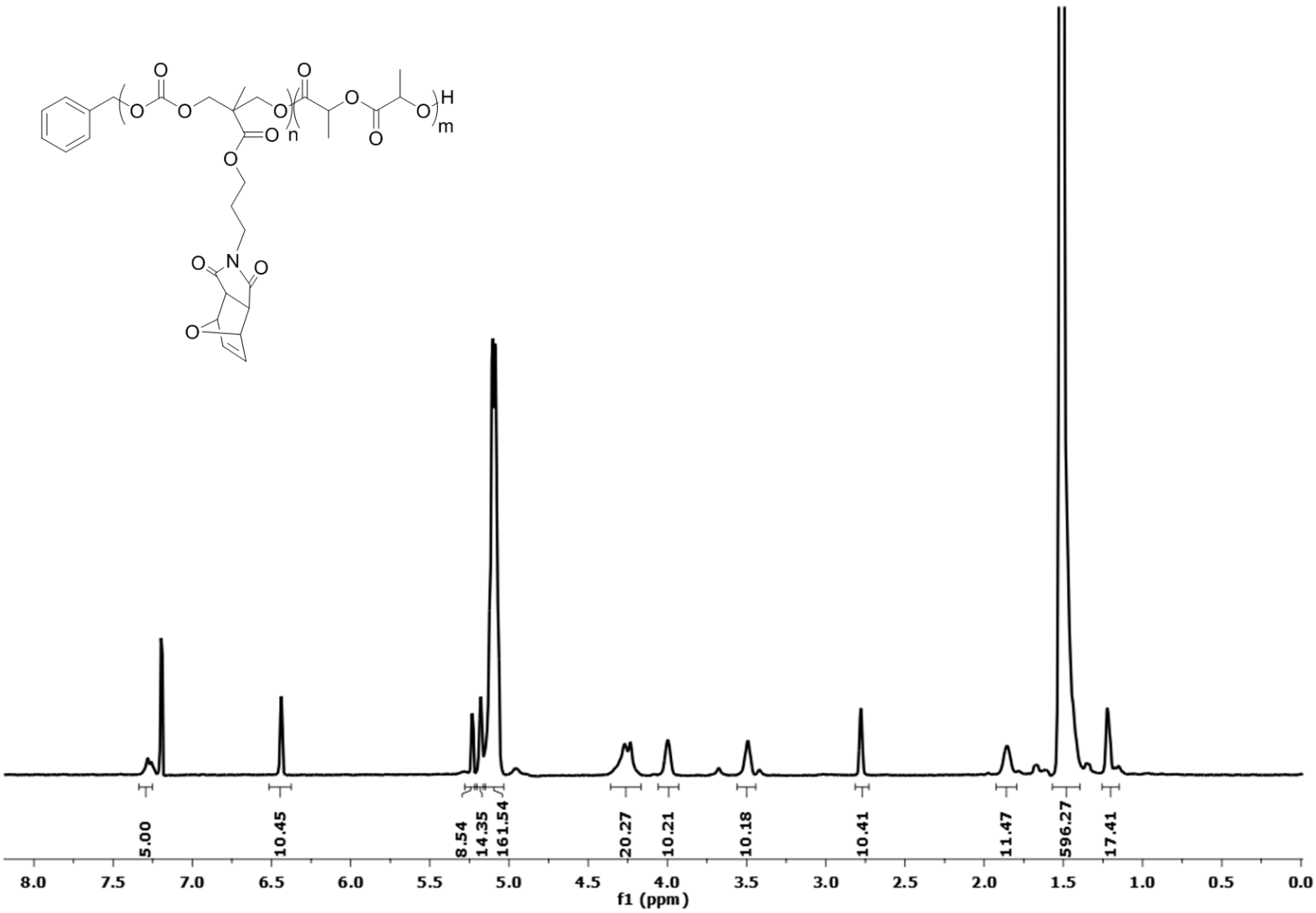

Figure A.10. ^{1}H NMR spectrum of maleimide functional copolymer 6.

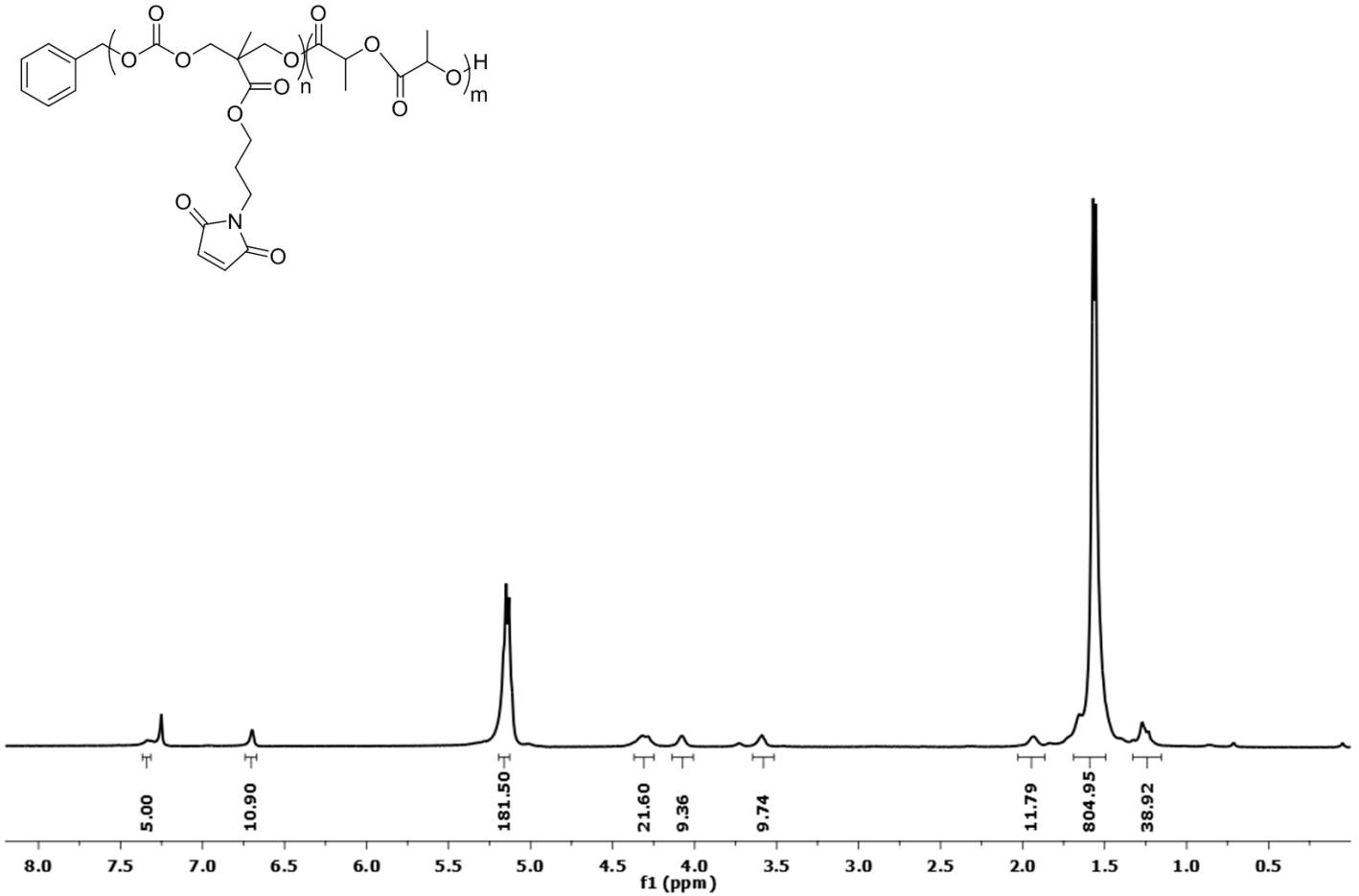

Figure A.11. ^{1}H NMR spectrum of activated copolymer 7.

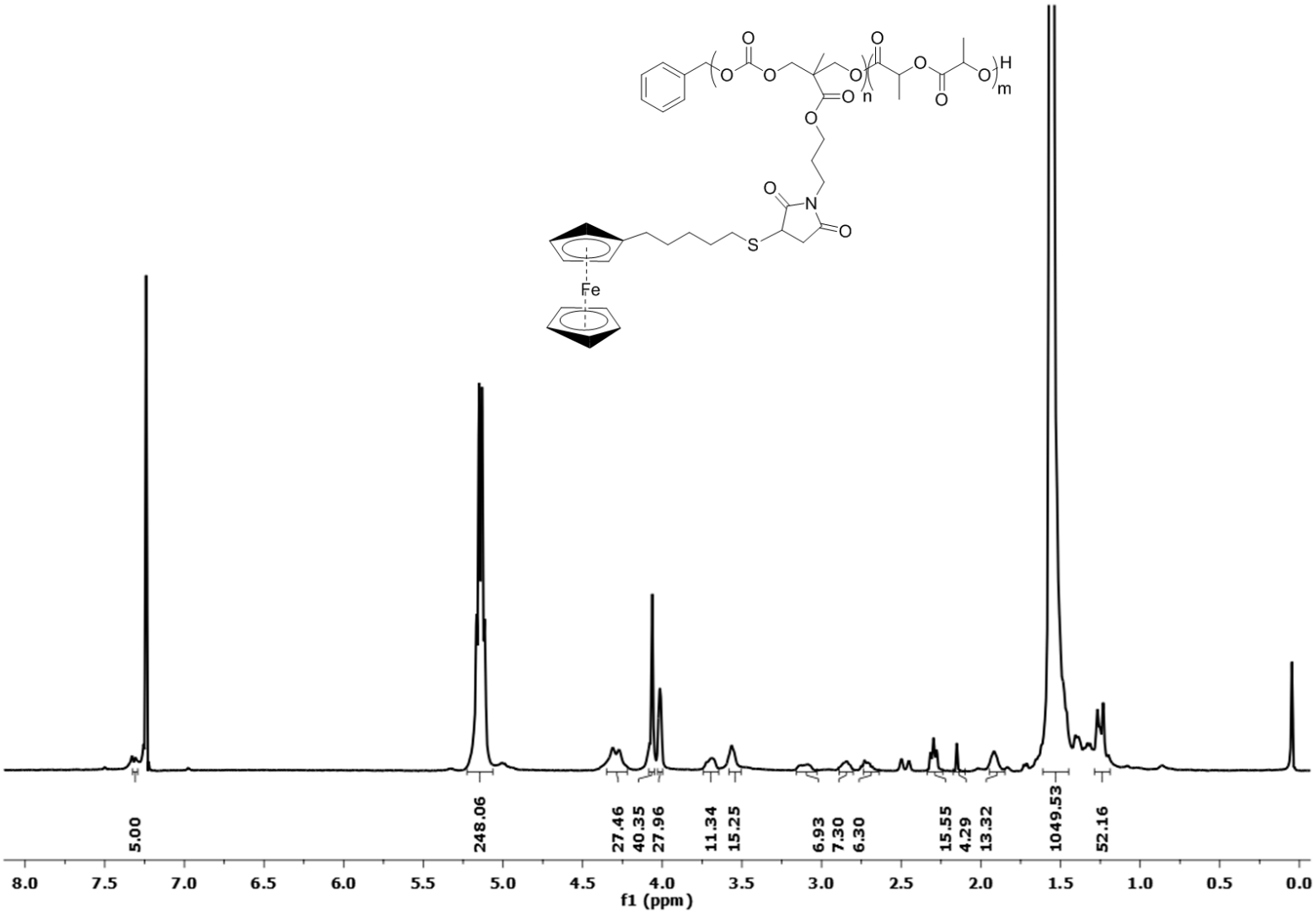

Figure A.12. ^{1}H NMR spectrum of 6-(ferrocenyl) hexanethiol functionalized copolymer 8.

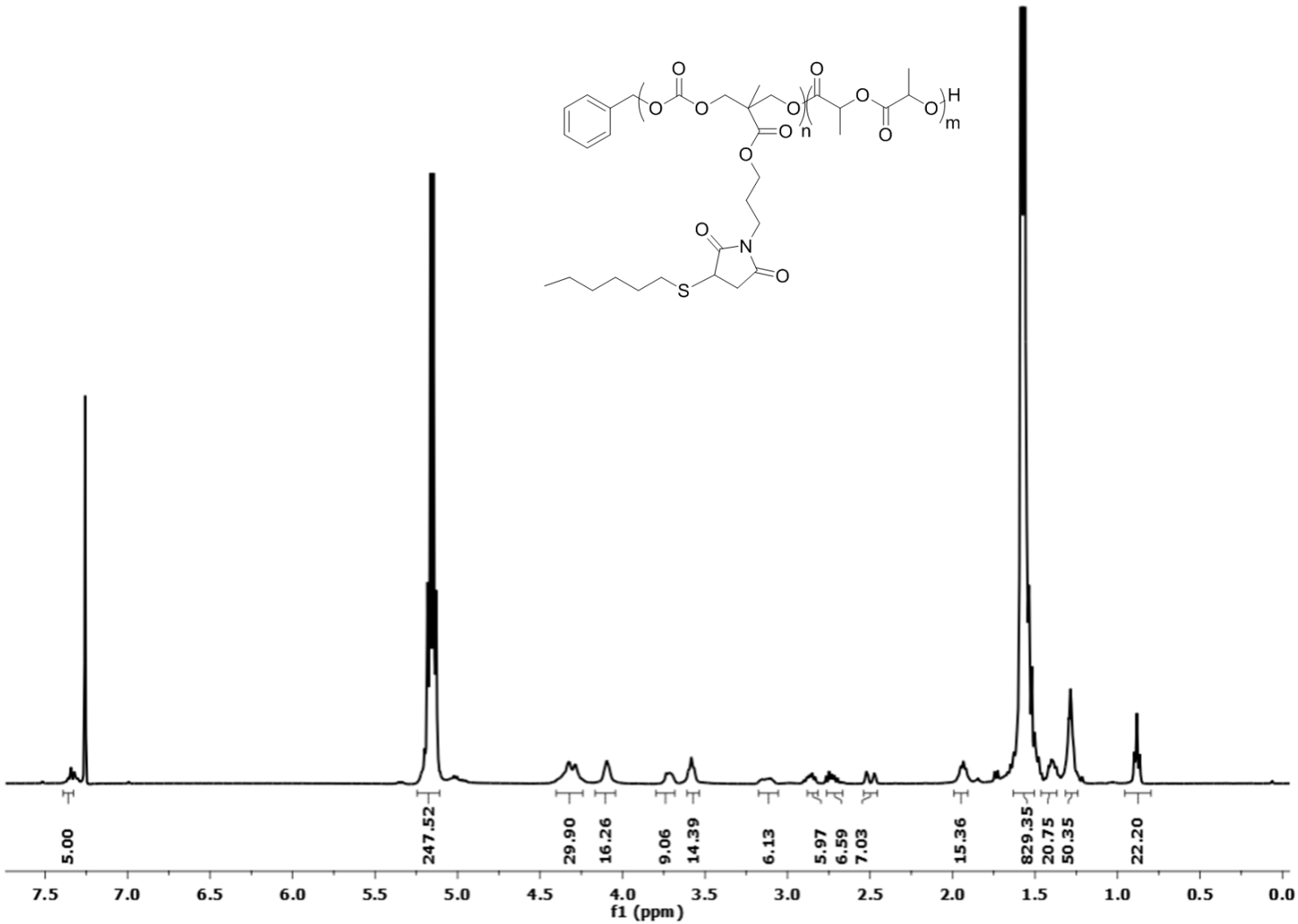

Figure A.13. ^{1}H NMR spectrum of 1-hexanethiol functionalized copolymer 9.

REFERENCES

1. Majoros, I. J., A. Myc, T. Thomas, C. B. Mehta and Jr. J.R. Baker, "PAMAM Dendrimer-Based Multifunctional Conjugate for Cancer Therapy: Synthesis, Characterization and Functionality", *Biomacromolecules*, Vol. 7, pp. 572-579, 2006.

2. Caminade, A. M., C. Padie, R. Laurent, A. Maraval and J. P. Majoral, "Uses of Dendrimers for DNA microarrays", *Sensors*, Vol. 6, pp. 901-914, 2006.

3. Yilmaz, M. D., O. A. Bozdemir and E. U. Akkaya, "Light harvesting and efficient energy transfer in a boron-dipyrrin (BODIPY) functionalized perylenediimide derivative", *Org. Lett.*, Vol. 8, pp. 2871-2873, 2006.

4. Frechet, J. M. J. and D. A. Tomalia, Dendrimers and Other Dendritic Polymers, John Wiley & Sons, New York, NY, USA, 2002.

5. De Brabander-van den Berg, E. M. M. and E. W. Meijer, "Poly (propylene imine) Dendrimers: Large-Scale Synthesis by Heterogeneously Catalyzed Hydrogenations", *Angew. Chem., Int. Ed.*, Vol. 32, pp. 1308-1311, 1993.

6. Hawker, C. J. and J. M. J. Frechet, "Preparation of Polymers with Controlled Molecular Architecture. A New Convergent Approach to Dendritic Macromolecules", *J. Am. Chem. Soc.*, Vol. 112, pp. 7638-7647, 1990.

7. Gillies, E. R. and J. M. J. Frechet, "Designing Macromolecules for Therapeutic Applications: Polyester Dendrimer-Poly(ethylene oxide) "Bow-Tie" Hybrids with Tunable Molecular Weight and Architecture", *J. Am. Chem. Soc.*, Vol. 124, pp. 14137-14146, 2002.

8. Wathier, M., P. J. Jung, M. A. Carnahan, T. Kim and M. W. Grinstaff, "Dendritic Macromers as In Situ Polymerizing Biomaterials for Securing Cataract Incisions", *J. Am. Chem. Soc.*, Vol. 126, pp. 12744-12745, 2004.

9. Wu, P., M. Malkoch, J. N. Hunt, R. Vestberg, E. Kaltgrad, M. G. Finn, V. V. Fokin, K. B. Sharpless and C. J. Hawker, "Multivalent, Bifunctional Dendrimers Prepared by Click Chemistry", *Chem. Commun.*, pp. 5775-5777, 2005.

10. Lee, C. C., E. R. Gillies, M. E. Fox, S. J. Guillaudeu, J. M. J. Frechet, E. E. Dy and F. C. Szoka, "A single dose of doxorubicin-functionalized bow-tie dendrimer cures mice bearing C-26 colon carcinomas", *Proc. Natl. Acad. Sci. U. S. A.*, Vol. 103, pp. 16649-16654, 2006.

11. Ghosh, S., S. Basu and S. Thayumanavan, "Simultaneous and Reversible Functionalization of Copolymers for Biological Applications" *Macromolecules,* Vol. 39, pp. 5595-5597, 2006.

12. Yang, S. K. and M. Weck, "Modular Covalent Multifunctionalization of Copolymers", *Macromolecules,* Vol. 41, pp. 346-351, 2008.

13. Yang, S. K. and M. Weck, "Covalent and orthogonal multi-functionalization of terpolymers", *Soft Matter,* Vol. 5, pp. 582–585, 2009.

14. Kose, M. M., S. Onbulak, I. I. Yilmaz and A. Sanyal, "Orthogonally "Clickable" Biodegradable Dendrons", *Macromolecules,* Vol. 44, pp. 2707–2714, 2011.

15. Lutz, J. F., "1,3-Dipolar Cycloadditions of Azides and Alkynes: A Universal Ligation Tool in Polymer and Materials Science", *Angew. Chem., Int. Ed.*, Vol. 46, pp. 1018-1025, 2007.

16. Hoyle, C. E. and C. N. Bowman, "Thiol–Ene Click Chemistry", *Angew. Chem., Int. Ed.*, Vol. 49, pp. 1540-1573, 2010.

17. Kolb, H., M. Finn and K. B. Sharpless, "Click Chemistry: Diverse Chemical Function from a Few Good Reactions", *Angew. Chem., Int. Ed.*, Vol. 40, pp. 2004-2021, 2001.

18. Rostovtsev, V. V., L. G. Green, V. V. Fokin and K. B. Sharpless, "A Stepwise Huisgen Cycloaddition Process: Copper (I)-Catalyzed Regioselective Ligation of Azides and Terminal Alkynes", *Angew. Chem., Int. Ed.*, Vol. 41, pp. 2596-2599, 2002.

19. Mantovani, G., F. Lecolley, L. Tao, D. M. Haddleton, J. Clerx, J. J. L. M. Cornelissen and K. Velonia, "Design and synthesis of N-maleimido-functionalized hydrophilic polymers via copper-mediated living radical polymerization: A suitable alternative to PEGylation chemistry", *J. Am. Chem. Soc.*, Vol. 127, pp. 2966-2973, 2005.

20. Carruthers, W., "Cycloaddition Reactions in Organic Synthesis", Pergamon Press, Oxford, 1990.

21. Sanyal, A., "Diels–Alder Cycloaddition-Cycloreversion: A Powerful Combo in Materials Design", *Macromol. Chem. Phys.*, Vol. 211, pp. 1417–1425, 2010.

22. Goussé, C., A. Gandini, and P. Hodge, "Application of the Diels-Alder Reaction to Polymers Bearing Furan Moieties. 2. Diels-Alder and Retro-Diels-Alder Reactions Involving Furan Rings in Some Styrene Copolymers", *Macromolecules*, vol. 31, pp. 314-321, 1998.

23. Wei, H. L., Z. Yang, L. M. Zheng and Y. M. Shen, "Thermosensitive hydrogels synthesized by fast Diels–Alder reaction in water", *Polymer*, Vol. 50, pp. 2836-2840, 2009.

24. Dispinar, T., R. Sanyal and A. Sanyal, "A Diels-Alder/retro Diels-Alder Strategy to Synthesize Polymers Bearing Maleimide Side Chains", *J. Polym. Sci., Part A: Polym. Chem.*, vol. 45, pp. 4545-4551, 2007.

25. Ratner, B. D. and A. S. Hoffman, "*Hydrogels for Medical and Related Applications*", ACS Symposium Series No. 31, American Chemical Society: Washington, DC, pp 1-36, 1976.

26. Peppas, N. A., "*Hydrogels in Medicine"*, CRS Press: Boca Raton, FL, 1986.

27. Hoffman, A., “Hydrogels for biomedical applications”, *Adv. Drug Del. Rev.*, Vol. 54, pp. 3–12, 2002.

28. Liu, S. Q., P. L. R. Ee, C. Y. Ke, J. L. Hedrick and Y. Y. Yang, “Biodegradable poly(ethylene glycol)-peptide hydrogels with well-defined structure and properties for cell delivery”, *Biomaterials*, Vol. 30, pp. 1453-1461, 2009.

29. Malkoch, M., R. Vestberg, N. Gupta, L. Mespouille, P. Dubois, A. F. Mason, J. L. Hedrick, Q. Liao, C. W. Frank, K. Kingsbury and C. J. Hawker, “Synthesis of well-defined hydrogel networks using Click chemistry”, *Chem. Commun.*, pp. 2774-2776, 2006.

30. Altin, H., I. Kosif and R. Sanyal, “Fabrication of “Clickable” Hydrogels via Dendron−Polymer Conjugates”, *Macromolecules*, Vol. 43, pp. 3801-3808, 2010.

31. Shoichet, M. S., “Polymer Scaffolds for Biomaterials Applications”, *Macromolecules*, Vol. 43, pp. 581–591, 2010.

32. Kosif, I., E. J. Park, R. Sanyal and A. Sanyal, “Fabrication of Maleimide Containing Thiol Reactive Hydrogels via Diels−Alder/Retro-Diels−Alder Strategy”, *Macromolecules*, Vol. 43, pp. 4140–4148, 2010.

33. Gross, R. A. and B. Kalra, “Biodegradable polymers for the environment”, *Science*, Vol. 297, 2002.

34. Suriano, F., O. Coulembier, J. L. Hedrick and P. Dubois, “Functionalized cyclic carbonates: from synthesis and metal-free catalyzed ring-opening polymerization to applications”, *Polym. Chem.*, Vol. 2, pp. 528-533, 2011.

35. Uhrich, K. E., S. M. Cannizzaro, R. S. Langer and K. M. Shakesheff, “Polymeric Systems for Controlled Drug Release”, *Chem. Rev.*, Vol. 11, pp. 3181–3198, 1999.

36. Pounder, R. J., M. J. Stanford, P. Brooks, S. P. Richards and A. P. Dove, "Metal free thiol–maleimide 'Click' reaction as a mild functionalization strategy for degradable polymers", *Chem. Commun.*, pp. 5158–5160, 2008.

37. Brunelle, D. J., "Ring Opening Polymerization/Mechanisms, Catalysis, Structure, Utility", Hanser Publishers, Chap. 11, pp. 309-336, 1993.

38. Cabaret, O. D., B. M. Vaca and D. Bourissou, "Synthesis of highly functionalized oligo and copolyesters from a carbohydrate lactone**"**, *Chem. Rev.*, Vol. 104, pp. 6147-6176, 2004.

39. Kamber, N. E., W. Jeong, R. M. Waymouth, R. C. Pratt, B. G. G. Lohmeijer and J. L. Hedrick, "Organocatalytic ring-opening polymerization", *Chem. Rev.*, Vol. 107, pp. 5813-5840, 2007.

40. Lohmeijer, B. G. G., R. C. Pratt, F. Leibfarth, J. W. Logan, D. A. Long, A. P. Dove, F. Nederberg, J. Choi, C. Wade, R. M. Waymouth and J. L. Hedrick, "Guanidine and amidine organocatalysts for ring-opening polymerization of cyclic esters", *Macromolecules*, Vol. 39, pp. 8574-8583, 2006.

41. Albertsson, A. C. and I. K. Varma, "Recent Developments in Ring-Opening Polymerization of Lactones for Biomedical Applicants", *Biomacromolecules*, Vol. 4, pp. 1466-1486, 2003.

42. Dechy-Cabaret, O., B. Martin-Vaca and D. Bourissou, "Controlled ring-opening polymerization of lactide and glycolide", *Chem. Rev.*, Vol. 104, pp. 6047, 2004.

43. Bourissou, D., S. Moebs-Sanchez and B. Martin-Vaca, "Recent advances in the controlled preparation of poly (α-hydroxyacids): metal-free catalysts and new monomers", *C. R. Chim.*, Vol. 10, pp. 775-794, 2007.

44. Dove, A. P. "Controlled ring-opening polymerization of cyclic esters: Polymer blocks in self-assembled nanostructures", *Chem. Commun.*, pp. 6446-6464, 2008.

45. Jerome, C. and P. Lecomte, “Recent advances in the synthesis of aliphatic polyesters by ring-opening polymerization”, *Adv. Drug Del. Rev.*, Vol. 60, pp. 1056–1076, 2008.

46. Allen, S. D., D. R. Moore, E. B. Lobkovsky and G. W. Coates, “High-Activity, Single-Site Catalysts for the Alternating Copolymerization of CO_2 and Propylene Oxide”, *J. Am. Chem. Soc.*, Vol. 124, pp. 14284-14285, 2002.

47. Nederberg, F., B. G. G. Lohmeijer, F. Leibfarth, R. C. Pratt, J. Choi, A. P. Dove, R. M. Waymouth, J. L. Hedrick, “Organocatalytic Ring Opening Polymerization of Trimethylene Carbonate”, *Biomacromolecules*, Vol. 8, pp. 153-160, 2007.

48. Templaar, S., L. Mespouille, P. Dubois and A. P. Dove, “Organocatalytic Synthesis and Postpolymerization Functionalization of Allyl-Functional Poly (carbonate)s”, *Macromolecules*, Vol. 44, pp. 2084-2091, 2011.

49. Kose, M. M., G. Yesilbag and A. Sanyal, “Segment block dendrimers via Diels-Alder cycloaddition”, *Org. Lett.*, Vol. 10, pp. 2353–2356, 2008.

50. Sinclair, A. J., V. D. Amo and D. Philp, “Structure–reactivity relationships in a recognition mediated [3+2] dipolar cycloaddition reaction”, *Org. Biomol. Chem.*, Vol. **7**, pp. 3308-3318, 2009.

51. Altintas, O., B. Yankul, G. Hizal and U. Tunca, “A3-type star polymers via click chemistry”, *J. Polym. Sci., Part A: Polym. Chem.*, Vol. 44, pp. 6458-6465, 2006.

52. Shepherd, J. L., A. Kell, E. Chung, C. W Sinclar, M. S Workentin and D. Bizzotto, “Selective reductive desorption of a SAM-coated gold electrode revealed using fluorescence microscopy”, *J. Am. Chem. Soc.*, Vol. 126, pp. 8329-8335, 2004.